The Role of Zirconium in Microalloyed Steels

T N Baker

Department of Mechanical and Aerospace Engineering
The University of Strathclyde, Glasgow G1 1XJ, UK.
E-mail:neville.baker@strath.ac.uk.

Abstract

Recently there has been a renewed interest in the addition of zirconium to microalloyed steels. It has been used since the early 1920's, but has never been universally employed, as have niobium, titanium or vanadium. The functions of zirconium in steelmaking are associated with a strong chemical affinity, in decreasing order, for oxygen, nitrogen, sulphur and carbon. Historically, the main use of additions of zirconium to steel was for combination preferentially with sulphur and so avoid the formation of manganese sulphide, known to have a deleterious influence of the impact toughness of wrought and welded steel. Modern steelmaking techniques have also raised the possibility that zirconium additions can reduce the austenite grain size and increase dispersion strengthening, due to precipitation of zirconium carbonitrides, or in high nitrogen vanadium-zirconium steels, vanadium nitride. This review gathers information on the compounds of zirconium identified in steels together with crystallographic data and solubility equations. Also brief accounts of the role of sulphides and particles in general on austenite grain size control and toughness are included.

Keywords: Zirconium compounds, mechanical properties, impact, microstructure

1 Introduction

The term microalloying, as applied to steels, is generally accepted as emanating from the paper by Beiser[1] published in 1959, which reported the results of small additions of niobium to commercial heats of a carbon steel. However, it has not been recognized that microalloying as such, first occurred some 35 years earlier, when small additions of zirconium were added to plain carbon steels, and the effects reported by Feild[2] and by Beckett[3]. Over the past few years there has been a renewed interest in the influence of zirconium additions to high strength low alloy [HSLA] steels, reported, for example, by Xi et al [4], Guo et al[5], Wang et al[6]. While reviews of the effects of aluminium nitride in steel by Wilson and Gladman[7],and the influence of additions in microalloyed steels of niobium by DeArdo[8] ,an overview of titanium microalloyed steels by Pickering[9] and of vanadium by Baker[10] have been compiled, the work on zirconium additions to steel is scattered throughout the literature from about 1923, when research on this subject was first published. It is therefore timely that the available publications are brought together in an up- to date review.

The functions of zirconium in steelmaking are associated with the strong chemical affinity of this element which in molten steel reacts, in decreasing affinity, with oxygen, nitrogen, sulphur and carbon[11] .Like many other scientific and engineering innovations, military conflict was also the driving force in the case of the development of zirconium steels. As reported by Becket [3], the reduction of zirconium ores and the preparation of zirconium alloys were conducted in the USA at the Niagara Falls plant of the Electro Metallurgical Co. who manufactured ferroalloys, during the period of a few years immediately preceding the entry of the United States into the First World War in 1918. This work was driven by reports, later questioned, that ‘remarkable ordinance steels containing zirconium’, had been developed in Germany. The US War Industries Board decided upon an intensive experimental programme

with the aim of possible large scale production of zirconium steels suitable for light armour. A fuller background to this project is to be found in the paper by Becket[3], while the results of the experimental work are described briefly by Becket and more completely by Field. [2]Both considered that zirconium additions to low carbon steels would reduce the levels of oxygen, nitrogen and sulphur, overcome red shortness in high sulphur steels and improve the mechanical properties. They also identified zirconium nitride by optical microscopy and concluded that the improvement in properties was associated firstly with the removal of nitrogen as Zr_3N_2, while the remaining zirconium combined with sulphur, which was thought to be less deleterious to properties than manganese sulphide. Zirconium is also known to protect other elements, such as boron, that would otherwise combine with nitrogen and oxygen in liquid steel.[11]

Many of the earliest studies which were carried out by Sims and coworkers [12-16] were concerned with producing improvements in toughness through shape control of sulphide inclusions. This was achieved by changing the composition of the inclusions, essentially manganese sulphides, to manganese zirconium sulphides [17], which are less plastic at rolling temperatures. The change in composition increased the resistance of the sulphides to high temperature deformation, thereby avoiding elongation parallel to the rolling direction, which was known to have a significant effect on the toughness in a transverse mode .[18-20] Later, steelmaking processing modifications made possible the reduction of the sulphur levels in steels to less than 0.005wt %, at which amount the deterioration in toughness was averted [21], although other work concluded that the improvement in toughness and formability associated with a zirconium addition is superior to that obtained with extra-low sulphur practice. [22] Around 1990, a series of papers from Japan, cited by Sawai et al [23], highlight the importance of ‘oxides metallurgy in steels’. These papers emphasized the effect of fine oxides dispersed in steel, including zirconium oxide, which may play a significant role during thermo-

mechanical treatments, as heterogeneous nucleation sites for various precipitates and control steel properties. At this time, it was also recognized that a uniform distribution of oxides resulted in an improvement in toughness in the heat affected zone (HAZ) of weld metal, and a number of publications deal with the influence of zirconium on weld metal. [4-6]Zirconium additions have also been added as a possible replacement for, or in combination with, the transition metals niobium, titanium and vanadium, to increase the yield strength through grain size control [24-29], and /or dispersion strengthening [30] by precipitation of fine carbides, nitrides or carbonitrides.

2 Background

Zirconium, Zr, atomic number 40, atomic weight 91.22, has been used for many years as an alloying element in low carbon (≤ 0.15) microalloyed steels, but has never been employed universally, as have the elements niobium, titanium or vanadium. The name zirconium is derived from the Persian 'zargon', meaning gold- like. Zirconium is a fairly abundant element and is widely distributed in minerals, but it is never found uncombined in nature. It always occurs with hafnium, which has almost identical chemical properties. Zirconium ranks 20th in the earth's crust and is as abundant as chromium. It was discovered as the oxide, zirconia, in the mineral zircon, the silicate by Klaproth in 1789 and was first isolated in an impure form by Berzelius in 1824. [31, 32,]

The chief ore is zircon ($ZrSiO_4$), while baddeleyite (the oxide, ZrO_2) also has some importance. Zircon is recovered, along with monazite, ilmenite, and rutile, from certain beach sands in New South Wales, Australia, and near Jacksonville, Florida. The metal is produced by the Kroll process. [33-34] Zircon is combined with carbon in an electric furnace to form a cyanonitride, which is in turn treated with chlorine gas to form the volatile tetrachloride. The tetrachloride is purified by sublimation in an inert atmosphere and then chemically reduced to

metal sponge by reaction with molten magnesium. This spongy metal is cleaned and further processed into ingots. Special care is taken to exclude hydrogen, nitrogen, and oxygen, which make the metal brittle. If the metal is too brittle to be worked, it can be further purified by the Van Arkel–de Boer process, in which the crude metal is reacted with iodine to form volatile iodides that are thermally decomposed on a hot wire, resulting in pure crystalline zirconium. A fuller account of the history, sources and production of zirconium is given by Motock and Offenhauer [11] and of the chemical behaviour by Blumenthal. [33]In addition to its use as an alloying element in steel, 90% of all the zirconium produced is used in nuclear reactors because of its low neutron –capture cross –section and resistance to corrosion. [34] The commercial metal usually contains between 1% and 3% hafnium. For nuclear reactor use, the hafnium is normally removed by solvent extraction from the tetrachloride. [35]Zirconium alloys are used in parts of space vehicles for their resistance to heat, especially important during the atmosphere re-entry. The oxide, ZrO_2 is a refractory material and used to produce laboratory crucibles and metallurgical furnace linings.[36]

3 Zirconium: the physical state

Zirconium is an element of the second subgroup, Group IVA, of the periodic table, the outermost surface layer electron structure of which is $4d^2 5s^2$. The relationship between zirconium and other elements which are in Groups IVA, VA and VIA is given[37] in Table 1.

Zirconium has two allotropic forms, alpha, which is hexagonal close packed and stable up to 862ºC, while beta, which is body centred cubic, is stable between 862ºC and the melting point, 1852 ± 2ºC.A comprehensive description of the research history of the transition of alpha to beta transition is provided by Miller [31,.32], who also collated the lattice constants and co-ordination numbers(CN) given below:

alpha, a = 0. 3230 ± 0.002nm, c = 0.5133±0.003nm, c/a = 1.589, CN= 6,6

beta, a = 0.361nm at 862ºC, CN=8.

Group	Element	Metal Structure	Carbide (Metal Atom Structure)	Composition Range
IV	Ti Zr Hf V	b.c.c., h.c.p. b.c.c., h.c.p. b.c.c., h.c.p. b.c.c.	f.c.c. f.c.c. f.c.c. f.c.c. h.c.p.	TiC ZrC HfC VC-V_4C_3 V_2C-V_8C_3
V	Nb Ta Cr	b.c.c. b.c.c. b.c.c.	f.c.c. h.c.p. f.c.c. h.c.p. complex structures	NbC-Nb_4C_3 Nb_2C-Nb_3C TaC Ta_2C-Ta_8C_3 $Cr_{23}C_6$, Cr_7C_3, Cr_3C_2
VI	Mo W	b.c.c. b.c.c.	h.c.p. hex. h.c.p. h.e.x.	Mo_2C-Mo_3C MoC W_2C WC

VII	Mn	b.c.c., f.c.c., and complex structures	complex structures	Mn_4C,$Mn_{23}C_6$, Mn_3C,Mn_5C_2, Mn_7C_3

Table 1 Relationship between zirconium and some of the elements in Groups IV_A ,V_A and VI_A that are present in ferritic steels [37]

The properties of zirconium, titanium and iron have been compared by Schwope. [38] These metals all possess allotropic transformations. Schwope [38] found that 'elements such as niobium, tantalum, molybdenum, tungsten, vanadium, uranium, chromium, manganese, iron, cobalt, nickel and copper, which have a larger number of outer d electrons, can be expected to be eutectoid formers, enlarge the β- field and lower the transformation temperature. On the other hand, elements such as boron, aluminum, tin, germanium, antimony, lead, thallium and indium, with a smaller number of electrons, can be expected to raise the transformation temperature. The elements oxygen, nitrogen and carbon are α stabilizers and also raise the transformation temperature. Like other members of Group IVA, zirconium is a strong carbide, nitride and oxide forming element. Hume –Rothery and Raynor [39] describe the carbides and nitrides as interstitial phases determined by the size factor. Hägg [40], in 1931, observed that in a large number of interstitial structures, the metal atoms (M) form a close- packed partial structure of either face- centred cubic or close- packed hexagonal type. The relatively small non-metal atoms(X), such as carbon and nitrogen, fit into one of the

two kinds of interstice, octahedral or tetrahedral. Also it should be noted that up to 25% of the interstices may be vacant at random, so that compositions of carbides and nitrides vary from MX to M_4X_3. Hägg deduced an empirical law which states that for systems having an atomic radius ratio between 0.41 and 0.59, interstitial structures can form, where the small non-metallic X atom has six neighbours. However, when the radius exceeds 0.59, more complicated structures are formed. [41] This law is followed by the transition metal carbides and nitrides of the elements forming the Groups IVA and VA. Bhadeshia [41] has noted that Cottrell [42] has been able to explain many of the observed trends in the stability, crystal structure and stoichiometry of the carbides of transition metals in terms of chemical bonds. Titanium, zirconium and hafnium [≡M], which in the periodic table are elements near the beginning of the long periods, form very stable MC carbides, but the affinity for carbon diminishes further along the rows of the periodic table. A part of the reason for this is that more electrons have to be accommodated for elements further along the rows, so antibonding states are progressively filled, thereby reducing the bond order. This does not completely explain the trend because the maximum bond order occurs with chromium, molybdenum and tungsten, whose carbides are less stable. With MC carbides, the metal has to sacrifice four electrons to form the bonds with carbon. Titanium has exactly the right number, so that on forming TiC, its *d*-orbitals are left empty. This is not the case with VC, since vanadium has an additional *d*-electron which forms a V–V bond. The electrons in the two kinds of bonds, V–C and V–V mutually repel, leading to a reduction in the stability of VC when compared with TiC. This problem becomes greater along the row of the periodic table until MC carbide formation becomes impossible or unlikely. Andrews and Hughes [43] have pointed out that an unusual feature of the carbides and nitrides of the transition metals, is that the metal atom

partial structures in the interstitial phase is different from that of the crystal structure found in the pure metal. These phases show little solubility for iron, and are readily formed at quite low percentages of carbon. They form solid solutions with each other if the size factors of the metallic elements are favourable, and the formation of continuous solid solutions has been observed in the systems. [41]

Table 2 shows the atomic radii of many of the transitions elements and their difference from iron. Here it can be seen that while the vanadium atom radius has the smallest difference compared to the iron atom, zirconium and hafnium have the largest difference.

Element	Atomic radius nm	% difference to that of the iron atom
Ti	0.147	+14.8
V	0.136	+ 6.2
Cr	0.128	» 0
Zr	0.160	+25.0
Nb	0.148	+15.6
Mo	0.140	+ 9.4
Hf	0.31.3	+31.3
Ta	0.148	+15.6
W	0.141	+1

Table 2 Atomic radii of refractory metals[45]

4.Compounds characterised and reported in the literature based on zirconium additions to steels

Several important sources are listed below. Brown [44] has collected the available data on the chemical thermodynamics of zirconium and its compounds while Goldschmidt [45] collated data on interstitial alloys. Surveys of the field of refractory carbides and nitrides have been undertaken by Toth[46] in 1971 and Pierson[47] in 1996.Motock and Offenhauer [11] summarized the literature relating to zirconium based inclusions at a time when it was only possible to observe large particles, visible under the optical microscope. Frequently the colour of nitride, carbonitrides or sulphide particles was the only guide to the possible elemental composition, but this was not entirely reliable. When X-ray diffraction techniques became available they were used with geological specimens as standards, but were not able to identify individual particles. Data from these sources has been assembled below for compounds that have been identified or might considered to be present in zirconium based steels. The details of their crystal structure is collated in Table 3.Characterisation of individual particles only became possible with the advent of electron probe microanalysis, a technique used by both Lichy et al[17] and Keissling et al [48] and later selected area electron diffraction[SAED], energy dispersive X-ray analysis[EDX] [25]and electron energy spectroscopy [EELS]. [27]

Zirconium Boride

Bulk zirconium boride was studied by Norton et al [54]and by Brewer et al [55] in early investigations of refractory borides, and the method of preparation was described by Kieffer et al. [56] The binary phase diagram of B-Zr contains two compounds, B_{12} Zr [Fm3m] , identified by Post and Glaser [57] , and B_2Zr [P6/mmm],identified by Keissling et al[58], the former at 40.9wt% Zr and the latter between 80 and 83.8 wt% Zr (ASM vol. 3,2.87). [59]Raghavan[60] explored the Fe-ZrB_2 phase diagram, which

predicted that precipitates of FeB_2 could be formed in austenite by cooling from elevated temperatures. This compound was utilized by Park et al [61] to investigate the effect of zirconium borides on the grain refinement in low carbon steels. They used convergent beam electron diffraction to identify sub-micron particles at ragged grain boundaries as ZrB_2.

COMPOUND	STRUCTURE	LATTICE PARAMETERS Å			SPDD Card No
		a	b	c	
ZrB_2	Hexagonal (P6mm)	3.169		3.530	6-0610
ZrB_{12}	Cubic (Fm^3m)	7.408			6-0590
ZrC	Cubic (Fm^3m)	4.698			19-1487
ZrN	Cubic (Fm^3m)	4.56			
γ-ZrO_{2-x}	Cubic (Fm^3m)	5.09			27-997
β-ZrO_{2-x}	Tetragonal ($P4_2/nmc$)	3.64		5.27	24-1164
ZrO_{2-x}	Monoclinic ($P2_1/c$)	5.1477	5.203 β=99.38^o	5.3156	13-307
Zr_4S_3	Tetragonal	3.542 3.549		8.05 8.017	10-204
ZrS	Tetragonal	3.55		6.31	Hahn[49]
ZrS	Cubic	5.240 5.250			Hahn[49] 10-259
ZrS_4	Cubic	10.23 10.25			Hahn[49] 10-210
ZrS_2	Hexagonal	3.68 3.660		5.85 5.8255	Hahn[49] 11-679
ZrS_3	Monoclinic	5.16	3.65 β=98.1^o	18.3	Hahn[49]
Zr_2S		5.123	3.627 β=97.18^o	8.986	15-790 Haraldsen[50]
$ZrgS_2$	Orthorhombic	12.322	15.359	3.508	24-1496 Conrad and Franzen[51]

$Zr_4C_2S_2$	Tetragonal	9.752		19.216	24-1497 Conrad and Franzen[51]
$Zr_4C_2S_2$	Hexagonal	3.395		12.11	16-848 Kudielka and Rhode[52]
α–MnS	Cubic	5.2236			6-518
α–MnS	Cubic	5.214 - 5.243			Kiessling[53]

Table 3 Crystallographic data of selected zirconium compounds

Zirconium Carbide

As shown in the binary alloy phase diagram derived by Sara [62] and revised by Okamoto[63], only one zirconium carbide is formed, ZrC [Fm3m] which has a composition range from ~6 to 12 wt-% carbon. It was identified among others in microalloyed steels by He and Baker [27]. More recently, experimental information on the thermochemical properties and the phase equilibria involving the condensed phases of the Zr-C system has been analysed using phenomenological models for Gibbs energy by Guillermet. [64]

Zirconium Nitride

Zirconium nitride was observed in carbon steels optically by Feild [2] and by Becket [3], at x500 magnification, and described as yellow cubic crystals. This appearance corresponded to a product prepared in 1859, by Mallet. [65] The formula, Zr_3N_2 was assigned in 1912 to a compound prepared at high temperatures from zirconium and nitrogen by Wedekind [66] ,which Field originally considered might agree with his particles. However, this formula is not upheld today.

The system nitrogen-zirconium was determined by Domagala et al. [67] Like the carbide, the binary alloy phase diagram of Zr-N as given in the ASM Alloy Phase Diagrams,

shows that there is only one nitride formed [68], ZrN [Fm3m], and this is present beyond 9wt-% nitrogen. Mihelich et al[22] confirmed the earlier observation by Lichy et al[17] ,that in a fully killed steel, which implies that the steel is completely deoxidised, zirconium combines with nitrogen in preference to sulphur or carbon. Using electron probe microanalytical [EPMA] techniques, Mihelich et al [22] identified manganese zirconium sulphides (Mn, Zr)S in their steels which they showed to have nucleated on ZrN particles. These authors also assumed that ZrN, which has a melting point~3000ºC, formed as solid particles, ~5μm in size, in the molten steel, and acted subsequently as heterogeneous nucleation sites for Zr(C, N).Large ZrN particles were also observed to exist independently in the matrix. More recently, Wang et al [6] used SAED and EDX to characterise particles on extraction carbon replicas, which were 25nm to 100nm in size, and described as ZrN. However, their EDX spectra show C peaks, which indicates that the C content of the cuboids is more than 100x greater than the N content. This level of carbon cannot be explained by the contribution to the peak from the replica, Also, many of the cuboids have smaller particles associated with them, suggesting that they nucleated at lower temperatures than the main cuboid. The authors make no comments about either of these observations. Some authors like Maia et al [29] did not characterise their precipitates, but stated that they expected zirconium to combine with nitrogen to produce ZrN particles.

Zirconium Carbonitride

Goldschmidt [45] predicted extensive solid solubility between ZrC and ZrN to form Zr(C, N) precipitates. These precipitates are mentioned as a possibility by Motock and Offenhauer [11] and were identified by Shiraiwa et al [69] in 1970 along with titanium carbonitride, using EPMA. However, quantitative analysis of the ~10μm cubic

inclusions was not possible due to the unavailability of data on the mass absorption coefficients at that time of zirconium (or titanium) for CK_α and NK_α. Shiraiwa et al [69] observed cubic inclusions of ZrC, ZrN and also cases where ZrCN existed in the core surrounded by ZrC. However Zr(C, N) particles were only infrequently observed by Mihelich et al [22], who also used EPMA to identify the carbonitrides. They found these particles were only present when additions of zirconium to their steels were ~0.15%.

Zirconium Oxides

Alcock et al [70], in work summarized by Brown [44], gives details of the crystal structure of zirconium oxides. Three polymorphs of crystalline ZrO_2 are known, monoclinic, tetragonal and cubic structures. At low temperatures, the monoclinic form is stable and has a theoretical density of $5.83 gcm^{-3}$.This phase occurs as the natural mineral baddeleyite. Under equilibrium conditions at 1 bar, the monoclinic-tetragonal transition temperature occurs at 1447±30K while the tetragonal-cubic transition is 2556±8K.At higher temperatures, 2953±15K, cubic ZrO_2 transforms to the liquid phase.

The binary alloy phase diagram of oxygen-zirconium system as determined by Abriara et al [71] shows the same three oxides. Face centred cubic γ-ZrO_{2-x} [Fm3m,] which forms between 22 and 25.9wt %O, tetragonal β-ZrO_{2-x} [$P4_2/nmc$], forms between 25.8 and 25.9 wt %O, and monoclinic α -ZrO_{2-x} [$P2_1/c$] forms at 25.9wt %O.

Some details of the method of manufacture by calcination at 500ºC of the tetragonal and monoclinic forms of ZrO_{2-x} and the dependency on the pH range used, are given by Srinivasan et al [72]. By comparing bright and dark field TEM images, Guo et al [5] found that complex inclusions present in the HAZ of a welded 0.05C,1.65 Mn, 0.057Mo,0.0008B,0.015Zr (all wt-%) line-pipe microalloyed steel, consisted of a

core of monoclinic ZrO_2 covered with a discontinuous layer of fcc MnS, oriented so that $[404]_{ZrO2} \| [112]_{MnS}$ .Both zirconium oxide and titanium oxide have been utilized to improve the toughness of steels in the as-rolled and heat treated conditions, the former by particle grain boundary pinning and the latter through the oxide nucleating acicular ferrite [23].

Zirconium Sulphides

One of the earliest references to zirconium sulphide inclusions in steel is that by Feild [73] in 1924. Zirconium sulphide, which was observed optically to have a grey colour was similar to MnS, and considered to have the formula ZrS_2. This characterisation by Feild was based on a comparison with the description given by Fremy [74] in 1853, who was probably the first to prepare zirconium sulphide, which he recorded as a crystalline compound with a steel- grey colour.

The ASM Handbook, volume 3, Alloy Phase Diagrams, does not give a phase diagram for zirconium sulphides. Kiessling and Lange [75] and Shatynski[76] note that Jellinek[77] considered that the system Zr-S had four intermediate phases. The sulphide with the highest zirconium content is ZrS, which is hexagonal and closely related to the corresponding titanium sulphides. A zirconium sulphide with metal vacancies may exist, with the composition Zr_{1-x} S, probably closely related to Ti_{1-x} S.X-ray diffraction patterns of both these zirconium sulphides are reproduced by Koch and Artner.[78] Hahn et al [49] list seven zirconium sulphides. However, eight zirconium sulphides are listed on the SPDD cards. These are ZrS_3 monoclinic, orange colour, Zr_2S- orthorhombic, Zr_9S_2- tetragonal, Zr_3S_2- tetragonal, Zr_3S_2- hexagonal, ZrS- cubic, Zr_3S_4- cubic (Fm3m, black colour), ZrS_2 –hexagonal (violet- brown colour). [79] More recently, Charquet [80] has produced a pseudo –binary Zr-S diagram. He found that the solubility limit of

sulphur in alpha zirconium was about 20ppm and his paper mentions that sulphur contents above this level lead to the presence of sulphur rich precipitates. Beyond 100ppm sulphur, the second phase is the tetragonal sulphide, Zr_9S_2, which he characterised using an EPMA, an SEM/EDX system and by SAED in an analytical transmission electron microscopy [TEM].

The most comprehensive investigation which was based on both x-ray and electron diffraction techniques was undertaken by Narita et al. [81] They studied two groups of resulphurised steels, one which could be described as a vacuum melted low carbon iron, with minimal carbon, manganese and silicon levels but 0.074 to 0.085%S and zirconium in the range 0.064 to 0.270%.With increasing molar ratio from 0.08 to 1.04,the sulphides identified changed from FeS +(ZrS_2) to Zr_3S_4 and finally to ZrS, as seen in Table 4.

The same group of techniques used by Charquet [80] was employed earlier by Suzuki et al [82], to characterise inclusions in zirconium treated steels. These authors verified zirconium sulphides as Zr_3S_2, in a rod or plate- like morphology, when the molar ratio of Zr/Mn was in the range 0.4~ 3.5.The inclusions changed to globular $(Zr, Mn)_3S_2$ when the manganese content of the steels was ~1 wt-%.The system Fe-Zr-S was examined by Vogel and Hartung [83] and by Lichy et al[17] who considered it to be very similar to the Fe-Mn-S system, in that there is a large miscibility gap extending from the ZrS_2 –Fe_2Zr system to the iron corner.

No.	Composition (wt%)			Molar ratio Zr*(mol)/S(mol)	X-ray diffraction	Electron diffraction
	Mn	Zr	S			
I-A-1 I-A-2 I-A-3 I-A-4	0.006 0.005 0.005 0.005	0.064 0.140 0.240 0.270	0.080 0.085 0.074 0.075	0.08 0.41 0.86 1.04	FeS+(ZrS_2) ZrV_2+(Zr_3S_4) Z_3r_4 ZrS	FeS+(ZrS_2) ZrS_2 Z_3r_4 ZrS
I-B-l I-B-2 I-B-3 I-B-4 I-B-5	0.97 0.80 0.77 0.81 0.96	0.12 0.18 0.32 0.50 0.58	0.28 0.26 0.31 0.31 0.25	0.04 0.14 0.28 0.49 0.74	MnS MnS+Zr_3S_4 MnS+Zr_3S_4 Zr*+(MnS) Zr_3S_4	Unidentified

Note : 1) The molar ratio(Zr*/S)is $\frac{(\sum Zr - Zr_{asZr0\ 2+ZrN})/91}{S/32}$

2) Suiphides in parentheses are minor in amount.

Table 4 Identification of sulphide inclusions by means of X-ray diffraction and electron diffraction[81]

Zirconium Carbo-Sulphide

One carbo-sulphide is noted in the first edition of the SPDD search manual as $Zr_4C_2\ S_2$, which is hexagonal. This compound was reported in 1960 by both Frick and Rohde[84] and Kudielka and Rohde.[52] It was identified in microalloyed steels by Arrowsmith [85] (cited by Little and Henderson [86]) using EPMA,TEM/SAED, as a grain boundary phase associated with ZrC. Schneibel et al [87] also identified $Zr_4C_2\ S_2$, as ~200nm size inclusions on extraction carbon replicas, using TEM/SAED/EDX and reported in a paper dealing with the influence of trace additions of zirconium on diffusional creep in Ni-20%Cr. However, the authors were unable to identify these inclusions in thin foils, which they considered might be due to inhomogeneity in the spatial distribution of the carbosulphides.

Zirconium Manganese Sulphide

The existence of zirconium as a component in sulphides isolated from zirconium-bearing steel was reported by Koch and Artner [78] in 1958.They suggested that MnS shows some solid solution for zirconium, and Zr_2S some solid solution for manganese. However, they did not mention specifically zirconium manganese sulphide.

The tendency for zirconium to form (Zr, Mn) S inclusions in zirconium steels, which have a similar colour and morphology to MnS, was noted by Urban and Chipman[88] and Portevin and Castro.[89]. Lichy et al [17] used EPMA to obtain quantitative analysis of blue grey oval silicide inclusions. These containing about 12-40%Zr, 5-50%Mn, 20-40%S and are detailed in Table 5.

In Steel Zr	In Inclusions Mn S Zr	Inclusion morphology
%	% % %	
0.04	35-49 28-39 12-16	oval
0.04	- - 68-71	yellow cube
0.013	8-19 6-16 42	oval
0.052	7 18 41	oval
0.052	10 25 44	grey phase around yellow cube
0.065	8 19 36	oval
0.090	5 17 42	oval

Table 5 Results of electron probe analysis of zirconium manganese sulphide inclusions[17]

Furthermore, Lichy et al[17] were the first to record the heterogeneously nucleation of (Zr, Mn)S on ZrN, as small lemon coloured particles. These were also identified by microprobe analysis as ZrN by Bucher et al [90] in 1969, who in addition to Mihelich et al [22], studied inclusions in zirconium steels also using EPMA techniques. While both sets of workers reported the presence of (Zr, Mn)S, neither provided any compositional data. The previously noted research of Narita et al [81], also considered

sulphide inclusions in steels containing 0.77 to 0.97 %Mn ,~0.28 %S and zirconium in the range 0.12% to 0.58%, giving corresponding Zr / S molar ratios of 0.04 to 0.74,seen in Table 4.The sulphides identified, at increasing Zr / S ratios, were MnS, the MnS+Zr_3S_4 eutectic and finally Zr_3S_4 . Zirconium OxySulphide

Both McCullough et al [91] and Jellinek [92] have explored the crystal structure of zirconium oxysulphide. The results of Schonberg, reporting a tetragonal ZrS, were examined by Jellinek [92], who concluded that this tetragonal phase was in reality ZrOS. The tetragonal ZrOS probably has a unit cell containing two formula units and a structure of the PbFCl- type. The observed intensities agreed well with those calculated from the parameters Z/sub Zr = 0.195 and Zs = 0.630. To date, this compound has not been reported to be present in zirconium microalloyed steels.

4 Stability of Zirconium Compounds

The stability of zirconium oxide, ZrO_2 is greater than that of the oxides of magnesium, calcium, silicon and titanium. Fig1 shows that it is only the complex oxides which have greater negative ΔG values up to the temperature limit of interest for steels, which is that associated with steelmaking, ~1850K.The corresponding ΔG values for the carbides and nitrides of niobium, titanium and zirconium are collated in Fig 2.Here it can be seen, that ZrC is more stable above 2000K than ZrN. At steelmaking temperatures of 1850K however, ZrN is slightly more stable than ZrC. Fig 2 shows that ZrC and ZrN both have the greatest - ΔG values at 2000K of ~180KJmol^{-1}.However, by comparing Figs 1 and 2, it can be seen that this value is around six times smaller than that of ZrO_2 at the same temperature, which has implications for steelmaking practice when additions of zirconium are made. If oxygen is not completely combined as a complex oxide such as $CaAlO_2$ or Mg Al

$_2O_3$, then the zirconium addition, which in microalloyed steels is usually added to form sulphides, carbides, nitrides or carbonitrides, will be lost in part or completely as zirconium oxides, which are normally reported as being too large to have an effective influence on the microstructure through Orowan dispersion strengthening or grain boundary pinning. To prevent a high loss of zirconium during steelmaking, it should be added to molten steel in the ladle. Field [2] added zirconium as a zirconium-silicon –iron alloy, which varied from 50%Si:44%Zr to 72%Si:10%Zr with smaller additions of iron, carbon and titanium.

Narita[93] has given data on the recovery of the elements in Groups IVA and VA, which are reproduced in Table 6

V: 90-1005	Ti: 50-80%	Y: 35-60%
Nb: 80-100%	Zr: 50-80%	La: 20-50%
Ta: 70-90%	Hf: 40-80%	U 20-50%

Table 6 Recovery of groups IVa and Va and rare earth elements in carbon steels[93]

This table indicates that the recovery expected from zirconium during steel making is similar to that from titanium, but less than that of both vanadium and niobium, due to the higher chemical affinity of zirconium for oxygen.

Solubility equations allowing the temperature of compounds in a solvent to be estimated, for example, zirconium carbide in austenite, are normally described in the form of an Arrhenius equation. This gives the dependence of the rate constant K of chemical reactions on the temperature T (in absolute temperature, kelvins) and activation energy E_a, as shown below

$$K=A^{-Ea}/RT \qquad (1)$$

where *A* is the pre-exponential factor and R is the Universal gas constant.

In microalloyed steels, the microalloying element, *M* is often combined with an interstitial *X*, to give a compound, *MX*, some or all of which, dissolves in austenite as the temperature is raised.

$$[M]+[X]=[MX] \qquad (2)$$

The rate constant *K* in equation (1) is now described as an equilibrium constant for the reaction given by equation [2].In practice, the concentrations of *M* and *X* are normally low, being less than 1% and therefore may be considered as having an ideal solution behaviour. *M* and *X* are expressed in terms of the weight percentage of the alloying element present in the steel chemical composition. This allows equation (1) to be expressed as

$$log_{10}[M][X] = k_s = -Q/RT + C \qquad (3)$$

Empirical Arrhenius equations have been determined for many of the important refractory carbides and nitrides known to form in steels, but similar equations for sulphides have not been found. Unlike the solubility equations of transition metal carbides and nitrides of niobium, titanium or vanadium, the corresponding equations of zirconium are almost entirely due to one source, and have some shortcomings. The equilibrium solubility products of zirconium carbide and zirconium nitride in iron have been determined experimentally by Narita [93] and are detailed below.

For zirconium carbide, in the case where carbon in iron is ≈0.1%, Narita[93] provides an equilibrium solubility equation for the reaction in the austenite phase field,

$$Zr_{\gamma} + C_{\gamma} = ZrC_{\gamma} \qquad (4)$$

and here

$$\log [\%Zr][\%C] = K_c = -8464/T + 4.26 \qquad (5)$$

which however does not give the data collated in Table 1 of Narita's paper, which is presented here as Table 7.

A second equation is given [93] for higher carbon steels (0.3%) in the section of his paper written in Japanese,

$$\log [\%Zr][\%C] = K_c = -8464/T + 3.84 \qquad (6)$$

T ºC	K_c
1300	2.9×10^{-2}
1200	1.2×10^{-2}
1100	4.7×10^{-3}
1000	1.5×10^{-3}
900	4.2×10^{-4}

Table 7 Solubility data for zirconium carbide in austenite according to Narita[93]

Arumalla [94] also derived an equation for ZrC solubility in austenite based on free energy data.

$$\log [\%Zr][\%C] = K_c = -9816/T + 3.84 \qquad (7)$$

A particularly useful form of displaying solubility data for different solution temperatures has been devised by Woodhead and published by Wadsworth et al. [95]While examples of the use of this approach can be found in the literature for various carbides and nitrides in steel [9, 96, 97], for some reason the paper is rarely referenced.

Using the appropriate solubility equations for a given temperature, solubility curves were obtained by usually plotting nitrogen or carbon on the abscissae or horizontal axis and the metal on the ordinate or vertical axis. As summarized by Nagata et al [97], the diagram presents loci representing the various combinations of transition metals and aluminium, added to steels, and carbon or nitrogen, in austenite or liquid iron, which are in equilibrium with the corresponding carbide or nitride at different temperatures. Steels which have different compositions, but with similar solution temperatures, should have comparable driving forces for precipitation. The diagrams often include as a reference, the stoichiometric line. The equilibrium solute concentrations after precipitation are identical for steel compositions falling on a line parallel to the stoichiometric line.

The solubility curves for ZrC in austenite at 1000ºC and 1200ºC based on equation (5) are shown in Fig3.

For zirconium nitride in austenite,

$$Zr_{\gamma} + N_{\gamma} = ZrN_{\gamma} \qquad (8)$$

The solubility equation derived by Narita[93] is

$$log_{10}\,[\%Zr]\,[\%N] = K_n = -16007/T + 4.26 \qquad (9)$$

According to Narita, at 1300ºC, K_n = 1.6 x 10^{-6}, and at 1200ºC, K_n <4 x 10^{-7}. Substituting these values of K_n into equation (9), gives T = 1318ºC and 1228ºC respectively. The values are close, but not identical to the corresponding temperatures, suggesting some minor shortcomings in equation (9). Equation (9) indicates that very little ZrN is soluble in austenite.

Narita [93] also gives an equation for the reaction of zirconium with nitrogen in liquid iron,

$$log_{10}\,[\%Zr]\,[\%N] = K_{ln} = -17000/T + 6.38 \quad (10)$$

A comparison of the solubility curves for ZrN in austenite and liquid iron at 1550C°C, a temperature approximately where both solid and liquid steel may exist, is shown in Fig4, which is based on the data of Narita [93].When the zirconium and nitrogen levels fall below the 1550ºC liquid line but above the 1550ºC solid line, ZrN precipitation is expected to begin at high temperatures after solidification. This is discussed in more detail for particular steel compositions in later sections of this paper.

A second equation for zirconium with nitrogen in liquid iron which held between 1550 and 1750°C, was published by Evans and Pehlke [98], and converted to the form given in equation (11) by Morita et al. [99]

$$log_{10}\,[\%Zr]\,[\%N] = K_{ln} = -13300/T + 4.80 \quad (11)$$

Fig5 shows a comparison of the two equations of Narita [91]and Evans and Pehlke [98], for zirconium with nitrogen in liquid iron at 1550ºC. The respective K_{ln} values at 1550°C 1.16×10^{-3} and 3.19×10^{-3}, the latter indicating a solubility product of 2.75 times that of Narita for ZrN in liquid iron. Morita et al [99], who compared the thermodynamic data of seven nitrides in liquid iron, only considered the solubility equation given by Evans and Pehlke [98].The effects of T, Zr, V and Cr on the rate of nitrogen dissolution in liquid iron were studied by Ono et al [100] over a temperature range 1873 to 2023K using an isotope method. They showed that while the interaction parameters for Zr and Ti with N were nearly equal, the rate of nitrogen dissolution was significantly greater in Fe-Ti than Fe-Zr alloys. This result was explained in terms of the alloying elements enhancing the dissolution rate by increasing the activity of vacant sites at the metal surface.

Several publications referenced in this review consider both ZrN and TiN precipitates.Fig6 compares the solubility curves of these compounds in austenite at

1200ºC .Both of the curves developed for TiN show a much greater solubility of this compound than that of ZrN. This is apparent from the respective K_{ln} values:

TiN in γ at 1200ºC

7.78×10^{-6} (Matsuda and Okumura [101])

4.36×10^{-6} (Narita [93])

ZrN in γ at 1200ºC

2.47×10^{-7} (Narita [93])

Matsuda and Okumura [101] predict a Kl_n value 1.8 x greater than Narita [93] for TiN in γ at 1200ºC.

At 1200ºC, the difference in Kl_n between TiN and ZrN in γ is 5.6x using the Narita [93] data and 3.17x using Matsuda and Okumura [100] for TiN. It is interesting to note that Nagata et al [97] used only the data of Matsuda and Okumura [101] in their study of TiN precipitation in low alloy microalloyed steels.

A method of comparing the solubility data for the transition metal carbides and nitrides which might normally be expected to precipitate in low alloy and microalloyed steels, by giving the equilibrium solubility product, K_c or K_n, at several temperatures, was arranged in a diagrammatic form by Gladman.[96] Fig 7 is based on Gladman's compilation, which in the case of solubility in austenite, is dependent mainly on the data presented by Narita [93]. In addition, Fig7 includes data for zirconium carbide in austenite and zirconium nitride in austenite and liquid iron, which was not given by Gladman. No data has been found for ZrN in ferrite, which is not surprising, considering the low levels of solubility in austenite. Many of the solubility curves presented in the literature [9, 96, 97] include AlN in austenite, which is also in Fig 7. The solubility products of ZrN and TiN in austenite, shown in Fig7 ,which are expressed as log k_s values, are similar, but in liquid iron, ZrN is less soluble than TiN, an

observation that has implications for the composition of precipitates when titanium, zirconium and nitrogen are present in microalloyed steels . The figure also shows that titanium carbide, and both vanadium and niobium carbides and nitrides are more soluble in austenite than zirconium and titanium nitrides, which again has implications for the role of the various precipitates in controlling austenite grain size and developing a significant degree of dispersion strengthening in zirconium alloyed steels alloyed in particular with vanadium.

Following a detailed literature search, no recent solubility data for ZrC or ZrN in iron has been discovered.

Goldschmidt [45] considered that 'the extensive homogeneity ranges of the cubic or close-packed hexagonal binary nitrides give rise to similar ternary regions, provided that the size ratios and electron valences of the partner metals are favourable. Thus TiN, ZrN, NbN, TaN (with their N defect ranges) are all intersoluble. The VN-ZrN system forms an exception, as here the metal atom size ratio is unfavourable for any appreciable intersolubility. This is quite similar in the corresponding carbides. It implies that in a ternary system such as TiN-ZrN-VN or ZrN-NbN-VN a miscibility gap should occur, in contrast to the complete solution systems such as TiN-VN-NbN.

The effect of multiple additions of carbide and nitride forming elements on the solubility data of carbonitride precipitates has been explored in many publications, see for example Gladman[96],Houghton[102], Zhou and Kirkaldy [103] , Liu[104], and also incorporated into standard commercially available computer programmes, such as ChemSage and those based on CALPHAD. While the outcome for mixed carbides and nitrides of niobium, titanium and vanadium are well established, when zirconium is present, the outcome is often less satisfactory. More recently, Ku et al[105] have presented' a computational model of equilibrium precipitation of oxides, sulphides, nitrides and carbides in steels, based on satisfying

solubility limits including Wagner interaction between elements, mutual solubility between precipitates, and mass conservation of alloying elements. The model predicts the compositions and amounts of stable precipitates for multicomponent microalloyed steels in liquid, ferrite and austenite phases at any temperature. The model showed a good comparison when validated by commercial packages, but at present, like many similar models, does not include zirconium compounds

Some details of the other binary and ternary systems of importance in the consideration of the role of zirconium in steelmaking, such as Fe-Zr, Zr-O, Zr-N, Zr-H, Zr-S, Zr-Si, Zr-Mn and Fe-Zr-C, are given by Motock and Offenhaur. [11] More recently, Raghaven [106] considered thermodynamic calculations for the C-Fe-Zr system. Most of his comments refer to the work of Jiang et al [107] who computed the isothermal sections of the C-Fe-Zr system at 1300ºC and 900ºC, which according to Raghaven[106] appear to be quite similar to those at 1100ºC of Holleck and Thummler [108] reviewed by Raghaven [107] in 1987. The computed isothermal section at 900ºC redrawn by Raghaven [109] , is shown in Fig 8. Jiang et al [105] compared their calculated data with that of Narita[93] for ZrC in γ iron, and also calculated the solubility of ZrC in an α iron, both sets of data which are included in Fig. 7. They found their calculations disagreed with the experimental data of Narita.[93] They preferred their own calculated data and discussed their reasons.[105] Selected thermodynamic data for solid metal sulphides, selenides and tellurides, and estimated an entropy values for Zr_2S, were reviewed by Mills[110]. Zr_2S is the only zirconium sulphide given in Barin.[111]

5 Austenite Grain Growth Control

Two of the well-established microstructural characteristics known to control both strength and toughness properties in steels are grain size and precipitates/inclusions [7-10]. Petch was the first to attempt to relate impact toughness to microstructure in terms

of grain size.[112]Equation 12 takes the same form as the well established Hall-Petch relationship between yield stress and grain diameter, *d*, only here the impact transition temperature T_c in °C is related to d through

$$T_c = T_o - K_y d^{-1/2} \qquad (12)$$

where T_o and K_y are constants. This classic work[110] did not include the influence of carbide films usually present at the ferrite grain boundaries in steels. In a later paper, Petch[113] refined his ideas to include the effects of both grain size and carbide thickness. However, he pointed out that over a $d^{-1/2}$ range of 3-10 $mm^{-1/2}$ (i.e.100-10μm) and with some carbide refinement concurrent with grain refinement, equation (12) can be used. With a finer grain size, as in microalloyed steels, where d is in the range 10 to 3 μm ($d^{-1/2}$ range of10-18$mm^{-1/2}$), then equation (12) gives a more accurate assessment of T_c.

$$5.5\ T_c = 770 - 46 d^{-1/2} - \sigma_c \qquad (13)$$

where σ_c is the cleavage strength. The derivation of equation (13) is discussed in detail by Petch.[113]

As acknowledged by Martin [114], it is well established that dispersed, hard incoherent particles can either retard or accelerate recrystallization of a metallic matrix', and this was affirmed by the work of Doherty and Martin. [115] Zener was the first to devise a relationship involving a dispersion of particles and the retarding force which they exerted on a grain boundary. The effect, after his original analysis, is known as the Zener drag and was first published by Smith. [116] Zener proposed that the driving pressure for grain growth due the curvature of the grain boundary would be counteracted by a pinning (drag) pressure exerted by the particles on the boundary. Consequently, normal grain growth would be completely inhibited when the average grain size reached a critical maximum grain radius, also known as the Zener limit,

(R_c) given by:

$$R_c = 4r/3f \qquad (14)$$

where f is the particle volume fraction and r the radius of the pinning particles. He considered that both grains and particles could be approximated to spheres. In its general form the Zener Equation is

given as :

$$R_c = K_g r/f^m \qquad (15)$$

where K_g is a dimensionless constant and m an index for f.

However, the model has been shown to overestimate R when compared with experimental data. [117] Several other models have been produced, collated and critically reviewed. [118,119] The most extensive consideration of the many modifications proposed to the Zener equation has been undertaken by Manohar et al [119], who examined in detail some 32 models published to 1987. Data taken from these models is plotted in Fig9 which shows that R_c / r as a function of f results in the data falling into three bands for the exponents m=0.33, 0.5 and 1.0.In addition, for the range of particle volume fractions commonly found in engineering materials (f =10^{-4} to 10^{-2}), values of R_c for m=0.33 also fall within the band m=0.5, and all the bands in this range of f overlap. The dashed line in Fig9 shows the limiting grain radius for K_g=0.17 and m=1, which values are close to those given by a number of equations in the 32 models considered. Furthermore, Manohar et al [119] collated experimental grain growth data from a variety of materials used to examine the models. These are plotted in Fig10 and show that a number of the data closely follow the line for K_g=0.17 and m=1.0, particularly at lower volume fractions. The authors conclude that for systems where f is less than 0.05, K_g=0.17 and m=1 are a reasonable choice.

In general, the pinning of sub-grain and high-angle grain boundaries [120,121] have been shown to occur when the particle radius, r, is the size range 30- 800nm, and particle

volume fraction (*f*) less than 0.01.To date no zirconium or zirconium -vanadium steels have been used to test any of these models. While data for R_c and to some extent *r* are available for zirconium and zirconium -vanadium steels, no reliable data on volume fraction of precipitates in these steels has been published.

There also exists a body of experimental evidence to show that in steels, particles, particularly oxides and carbides greater than 0.5μm with interparticle spacings, also greater than 0.5μm, can lead to acceleration of recrystallization due to nucleation of new grains at carbide particles [122] and oxide slag inclusions. [123]These particles are assumed to create lattice curvature at particle –matrix interfaces in the deformed matrix, which enhances recrystallization and gives rise to accelerated recrystallization. Depending on the composition of the steel, zirconium additions have been shown to precipitate compounds which have a strong pinning effect on austenite grain boundaries, and in certain conditions, zirconium additions may be considered for this purpose as a replacement for niobium or titanium. The early work by Feild [2], referred to above, who, as part of a major study involving over 350 heats of steel, explored the effect of zirconium additions to steels with varying carbon, manganese, sulphur levels and was almost certainly the first to show the effect of zirconium on the ferrite grain size. In his paper, several pairs of optical micrographs from identical steels with and without zirconium additions, show a significantly smaller grain size in the former. However, Feild completely missed this grain refining effect of zirconium on his steels and only noted the effect of zirconium additions in reducing banding, which occurred in the as- rolled plate.

In a well cited paper, Halley [24] considered in a series of 0.30%C steels, the effect of zirconium additions compared with aluminium and titanium on the grain coarsening temperature (GCT), in a study of the change in Charpy toughness of a series of

0.30%C steels. The zirconium steels contained up to 0.134%Zr. He used a calibrated temperature gradient furnace to heat 150mm x 12mm square bars, oil quenched after 2 hrs at temperature and metallographically prepared along the longitudinal axis, to relate the temperature at which grain coarsening commenced, as indicated by the size change of the austenite grains. The results, summarized in Fig11, show clearly that additions of zirconium are less effective than either aluminium or titanium as a grain refiner. However, while the paper does include the carbon content of the steels, it does not include the nitrogen or oxygen levels. Also, at the time the paper was written, solubility data was sparse, and the importance of carbides and nitrides as grain boundary pinning particles was not yet realised, Halley's paper predating the Zener model by two years. It is therefore not possible to accept Halley's conclusion on the effectiveness of zirconium, relative to aluminium or titanium as a grain refiner. However, it is clear from his work that additions of zirconium greater than 0.04 wt-%, raised the GCT by about 80ºC. Despite its modest effect on tensile properties, the data in Table 8 demonstrate that zirconium has a profound effect on notched impact resistance.

Steels with additions of zirconium in the range 0.021 to 0.028%, have better toughness than those with no addition or with an addition of 0.134%Zr. Halley [24] made little attempt to explain his data in terms of which precipitates associated with aluminium, titanium or zirconium, might be responsible for the grain growth inhibition he observed, and seemed to be unaware of the work of Feild [2].

Zirconium Content		Charpy impact energy (J) obtained over a range of test temperatures				
%	24 °C	-18°C	-32 °C	-40 °C	-59 °C	-73 °C
None	54-49	38-33	33-20	4.0	3.4	3.4-2.7
0.009	52-50	45-42	43-38	34-22	4.0	2.7
0.021	60-59	47-40	40-39	34-31	29-28	30-3.4
0.038	62-54	47-43	41-38	33-31	32-31	30-4.7
0.134	56-52	46-44	37-36	37-33	28	23-11

Table 8 Notched impact resistance of zirconium steels, after Halley [24]

.

The two papers in Japanese by Masayoshi [124,125] published in 1951, summarize his work on zirconium steels carried out over a ten year period and mention that this is probably the only major study in Japan at this time. It is regrettable that this work, which was the first major examination of the effect of zirconium additions in steels since the second world war is not better known. Masayoshi examined over 60 casts, mainly from laboratory melts, and in addition to zirconium, considered varying levels of carbon, nitrogen, silicon sulphur, phosphorus, and aluminium. As well as C-Mn steels, he investigated microstructure-properties in zirconium steels containing 2.7%Ni, 0.7-0.8%Cr with 1.7-2.02%Ni, and Si-Cr-Mn. His first paper [124] includes detailed results on the composition, and optical micrographs showing the morphology and size of the inclusions present in his steels. Of particular relevance to microalloyed steels is his work [125] which showed that an addition of 0.01%Zr (steel E43 in his paper)

refined the austenite grain size and retarded grain growth at high temperatures, compared to a zirconium free steel (E41).

In much of the earlier work, zirconium was the only transition metal present. In modern steels, it is frequently the case that combinations of niobium, titanium, vanadium and zirconium are used. Table9 gives the chemical composition of ten steels used in one of the most detailed studies of the influence of zirconium carbonitrides on austenite grain coarsening behaviour in controlled rolled aluminium killed microalloyed steels which was carried out by He and Baker [26].The precipitates in Zr and Zr-Nb steels, with Zr/N ratios between 2.8 and 22, were compared with Ti-bearing carbonitrides in Ti-Nb and Ti-Nb-Zr steels. TEM observations and parallel electron energy loss spectrographic [PEELS] analysis showed that in the Zr and Zr-Nb steels, with hypo Zr additions (Zr/N =2.8 to 6.3), the precipitates containing zirconium were large Zr-N rich carbonitrides of irregular shape and with sizes varying from ~ 100nm to several micrometeres, Fig12.

With hyper-additions (Zr/N = 15 to 22), which were far from stoichiometry , which occurs at a ratio of Zr/N=6.5, fine spherical particles of Zr rich zirconium carbonitrides, in the range 10 to 100 nm, were formed, Fig13 ,together with many more larger ZrC-rich carbonitrides, as detailed in Table10. Moreover, only in the steels with the lowest Zr/N ratios, which were 2.34 for the 0.011Zr steel and 2.75 for the 0.022 Zr-Nb steel, was a significant fraction of AlN detected.

Steel	Type	C	Si	Mn	P	S	Al	N	Ti	Nb	Zr	Zr/N
1	Zr	0.069	0.40	1.44	0.014	0.004	0.034	0.0051	<0.005	<0.005	0.014	2.75
2	Zr	0.068	0.40	1.44	0.014	0.004	0.036	0.0047	<0.005	<0.005	0.011	2.34
3	Zr	0.072	0.40	1.44	0.013	0.004	0.037	0.0058	<0.005	<0.005	0.030	5.17
4	Zr	0.070	0.40	1.44	0.013	0.004	0.040	0.0053	<0.005	<0.005	0.120	22.64
5	Zr-Nb	0.094	0.40	1.43	0.012	0.004	0.036	0.0043	<0.005	0.017	0.013	3.02
6	Zr-Nb	0.018	0.40	1.45	0.012	0.004	0.036	0.0080	<0.005	0.018	0.022	2.75
7	Zr-Nb	0.021	0.40	1.44	0.012	0.004	0.035	0.0071	<0.005	0.017	0.045	6.33
8	Zr-Nb	0.100	0.40	1.46	0.012	0.003	0.041	0.0039	<0.005	0.017	0.060	15.38
9	Ti-Nb	0.110	0.40	1.44	0.013	0.003	0.039	0.0051	0.017	0.016		
10	Ti-Nb-Zr	0.100	0.42	1.44	0.013	0.003	0.045	0.0048	0.013	0.016	0.016	2.71

Table 9 Chemical composition of steels investigated by He and Baker [26]

1	0.014Zr	ZrN-rich (0.1 -several µrn)
2	0.011Zr	ZrN-rich (0.1-several µm)+AIN (15-500µm)
3	0.03Zr	ZrN-rich (0.1 -several µm)
4	0.12Zr*	ZrC-rich (0,1 -several µm) + dense spherical ZrC (10-100 µm)
5	0.013Zr Nb	ZrN-rich (0.1 -several µm)
6	0.022Zr-Nb	ZrN-rich (0.1 -several µm) + AIN (15 500µm)
7	0.045Zr-Nb	ZrN-rich (O.l -several µm)
8	0.060Zr-Nb*	ZrN-rich (0.1 -several nm) Ismail spherical ZrC, Zr-Nb (10-100 µm)
9	Ti Nb	Ti-rich Ti-Nb (0.01 -several µm)
10	Ti-Nb~Zr	Ti-rich Ti~Nb (0.01-several µm) +Ti~Zr and Ti-Nb~Zr carbonitrides (0. 1 – several µm)

*Some ZrC_2S_4 particles were also observed in these steels.

Table 10 Precipitate types in steels in the as –rolled condition.[26]

Austenite grain coarsening occurred around 1050-1100ºC in all the hypo-Zr and Zr-Nb steels, Fig14, because very few small carbonitrides (<100nm) were still present, while a much more gradual austenite grain growth was recorded for the Ti-Nb, Ti-Nb-Zr and hyper-Zr steels, due to the effective pinning of austenite grains by Ti-Nb or zirconium carbonitrides (<100nm).Detailed particle characterisation was undertaken in this work The lattice parameters of zirconium carbonitrides in the Zr treated steels calculated

from SAED patterns showed that for the hypo Zr and hypo Zr-Nb steels , the values were close to that of ZrN, while for the hyper-Zr steels, these values were close to those of ZrC, Fig15. The study concluded that in the hyper Zr treated steels, the fine ZrC-rich carbonitrides, confirmed by PEELS analysis, Fig16, did control austenite grain growth in the temperature range 900 to 1300ºC, but not as effectively as the Ti-Nb carbonitrides in the Ti-treated steels. The authors consider that this was due to the wide particle size range of zirconium carbonitrides which hampered the use of zirconium as an effective austenite grain refiner. Due to the low sulphur levels of 0.003 to 0.004% in the steels, no trace of sulphides as such was recorded in this work.

More recently, austenite grain boundary pinning in zirconium steels has been studied by Maia et al [29] who used higher levels of zirconium. They compared induction melted steels under an argon atmosphere containing 0.09%C,1.5% Mn,0.02%S,0.05%Al,0.05%N, at three levels of silicon,0.2%,0.4% and 0.6% corresponding to three levels of zirconium, 0.4%,0.6% (stoichiometric) and 0.12%,all weight percent. These steels were compared with three commercial microalloyed steels. Specimens for grain size studies were reheated in the range 950-1300ºC for 3600s, while 20mm sized samples used to investigate the extent of austenite recrystallization, were reheated at 1150ºC for 3600s and then rolled, finishing between 910 and 770ºC. The authors considered that zirconium would combine with nitrogen to produce ZrN particles, which restrained the movement of austenite grain boundaries. No evidence was presented in this work to confirm that ZrN precipitation did in fact take place, as no characterisation of the precipitates was undertaken and the main data was that of grain sizes. Fig 17 shows that the steel containing 0.12%Zr had a marked influence on restraining austenite grain growth, and was significantly more effective than the 0.04%Zr steel in this respect , but still less than the TiNb steel .In this respect,

some of these results are very similar to those discussed by He and Baker.[26] However, Maia et al [29] make the point that the difference in austenite grain size at say 1250 ºC, between the 0.12%Zr and the TiNb steel,80μm and 40μm respectively, would in practice be equalised during rolling. The results of the investigation into the retardation of recrystallization due to zirconium additions, showed no difference between the steels containing 0.04% and 0.06%Zr. Also no significant difference was recorded when the finishing rolling temperature (FRT) was $<A_3$ (≤830ºC) between the low (0.020%) and high (0.12%) Zr steels. However, when the FRT was in the temperature range 850-910ºC ($>A_3$), steels with ≤ 0.06%Zr, recrystallized, resulting in equiaxed austenite grains, while in the case of the 0.12% Zr steel, elongated austenite grains were observed up to 870ºC, which was interpreted as being due to the presence of zirconium in solution retarding austenite grain growth by a solute drag mechanism

6 Effect of Zirconium on the Mechanical Properties of steels.

The earliest investigation on the effect of zirconium on the mechanical properties of carbon steels, was reported by Feild [2], who compared the data obtained from an 0.70%C steel with and without a zirconium addition, after quenching from 825ºC into water and tempering between 370ºC and 600ºC.While the steel composition is beyond that considered for microalloyed steels, the results taken from his paper and presented in Table 11, are of interest. Here it can be seen that the zirconium addition results in a substantial improvement in ductility at all tempering temperatures, but that following tempering above 370ºC, the strength shows a progressive slight decrease with increasing tempering temperature to 600ºC.

Tempering temperature ºC	Zirconium %	Tensile strength (UTS) MPa	Yield strength (YS) MPa	El 5cm %	RA %	Brinell hardness

370	nil	1363	883	5.2	6.6	433
	0.13	1566	1282	8.3	23.3	414
410	nil	1428	1242	7.5	22.9	418
	0.13	1371	1195	12.7	45.8	407
440	nil	1362	1185	8.5	30.0	387
	0.13	1265	1103	13.0	46.0	388
540	nil	1013	889	14.7	39.4	298
	0.13	970	843	18.9	48.2	288
600	nil	880	759	19.6	51.2	238
	0.13	863	728	21.3	54.7	233

Table 11 Mechanical properties of 0.70%C steel with and without zirconium. Quenched into water from 825ºC and tempered at the temperatures indicated, after Feild [2].

In his second paper, Feild [73] considered that the improved ductility in the zirconium containing steels was associated with the precipitation of ZrS_2, which replaced MnS found in the zirconium free steels. On the other-hand, Crafts and Lamont [126] found that zirconium additions up to 0.06% produced relatively small changes in the mechanical properties of oil quenched carburized 0.10%C-1.5% Cr steels. They made no observations on microstructure in their work. Research in the 1950's by Masayoshi [124, 125] mentioned earlier, recorded improvements in the mechanical properties in steels that had been normalized and tempered at high temperatures. Other reports on mechanical properties include work by Falce et al [127], who as part of an investigation into the effect of zirconium on the weldability of niobium HSLA steels, tested samples with additions of 0%,0.07% and 0.11%Zr and concluded that 'the as –rolled yield (~500MPa) and tensile (~600MPa) strengths were practically unchanged and unaffected by the presence of zirconium'. This conclusion is supported by Xi et al [4]

who explored the effect of five levels of zirconium in the range 0.00 to 0.06% in a 0.01% Nb steel containing 0.09% C, 1.42% Mn and 0.0003 to 0.0005% N, on the mechanical properties and toughness of microalloyed steels. The experimental steels were vacuum melted, hot rolled and normalised at 930ºC for 1hr followed by air cooling. The lower yield strength (LYS) was invariant with composition to 0.03%Zr, at about 335MPa, but decreased to 320MPa after the 0.06%Zr addition. The ultimate tensile strength [UTS] increased from 500MPa to 510MPa as the zirconium addition increased from 0.02%. This percentage must be within the UTS error resulting from testing, but no errors were considered in this work. Only minor changes were recorded for the ductility. The main conclusions from the papers cited above which concern mechanical test results, is that they show very little change with small additions of zirconium.

Akbarzadeh et al [128] compared selected properties and microstructure from a plain carbon steels, microalloyed steels containing 0.06%C, 0.0045%N of two levels of zirconium,0.0055 and 0.02% and those containing 0.01% and 0.10% zirconium. The nitrogen level was not given in this latter case. The steels were investigated in three conditions, as-cast and homogenised at 1000ºC for 6 hrs, austenitised at 950ºC for 2hrs and quenched, and tempered at 450ºC for 4hrs followed by air cooling. The tempered steel containing 0.01%Zr showed the greatest UTS, YP, El% and RA%.XRD results for this steel and indicated that ZrN and ZrC precipitates were present in the as-cast specimen, but only ZrN precipitates after homogenisation or after tempering.. However, no crystallographic data were given to support these results. The presence of separate ZrN and ZrC precipitates is unexpected, bearing in mind Goldschmidt's [45] conclusions on mutual solubility of these compounds. The paper also contained an EDX spectrum obtained from a~1μm size particle in the 0.005% Zr tempered steel

contained a Zr_L peak, but made no comment about the absence of C_K or N_K lines. Precipitates of 1μm in size are too large to contribute to dispersion strengthening, but could restrict grain growth. No grain size data was presented. A second paper [129] published five years later, which omitted to cite the first paper[128] and has a slightly different spelling of the name of the first author, compared the 0.005%Zr steel to the zirconium free steel , but adds nothing new and repeats the earlier conclusions. Neither paper helps to unravel the role of zirconium in microalloyed steels as both avoid detailed comparison and omit important data. The conclusions should be treated with caution.

Other research has explored the role of zirconium in combination with the other transition metals niobium, titanium and vanadium, singly or in combination. One of the earliest papers to compare the roles of niobium, vanadium and zirconium in weldable controlled rolled microalloyed steels, ~0.18%C,~ 0066 ± 0.0008%N was by Heisterkamp et al [130,] and Meyer et al. [131] They investigated 19 steels,14 of which contained zirconium, with either single additions at levels of nominally 0.043%0.057%,0.072%, or in combination with two levels of niobium,0.020% or 0.035%.These were compared with five vanadium-zirconium steels arranged in two groups, one of three steels based on 0.030% V containing respectively, 0.019%,0.035% and 0.057%Zr, and a second of two steels with 0.049%V, and 0.053%Zr or 0.092%Zr.The steels were examined in the as-rolled and normalised conditions. Little effect of zirconium additions were found on the strength of the niobium –zirconium steels, the as- rolled strip having a yield strength of ~500MPa. A decrease from 460MPa to 420 MPa was found when a zirconium addition was present with 0.030-0.050% vanadium. This data will be considered along with that on toughness later in this review.

It was the same basic steel composition as that of Heisterkamp et al [130,] and Meyer et al. [131] which had a strong effect on the formation of zirconium phases in two Zr-Nb steels was considered by He and Baker[26]. While most of the work discussed above concerned steels on which the authors do not comment on the nitrogen level, the two niobium zirconium steels with compositions shown in Table 12 contained deliberate additions of nitrogen to give hypo and hyper-Zr steels, described respectively as N1and N2. The work compared the properties and microstructural data given in Table 13 following controlled rolling to a thickness of 16mm

Steel	C	Si	Mn	P	S	Al	N	Nb	Zr	Zr/N
1	.018	.40	1.45	.012	.004	.036	.0080	.018	.022	2.75
2	.100	.40	1.46	.012	.003	.041	.0039	.017	.060	15.38

Table 12 Chemical composition (wt%) of nitrogen steels investigated by He and Baker[27]

Steel	LYS (N/mm^2)	27JITT (°C)	Grain Size ($mm^{-1/2}$)	Pearlite (%)	Bainite+Martensite (%)
1	378	-110	11.8	1	0
2	403	-50	12.1	12	4

Table 13 Mechanical properties and microstructural parameters [27].

A 15 Nmm^{-2} difference in the LYS between N1 and N2 was explained by using a Hall-Petch analysis which showed that with the same solid solution strengthening and similar dislocation density for the two steels, the grain size difference accounts for only 6 Nmm^{-2},which is within experimental error. As fine NbC particles (<10nm) were identified in both steels, the increase in the LYS for N2 was considered to result from the precipitation of ZrCN particles (<100nm), as 0.035%Zr remained available after combination with all the nitrogen. The average dispersion strengthening

coefficient (K) of NbC given by Morrison [132] is 1500Nmm^{-2} per wt% .The present work gives a dispersion strengthening contribution from the fine ZrCN particles of 19Nmm^{-2}, which suggests a corresponding K factor of 550 Nmm^{-2}per wt.%. This is a lower value than that found in niobium steels, and is thought to be due to the higher overall precipitation temperatures of ZrN and ZrC than those of NbN/NbC, resulting in the larger observed particle size, giving a lower strengthening contribution. In the hypo Zr-SteelN1, no intermixing of the zirconium compounds with the Nb-N system was observed, the Zr-bearing precipitates being predominantly ZrC. In the hyper-Zr-SteelN2, some intermixing of the two systems was observed, and zirconium -bearing precipitates were predominantly ZrC. The interaction between Zr, Nb and N in this work, was found to be much weaker than between Nb, Ti and N, previously reported.

An interesting, but unsatisfactory paper by Michel and Buršak[133] compared the mechanical and toughness properties of two controlled rolled microalloyed steels,

Steel A -0.09%C,1.49%Mn,0.024%Al,0.031%V,0.04%Nb.0.022%Zr and

Steel B-0.088%C, 1.16%Mn,0.024%Al,0.035%V,0.013%Nb.

The percentages of nitrogen and oxygen were not given, neither were any details of the controlled rolling schedule or the metallographic methods. The microstructure was characterized, producing for Steel A an average grain size of 3.2μm and an interparticle distance of 85nm, while for Steel B an average grain size of 3.7μm and an interparticle distance,75nm. Michel and Buršak[133] undertook a modified Hall-Petch analysis [30,96] using this data to estimate the contributions to the measured proof stresses for Steel A of 540MPa and Steel B of 520MPa.The respective contributions through grain size were 265MPa and 246MPa and for dispersion strengthening via the interparticle distance data above,110MPa and 140MPa respectively. These two contributions constituted over 70% of the calculated proof stresses which were in good agreement with the measured data. Both steels were also

found to have good ductility and toughness. However, no details of the precipitate composition was given, and therefore no conclusions were provided on the role of zirconium, niobium or vanadium. A more recent study by Mintz et al[134] of the behaviour of nitride formers in a plain carbon steel , included zirconium additions. The steels were based on a composition of Fe-0.2C-0.02S-0.02P-0.6Mn-0.3Si,with Zr in the range 0 to 0.014 and total N 0.0050 to 0.0074, all in weight percent. The eight 18Kg laboratory vacuum melted steels were hot rolled to 12mm thick plate with the FRT being 1000 to 900ºC.In addition to the determination of the yield stress and 54J ITT, the free nitrogen remaining in solution after hot rolling and air cooling was determined by a strain ageing technique described in the paper, and related to an increase yield stress, ΔY. The results are given in Fig 18.It was concluded that: 'Zr up to the stoichiometric composition (SC) for ZrN, (0.034%), gives good impact behaviour but the yield strength continually decreases'. Beyond SC, the impact behaviour starts to deteriorate, which was 'probably occurs because coarse zirconium carbonitrides are now able to form at grain boundaries'. While Arrowsmith[85] identified zirconium carbonitride in the matrix, his is the only reported identification of this compound in a steel. The optimum zirconium addition for good impact properties found by Mintz et al [134] agrees with that of Heisterkamp et al[130], but is lower than that of Bucher et al [90]. No characterisation of the precipitates was undertaken in this work. Fig 18 also shows that the yield decreases from 315 to 270MPa.

The influence of niobium, titanium, vanadium, and zirconium additions in 0.06%C, 1.4%Mn ~0.01%N microalloyed steels, processed by a simulated thin slab casting direct charging route was considered by Li et al. [30] For an 0.1% V-0.008%Zr steel, equalized at 1200ºC and end cooled at 642ºC, values of LYS, 525MPa ,UTS, 655MPa, El,~22% and Charpy toughness of 13JTT at -80ºC were recorded. The average ferrite grain size was 4.8μm and the dispersion plus dislocation strengthening contribution to the LYS, 145MPa. Optical

microscopy showed that for the zirconium addition of 0.01%, a ferrite-pearlite structure was observed, but with an increase in Zr to 0.03%, the lamellar pearlite structure became discontinuous, and the at 0.06%Zr, spheroidal carbide was present. In addition, VN cuboids at prior grain boundaries and small VN particles within ferrite grains were analysed by PEELS and the results given in Fig 19.It is interesting to note that the yield stress data and dispersion, plus possibly dislocation, strengthening contributions here are similar those given above for the steels investigated by Michel and Buršak.[133] More recent research undertaken by Wang et al [6] investigated two ~0.07% carbon steels with Al contents of ~0.034%, one (S1) containing 0.017%Zr,0.0039%N, giving a hypo Zr/N ratio = 4.36, the other (S2) containing 0.040%Zr,0.0037%N, with a hyper Zr/N ratio = 10.8. 50Kg ingots were vacuum melted, homogenized at 1200ºC for 2h, and then thermo-mechanically rolled to 20mm thick plate, followed by two – pass water cooling to ~520ºC and finally air cooled to ambient. The authors studied (1) the effect of the Zr/N ratio on the mechanical and toughness properties and (2) the thermal stability of ZrN particles at high temperatures. It was found that the Zr/N ratio had a significant effect on the impact toughness, the 27JITT increasing from -78ºC for the hypo Zr/N ratio steel to -55ºC for the hyper Zr/N ratio steel. They verified the precipitates by TEM/SAED in both steels as cuboidal ZrN particles, with those in S1 having a mean size of 25nm compared with 100nm mean size for those measured in S2. Holding for 1min after heating to 1350ºC, the precipitates coarsened to 50nm for S1 and 20nm for S2.This suggested that the ZrN particles found in hypo Zr/N steel S1 had the potential to inhibit grain growth in austenite. One anomaly in their work is that the EDAX spectra they show for both S1 and S2 steels have significantly higher peaks for carbon than nitrogen. The bright field images of these small particles do not reveal any significant sign of contamination and it is assumed that the carbon arising from the carbon replica is stripped out of these spectra. This would suggest

that the particles are indeed zirconium- high carbon containing carbonitrides and not pure zirconium nitrides as claimed in their paper.

The above discussion of several papers highlights apparent disagreements in the literature concerning the effect of zirconium on the mechanical properties, depending on the level of the addition and the heat treatment undertaken. However, much more agreement has been reached on the effect of zirconium on the notch toughness following the initial work by Feild[2].A publication by Egan et al [135] in 1933, showed that zirconium in the range 0.11% to 0.97% was more effective than vanadium in improving the impact strength of 0.2%C steels, as seen in Fig 20. This effect was later supported by the work of Halley[24] considered previously. While much of the earlier research on zirconium additions to low carbon steels carried out during the 1930's and 1940's reported the favourable effect on notch toughness and ductility of steel [24,135,136] more recent publications have ascribed these improvements to a control of sulphide morphology. [17,90,137-139] However, economically, a more attractive approach is to modify the sulphide inclusion composition, so as to reduce its plasticity at hot rolling temperatures, resulting in enhanced impact toughness in a transverse orientation.

7 Toughness and ductility improvements through sulphide modification

While many workers have shown that additions of zirconium have little effect on the tensile properties, changes found in the ductility and Charpy toughness are well documented. For example, Xi et al [4], found significant differences for the Charpy V-notch toughness energy, which was the lowest at all test temperatures for 0%Zr and 0.06%Zr steels, while the steels

containing 0.01 to 0.03%Zr had values ≥ 80J for test temperatures above -50ºC, the lowest value of 70J at -60ºC.

To understand the role of zirconium on toughness, it is first necessary to consider the effect of sulphides on toughness in non-zirconium steels. The need for higher levels of impact strength in structural steels and the requirement for cold formability in strip products have focussed attention on the development of cleaner steels and inclusion shape control[131, 140]. The main inclusions of concern in steels are oxides, silicates, and sulphides.[141-142] A study by Charles and Uchiyama[143] concluded that little or no plastic deformation of silicates occurs below 900ºC, which explains the more deleterious influence of sulphides compared to silicates at rolling temperatures, Fig.21. Gove and Charles[141] related the resistance to deformation of inclusions through in-situ high temperature microhardness data. They determined the inclusion and steel matrix hardness at different temperatures for a number of real and artificial inclusion systems, to obtain the relative plasticity ν, which was defined as the ratio of the inclusion true strain to overall matrix true strain, where

$$\nu = 2 - h_i / h_m \quad (0 \leq \nu \leq 2) \qquad (16)$$

h_i is the inclusion hardness and h_m is the matrix hardness. Baker at al [142] considered the hardness of both silicate and sulphide inclusions. Fig 21is complied from the data they collated, and clearly shows that the variation in ν with temperature of a type I MnS inclusion. A peak occurs where the matrix is ferritic followed by decrease in ν at the transformation temperature, a slight increase in ν in the wholly austenitic region, and finally a decrease as the temperature increases to 1200°C.The curve for large two phase silicates shows that at 1000°C ν = 1,decreases rapidly around 900°C to zero at 800°C,where ν of 0.1 is significantly less than of the sulphide, 0.7 .

As pointed out by Baker and Charles [144], one of the reasons for the confusion surrounding the deformability of MnS inclusions is that they can be precipitated from the molten steel in three different morphologies (types I, II, and III), first described by Sims [12-16] in cast steels and later considered by Lichy et al[17] in as-rolled (wrought) steels.

Globular type I sulphides are distributed randomly with a wide range of sizes, often duplex with oxides. They are formed in steels such as silicon-deoxidised steels where the oxygen contents are relatively high, in excess of 0.02wt%, and sulphur contents relatively low, so that they precipitate from the liquid phase at an early stage of solidification. The nuclei in silicon - deoxidised steels are considered to be particles of FeO or MnO, as both are isomorphous with α-MnS and wetted by it. [133] Single phase type I MnS inclusions analysed by Baker and Charles [144] had a mean composition of 59.8% Mn, 35.4% S, 3.0%Fe, together with small amounts (<1%) of chromium. Duplex regions indicated a mean composition of 50.9%Mn, 10.3%S, 1.7% Fe with the balance being oxygen.

Type II eutectic sulphides are encountered at primary grain boundaries in a dendritic pattern. They occur in steels where the oxygen content is below 0.01wt% and the sulphur solubility high. This situation can be found in steels thoroughly deoxidized with aluminium, titanium or zirconium. However, it is considered that the oxides precipitated in this case, are too small to be effective nuclei for MnS, which means that the sulphide phase precipitates with high supercooling in the last regions to solidify, i.e. in the primary grain boundaries. Between 0.01 and 0.02 wt. % oxygen may be found either or both of types 1 and II sulphides. [10,17, 143]

Low oxygen contents are also necessary for the formation of type III MnS. Whereas the oxygen content is a sufficient condition for the formation of type II from type I, but the presence of other alloying elements is necessary to ensure the production of type III. The most effective of these elements are carbon, silicon and aluminium, but they may also be augmented by phosphorus, calcium, chromium and zirconium. Type III MnS precipitates are

therefore unlikely to be found in plain carbon steels. They are precipitated earlier than type II, usually as monophase angular particles, as described by Little and Henderson. [86] Karmazin [146] considered that oxides are the nuclei for these sulphides. For example, in the case of deoxidation with aluminium, the Al_2O_3 particles are considered to be sufficiently large to serve as nuclei. On these nuclui, Al_2S_3 which is both isomorphous and wets Al_2O_3, will precipitate. According to Kiessling et al [48], further precipitation of sulphides occurs through absorption of the Fe-Mn-S phase on the growing particles, giving type III sulphides. A detailed chemical analysis of the three types of MnS sulphide was reported by Kiessling et al. [48]Their data is reproduced in Table 14.The Fe wt% is given as a range for MnS types 11 and 111.

Sulphide type	Composition (wt%)				
	Mn	Fe	Al	S	total wt%)
MnS (theory)	63	-	-	37	100
I	60	1	no indication	37	98
11	60	1-6	no indication	37	98
III	60	1-3	no indication	37	98

Table 14 Mean composition of the characteristic sulphide types [48].

Kiessling et al [48] and Lichy et al [17] must have been among the first to use electron probe microanalysis (Cameca EPMA) to chemically analyse micron sized particles, both in situ and following isolation by electrolytic extraction. The analyses given in Table 14 are mean values from six determinations. All three types of sulphide consisted of α-MnS with a low iron content and were found to have, within experimental error, identical compositions, crystal structure and unit cell dimensions. Aluminium was not found, but could not be detected with this instrument at levels below 0.3-0.5 %.However, these observations led the authors who

disagreed with Karmazin [146], to conclude that 'it was unlikely that Al_2O_3 was active in the formation of any of the three types of sulphide, and that it is more likely that the precipitation of the sulphides is associated with oxygen content in the steel.

The importance of inclusion shape as a major factor influencing the anisotropy of Charpy shelf energy in wrought products was shown by Vogels et al[18], Dahl et al[19], and Wahlster et al. [20] A useful succinct review of the background to sulphide shape control by additions of zirconium has provided by Pollard. [138] He reminds us that 'ductile fracture of metals and alloys is initiated by the nucleation of voids when a non-metallic inclusion cracks or its interface debonds from the matrix. The voids grow and coalesce until complete failure occurs'. A hyperbolic relationship between ductility, as measured by the total elongation, and the volume fraction of inclusions was shown to apply initially for inclusions in copper by Edelson and Baldwin[147] and confirmed for steels by Gladman et al.[148] In steel processed by rolling, inclusions tend to elongate in the rolling direction, thereby decreasing the interparticle spacing in the rolling direction and providing an easy path for fracture. The elongation of inclusions into planar arrays causes anisotropy of toughness and ductility, and both manganese sulphide and stringers of oxides are damaging in this respect. In steels, directionality of mechanical properties manifests itself in lower impact notch toughness when the fracture plane is parallel to the rolling direction as found by Mihelich et al. [22] Tensile, impact and bend specimens with their principal stress axes transverse to the rolling direction therefore exhibit less ductility, toughness and bendability than those with their principal stress axes parallel to the rolling direction. However, the problem is largely eliminated if the inclusions are present as small isolated non-deformed particles.[86] The volume fraction of inclusions is related to both the steel- making practice and the steel chemical composition. Franklin and Tegart [21] showed that lowering the sulphur content from ~ 0.02 to 0.005% resulted in a marked increase in the ductile impact energy for a number of low alloy steels of

varying microstructures, Fig 22. In practice, this approach is not always possible to implement. The degree of anisotropy depends on the rolling temperature [146, 149] the amount of deformation [19,142,146] and the deoxidation .practice. [10, 17, 150,151]

Earlier work on the effect of deformation temperature by Scheil and Schnell [152] indicated that initially, MnS deforms to the same extent as steel. However, more detailed work by Maunder and Charles [153] observed that sulphides deformed little above 1200ºC, but became more plastic with decreasing temperature until they approached the deformability of the matrix at 900ºC. After hot rolling, Mardinly et al[154] have shown that MnS inclusions in steel, Fig 23, tend toward an ideal <100> (001) orientation. Baker and Charles[144, 151] chemically analysed manganese sulphides by electron probe microanalysis and determined their size in detail by in both the cast and as –rolled state. The latter also confirmed the observations of Sims and Dahle [12] , Dahl et al[19] and Crafts and Hility[150], that the morphology of the sulphides is controlled by the steel composition, in particularly the degree of deoxidation, and that the deformation of the sulphide phase during rolling in the temperature range 850-1300ºC increases in the order of types I,II and III. Sulphides of type I were only slightly deformed, sulphides of type II formed closely connected groups of elongated inclusions, while sulphides of type III were the most easily deformed and elongated into long stringers. Based on the results of impact tests on cast specimens, Sims [16], concluded that type I sulphides were highly desirable in steel, that type II should be avoided, while type III sulphides, although not as desirable as type I, were preferable to type II, for a given sulphur level.

The influence of sulphide shape on the machinability of high sulphur free- cutting steel bar was investigated by Paliwoda [155] , who showed the beneficial effect of globular sulphides, as opposed to stringer sulphides. Knowledge of this work [151] and also that published earlier by Sims et al[13], encouraged Lichy et al [17] to investigate whether the desirable oval type sulphides could be obtained in a rolled product when various deoxidizers, or other elements with a high

affinity for sulphur, were added to steel. Their previous work on sulphide shape control in steels with and without zirconium additions had shown that the 'heavy stringer sulphides which occurred in the non-zirconium steels were changed to an oval type when 0.10 to 0.18%Zr was present. Here they examined the influence of mould additions of aluminium, zirconium and Misch metal as a means of eliminating a differential etch pattern caused primarily by a greater frequency of stringer sulphides.[17] They concluded that 'additions of 0.03 to 0.14%Zr completely eliminated this pattern in the rolled product, which was accompanied by a change in the stringer type manganese sulphides into barely ductile oval sulphides, consisting mainly of zirconium and manganese'.

Influenced by this work, Bucher et al [90], in an investigation into the ductile fracture resistance of ferrite- pearlite steel, paid particular attention to the effect of zirconium on inclusion morphology. Twenty three aluminium -killed heats were prepared in a laboratory air induction furnace under a protective argon atmosphere. The sulphur content was varied from 0.004 to 0.038%, while zirconium was in the range 0.030 to 0.14%. In the as-rolled state, the sulphide morphology was in an elongated form in steels with below 0.05%Zr, which was considered to be due to preferential oxidation of zirconium. Progressively less elongated, rounder inclusions were obtained as zirconium was increased to 0.10%, with less improvement in the ductile fracture above this level. EPMA revealed that all the sulphide inclusions formed a (Mn, Zr) S compound. To raise the ductile impact resistance, the authors recommended a zirconium addition in the range 0.05-0.10%.

Reviewing the effects of microalloying due to sulphide forming elements, Ejima [156] made the point that even with such elements as titanium, zirconium, calcium and rare earth alloys, to guarantee the complete precipitation of these sulphides formed in preference to MnS, required a reduction in the sulphur composition of the steel, as shown earlier and discussed above in the work of Franklin and Tegart. [21]

The effect of a zirconium addition on the sulphide shape in three ferrite-pearlite ~0.011%C Al killed steels was studied by Mihelich et al. [22] The first two steels were without a zirconium addition, but contained 0.020%S and 0.012%S respectively, while the third contained 0.09%Zr and 0.018%S.The tensile properties and grain size of all three steels were similar, but the cold formability and notch toughness in the transverse direction of the zirconium treated steel was superior to the other two steels. Microstructural studies showed that the zirconium addition had a significant influence on the globularisation of the sulphides, which were observed to be (Mn, Zr)S particles nucleated on a ZrN core,Fig24. Mihelich et al [22] also considered that the aluminium deoxidation practice used in their experiments was effective in removing oxygen, and the allowed the formation of the next stable compound, ZrN, predicted in Figs 1 and 2, and seen optically as lemon yellow cubic particles. Zr(C,N) particles are known to have an orange colour, but these were less frequently observed [22] , as they are promoted with additions of Zr ~0.15%.The sequence of nucleation events was also considered by Mihelich et al. [22] They concluded that ZrN, with a melting point of ~3000ºC, formed as solid particles, ~5μm in size in the molten steel, and in some cases, acted subsequently as heterogeneous nucleation sites for Zr C, N) precipitates. Large ZrN particles were also observed to exist independently in the matrix. In their studies, to achieve sulphide shape control, arbitrarily defined by inclusion shape factor, length to width ≤ 0.2, they concluded that sufficient zirconium must be added to remove nitrogen, allowing a minimum of 0.02%Zr to combine with sulphur. To effect the change from elongated to globular sulphides in the fully killed steel containing 0.015-0.020%S, Mihelich et al [22] found that the amount of zirconium (recovered) was related to the total nitrogen by,

$$\%Zr_{tot} = 0.02\%Zr + 6.5(\%N_{tot}) \qquad (17)$$

where the coefficient of the nitrogen is fixed by the stoichiometry of zirconium nitride. Because zirconium removes nitrogen from solid solution, zirconium treated steel, in addition

to having improved sulphide shape, is completely free from strain ageing, strain ageing embrittlement, and blue brittle behaviour. [11] Mihelich et al [22] also pointed out that since zirconium is such an effective denitriding element,(for 0.09%Zr, the nitrogen remaining in solution is ≤ 0.002%), the possibility of obtaining dispersion strengthening by other nitrides such as vanadium nitride in V-Zr steels, which has a lower affinity for nitrogen, is ruled out. However, in practice this may not be the case when zirconium is added to high nitrogen, ≥0.01%, and low sulphur, ~0.005%, steels. [6, 30]

One of the most detailed investigations of the effect of zirconium additions in low carbon steels on the Charpy shelf energy was undertaken by Little and Henderson [86].They produced two series of experimental 88Kg vacuum melted casts to study the effect of varying zirconium additions on the mechanical properties of C-Mn steels, through their influence on the sulphide inclusion morphology. The steel compositions, in weight percent., are given here in detail to highlight the extent of the work.

In the first series, the compositions were: 0.16-0.23%C, 1.2% Mn, 0.23%Si, 0.02-0.032%S, 0.02-0.03%Al, 0.0027%N, with 0,0.02%,0.04%,0.055%,0.100%,0.175%Zr, while in the second series, the compositions were: 0.16-0.17%C, 1.26%Mn, 0.030%Si, 0.030%S,0.02-0.024%Al,0.0049-0.0068%N, with 0.03%,0.05%,0.07%,0.08%,0.09% and 0.11% Zr. After holding for 1hr at 1290ºC, the ingots were rolled to 13mm thick plate in an experimental rolling mill, each plate receiving 50% reduction below 900ºC.The metallographic examination of the melts revealed no evidence of oxide inclusions, the majority of the inclusions observed being sulphides. Occasional ZrN cuboids were found in the zirconium containing casts. In the 0.02%Zr cast steel, mixed eutectic type Π MnS and angular type III, (Mn, Zr) S particles were present, which deformed after rolling. In the steels containing between 0.02% and 0.055%Zr, isolated angular (Mn, Zr) S particles were present, which were unaffected by rolling. However, when the zirconium addition reached 0.10%, in

addition to the isolated angular (Mn, Zr)S particles, a light pink/grey grain boundary phase, identified by electron microscopy selected area diffraction as $Zr_4C_2S_2$, which exhibited little or no plasticity, was present.[85] This phase did realign parallel to the principal rolling direction. Its mechanism of formation appeared to be through the initial precipitation of thin ZrC films at austenite grain boundaries, which thickened as sulphur partially replaced carbon.

In the second series of experimental melts, the steel- making procedure was modified to mirror that of commercial practice used in the 1970's, with a higher nitrogen content ,~0.006%.Oxide particles were observed. However, the inclusion behaviour was similar to that recorded for the first series. Fig 25 shows the effect of the zirconium addition on the Charpy shelf energy for the second series of experimental melts.

An extensive review of the literature shows that not all the investigations on sulphide shape control in high strength low alloy (HSLA) steels have decided in favour of zirconium additions. Of their chosen contenders for sulphide shape control, which were titanium, zirconium, calcium, magnesium and rare earth alloys, based on detailed thermodynamic considerations, Luyckx et al[157] eliminated zirconium on the grounds that with a high affinity for nitrogen, together with a tendency to form coarse particles, these factors precluded its use in hot rolled steels strengthened by finely dispersed nitride precipitates. On the other hand they also state that despite the high stability of ZrC, there is no evidence that Zr-C interactions adversely affect mechanical properties for carbon levels below 0.2%.However, at higher carbon levels, and for zirconium concentrations in excess of 0.1%, lath shaped crystals of ZrC and $Zr_4C_2S_2$ can cause embrittlement [52, 85], as mentioned earlier. It is interesting to note that two of the authors, Bell and Korchynsky, involved in the Luyckx et al[157] publication, were co-authors with Mihelich et al [22] in a paper published the following year, which advocated controlled additions of zirconium to improve the ductility of ferritic steels

which were to be bent by a cold-forming operation. They also considered globular sulphides to be important in HSLA steels which are normally subject to brake press forming.

It is most probable that the first detailed study of inclusions in steel, which was based on very high quality optical metallography, was undertaken by Portevin and Castro. [89] As part of this work, they may have been the first to attempt to separate the compounds in steel commonly described as inclusions, from those described as precipitates. They defined compounds based on silicates, aluminates, oxides and sulphides as inclusions, while borides, nitrides, carbides and possibly phosphides, were defined as 'metallic constituents', which we now regard as precipitates. Part IVB of this study includes their observations on inclusions associated with zirconium, some of which have been superseded by later work. For example, they discussed the observations of Urban and Chapman[88] on zirconium compounds. At the time of this publication, many compounds were characterised by the colour and morphology of the crystals. Based on the description given by both sets of workers, they dispute the conclusion that these are zirconium oxysulphides [88], but consider them to consist of small ZrN nuclei surrounded by ZrC. Now we would probably expect them to be characterised as Zr(C, N) particles with varying N/C ratios from centre to surface, based on the known mutual solubility of the carbide and nitride. [45]

Significant improvements in the impact toughness were found when the zirconium addition exceeded about 0.05% by Heisterkamp et al[130] and Meyer et al. [131] For the 19 steels mentioned in Section 6 above, they plotted the length and hardness of the sulphide inclusions as a function of zirconium, Fig 26. Above ~05% Zr, the inclusion length decreases significantly while the corresponding hardness increases, as expected from previous studies[22]. Hence it is considered that knowing the nitrogen content, one can forecast quite accurately the minimum content of nitrogen necessary to influence sulphide formation. For steels with 0.006%N this would be about 0.04%Zr. Fig 27 compares the impact toughness of two sets of

three steels, one set without a zirconium addition, the other with zirconium alone or in combination with niobium or vanadium. Steel8, with 0.072%Zr showed the highest toughness values. The effect of zirconium additions on the impact transition temperature of the combined additions is shown in Fig 28. Heisterkamp et al [130] and Meyer et al [131] then considered what toughness (and strength) were attainable by various alloy combinations for 0.006%N steels. Of the elements considered, only titanium with zirconium gave both an increase in tensile strength and transverse impact value, the latter only being increased along with a marked increase in yield strength. However, the dispersion strengthening which raises the yield strength, adversely affects brittleness. Hence, titanium, despite its relatively favourable price, they considered could not be regarded as an ideal alloying agent along with zirconium. Examining the two other combinations, niobium plus zirconium retained its strengthening and toughening effects, whereas with vanadium and zirconium, these effects are reduced. The reasons for these variations were considered to be that niobium, which precipitates as a carbon rich carbonitrides, is hardly affected by the formation of zirconium nitride, and dispersion strengthening and grain refining reach completion, even in the normalised condition. On the other hand, as far as vanadium is concerned, nitrogen at the 0.006% level, which is important for vanadium precipitation, is not available as it is already combined with zirconium.

The work of Li et al [30] has been referred to above, in which zirconium was studied in high nitrogen vanadium steels containing0.062%C,0.022%Al,0.01%N,0.010%V and 0.008%Zr. Because vanadium and zirconium nitrides are not intersoluble[45], it was considered that ZrN would form at high temperatures, but that only part of the nitrogen would be taken up by zirconium, leaving vanadium to combine with the remaining nitrogen in austenite at lower temperatures . From the steel composition, the solubility product for ZrN, $\log_{10}k_{ZrN}$ is -4.1.Fig7 indicates that ZrN should start to precipitate in the liquid phase. The stoichiometric

ratio is Zr/N=6.5, so that 0.008%Zr combines with 0.0012%N to form ZrN, assuming no vacant sites and that ZrC or Zr(C,N) are not formed. The remaining 0.0088% nitrogen is available to form VN as a separate compound [45]. The solubility product for VN, $\log_{10}k_{VN}$ is -3.06.Fig 7 indicates that this compound should start to precipitate in austenite below about 1200ºC. ChemSage calculations which consider the complex interactions of C, N,V and Zr, plus the influence of Si and Mn , showed that 20% of the total vanadium in the V-Zr steel composition was present as vanadium carbonitrides at 900ºC, and this decreased to zero around 1080ºC. Small particles within ferrite grains which could provide dispersion strengthening, were observed. PEELS analysis was undertaken by Craven and Wilson, as part of this study, on five precipitates of 8 to 11 ± 1nm in size. The results shown in Fig 19, provide convincing evidence from the chemical analysis of nitrogen and vanadium that they are essentially vanadium nitrides.

This approach of considering nitrogen as propitious alloying element commenced with the development of microalloyed steels utilizing NbN for controlling grain growth, and even earlier, the realisation that AlN could perform the same role. Previously nitrogen in steel was regarded as an element to be treated with caution.

8 Effects of Zirconium on Machinability

Improvements in machinability associated with small increases in sulphur in steel are well known. However, it has also been established that while resulphurisation is advantageous to machinability it can have a detrimental effect on ductility. [158] This view is supported by the work of Bhattacharya[139], who found that the addition of sulphur has dual effects. He found that machinability measured in terms of cutting energy per unit volume of metal machined (the specific cutting energy), increased linearly with increasing sulphur in the range 0.006 to 0.11%.The ductility parameters, reduction of area and impact shelf energy on the other hand, decreased significantly with increasing sulphur. The rational for the addition of zirconium

(0.15 to 0.19%), was based on the well established observation that it resulted in globularization of the sulphide inclusions which coincided with a significant improvement in the transverse mechanical properties and that secondly, globular sulphides had been reported to enhance machinability.[152] Bhattacharya[139] studied the effects of addition of zirconium in conjunction with sulphur on the machinability and mechanical properties of a laboratory produced AISI 1045 steels. While this is a class of forging quality medium carbon steel, the work is of interest because of the 0.15-0.19%Zr addition added to globularize sulphide inclusions. It was found that the impact ductility in the transverse direction was significantly improved by a zirconium addition as 'effective zirconium, *EZ*' ,calculated from the following equation:

$$[EZ] = wt\ \%\ Zr - 91/32 wt\%\ 0 - 91/14\ wt\ \%N \qquad (18)$$

For globular sulphides, *EZ* >0.02% [153], which here was 0.07 to 0.09%.Both angular orange or yellow coloured (zirconium nitrides) and grey (sulphides) particles were observed by optical microscopy. Analytical SEM was used to produce X-ray maps of the 'sulphide' inclusions, which showed that they were a combination of both manganese and zirconium sulphides, as reported by others.[17, 149] However, quantitative analysis of the inclusions was not reported.

A general loss in ductility with increasing sulphur was found in the zirconium steels. In the high sulphur steels (0.12%), small losses in both reduction of area and total elongation were recorded in the zirconium steels. These results disagree with those of Yamaguchi et al [159] who observed no effect on the longitudinal tensile ductility but an improvement in transverse ductility. On the other-hand, Arakawa et al [160] showed no significant effect of zirconium on tensile ductility at low zirconium contents but a slight deterioration at 0.18% zirconium. Bhattacharya [139] concluded that more work was required to resolve the effect of zirconium on machinability of steels in the presence of sulphur.

9 Effect of Zirconium on Weld Metal and HAZ

Falce et al [127] were probably the first to consider the effect of zirconium on the weldability of low carbon steels. They investigated Al- killed X-60 grade steels with a nominal composition of 0.15%C,1.35%Mn,0.034%Nb (N% not given) together with additions of 0.07% or 0.11%Zr, on the structural behaviour in the heat affected zone (HAZ) of welded HSLA steels compared to a zirconium free steel. HAZ continuous cooling transformation(CCT) curves were produced using a Gleeble machine to simulate welding cycles with cooling conditions in the range 800/500ºC and over 3 to 100secs,which covered ‘practically all those encountered in welding , including manual arc welding to automatic submerged arc welding’. It was found that when the cooling rate was such that a martensitic structure was formed (55ºC/sec), the HAZ was unaffected by the zirconium addition. However with 0.07 to 0.110%Zr in the plate, this extended the mixed martensite-bainite area to slightly slower cooling rates, decreasing from19ºC/sec to 14ºC/sec. The zirconium addition had almost no effect on the bainite-ferrite region. In the mixed martensite-bainite area, the hardness reached a maximum at a cooling rate of 27ºC/sec. The zirconium free steel recorded a hardness of 325Hv_{40}, corresponded to a martensite-bainite structure with over 70% bainite, whereas the hardness of 390 Hv_{40} for the 0.070%Zr steel represents a martensite-bainite structure with over 70% martensite. The authors found that the presence of zirconium seemed to have an effect on the weldability for cooling rates between 20 and 33ºC/sec.

While Falce et al [127] confined their work to the effect of only zirconium on weldability, Koukabi et al[161] compared the effects of zirconium with those of titanium and vanadium on submerged arc deposits. Their work[161] was prompted by the conclusions of Michelich et al [22], who found that zirconium additions had several beneficial effects through decreasing the volume fraction of inclusions, which resulted in improved transverse ductility and hot workability. They [22] also showed that sulphide shape and plasticity modification resulted in

an improvement in the weldability of steels. Koukabi et al [161] concluded that vanadium had a greater effect than zirconium on the increasing toughness in both the as-welded and stress relieved welds. It is well established that both TiN and ZrN particles have little solubility in austenite, as seen in Fig7. Titanium is known to decrease the soluble nitrogen content in welds by forming TiN particles, which in turn promote acicular ferrite found to be associated with improved weld toughness. Koukabi et al [161] had expected zirconium additions to behave similarly, but they found that ZrN particles did not promote acicular ferrite and the weld toughness was only slightly improved, due, they considered, to the removal of the soluble nitrogen. In other work, a brief report on an EU funded project, the role of boron, titanium, zirconium, aluminium and nitrogen in quenched and tempered weldable construction steels was investigated in Germany. Here a Zr-N ratio greater than 6.5 recommended to protect boron. [162]

In a more substantial paper, Pacey et al [163] summarized the general effects of weld microstructure on toughness, dividing them into two groups, depending on the test temperature: 'at low temperatures, $\leq$ -40ºC, the toughness may generally be increased by increasing the percentage of fine-grained acicular ferrite at the expense of either blocky proeutectoid ferrite or lath structures such as Widmanstatten ferrite side plates and upper bainite. At higher temperatures $\geq$ -20ºC, where fracture involves microvoid formation and coalescence, the volume and size distribution of inclusions is important in determining toughness.' Various other factors are known to influence toughness, including strengthening mechanisms, the fraction and distribution of other minor phases such as martensite-austenite (M-A) phase, the strain hardening coefficients and strain ageing. [164] Pacey et al [163] also studied in detail the microstructure of submerged arc welds of ~0.04%C steel containing~ 0.36% Mo and four levels of zirconium between 0.002 and 0.029%.They found that small amounts of zirconium initially slightly increased the percentage of acicular ferrite, but at a

level of 0.011%Zr and above, increased the percentage of bainitic laths and replaced inter-ferritic carbides with M-A phase. These effects were interpreted as being due to zirconium lowering the transformation temperature. In their work [163], zirconium additions were in general found to decrease the toughness particularly in the temperature range -30 to + 50ºC. This was due to a combined effect of an increase in the percentage of bainitic lath structure, an increase in yield strength and a decrease in the upper shelf energy, attributed to a change in the composition of the inclusions. An addition of 0.002%Zr increased the toughness at -40ºC, which they found was associated with the small increase in the fraction of acicular ferrite. However, at other temperatures, the toughness decreased due to the above detrimental factors.

The control of the grain shape and size in welded structures is particularly important in high heat input welding, which aims to improve the economics of the joining process by reducing the number of welding passes, and where thicker plate is to be welded, in such applications as ship-building, line-pipe and pressure vessels. High heat input welding can result in a coarse grain HAZ due to a longer time being spent at peak temperatures, which causes grain growth of austenite with a resultant deterioration in toughness. [165-167]Austenite grain size control in welded regions has been sought by several techniques involving titanium additions. [164] The most effective method involved the use of the titanium-boron and the titanium oxygen systems to generate plate-like intragranular ferrite in austenite grains, or the precipitation of TiN particles to pin austenite grains, thereby restricting grain coarsening. However, it has been found that partial dissolution of TiN near the weld bond reduces its effect. This has been overcome by the utilization of a TiN-MnS complex precipitate that is effective over a wide range of heat inputs, or by additions of zirconium.[164]The distribution of oxides after solidification during steelmaking and welding may be greatly affected by the interaction between oxides and the advancing solid/ liquid interface during solidification. Using

computer aided X-ray microanalysis, Sawai et al [23] compared the distribution of oxides in unidirectional solidified and controlled cooled steels containing 0.08wt-%C steels deoxidized with either 0.004wt-% Ti or an addition of 0.04wt-% Zr. The steels were quenched from 1480ºC, which was considered to correspond to the temperature just after the completion of solidification. Using SEM and EDX, oxides were identified as complexities of manganese silicate and Ti_2O_3 or ZrO_2, distributed in the dendrites. It was concluded that in the zirconium deoxidized steel, ZrO_2 distributed more uniformly than Ti_2O_3 in the titanium deoxidized steel. In both steels, oxides tended to be in the range 3 to 15μm in diameter, and the number of oxides whose diameter was above 10μm became bigger with greater fractions of solid. Liquid oxides that form as complex oxides in the titanium deoxidized steel are rejected by the solid/ liquid interface more easily than the solid oxides that are produced by zirconium deoxidization, because the interfacial energy between liquid oxides and liquid metal is smaller than that between solid oxides and liquid metal. [23] While not directly associated with welding, a paper by Fox et al [168] studied the dissolution rate of a number of oxides within the size range of 100 to 300μm, in a slag whose composition was chosen as suitable to simulate a mould flux used in continuous casting. The study found that dissolution rates of Al_2O_3, MgO, and $MgAl_2O_4$ were comparable to one another, while that of ZrO_2 was four times slower. It should be noted that the rate of dissolution is controlled by a surface reaction, the activation energies of ZrO_2 being 128.8kJ/mol and Mg Al_2O_4, 77.8 kJ/mol. It was concluded[168] that as the dissolution of ZrO_2 is so slow at any temperature of interest, removal of such particles by dissolution in this slag was not feasible. Both these pieces of work [23,168] highlight the effectiveness of a zirconium addition compared to that of titanium, due to the more uniform distribution and slower dissolution rate at high temperatures of ZrO_2. These effects are expected to influence the microstructure of steels and result in improved properties, especially in the case of toughness.

Most of the publications which consider oxides of zirconium in microalloyed steels do deal with inclusions precipitated during a welding process, for example [5, 161,163,164,167]. The observations of Koukabi et al[161] on the relative effects of titanium and zirconium additions in promoting acicular ferrite were explained in later work by Chai et al [167] who investigated the effect of zirconium bearing inclusions on the microstructure and toughness of the coarse grained HAZ formation during the welding of titanium -killed steels. Four steels containing ~0.080% C -1.5%Mn – 0.020%Ti with four levels of zirconium, <0.0010%(ZO), 0.0023% (Z1),0.0042%(Z2) and 0.010%(Z3), and oxygen levels of ~0.0010% (all wt. %) were studied. CGHAZ simulations were undertaken in a Gleeble machine. The specimens were heated rapidly to a peak temperature of 1350ºC, held for 1 second and cooled to 800ºC, at cooling rates in the range 20 to 40 ºC/s, and then further cooled to 500ºC, at cooling rates of 0.4-40ºC/s, rates which are equivalent to thermal cycles with heat inputs from 20 to 200kJ/cm, obtained when SAW is applied to a 20mm thick plate. The inclusions were studied by an analytical SEM technique and Thermo-Calc software was used to interpret the experimental observations. It was suggested that the equilibrium number and composition of the inclusion phases changed with the zirconium addition from Ti_2O_3 to ZrO_2.When the zirconium content was lower than 0.0085%, the inclusions in steels Z1 and Z2 were mainly Ti_2O_3 and ZrO_2 , and the oxides shared the same proportion of ~0.0045%Zr content.

Further evidence of the role played by ZrO_2 is provided in the paper by Guo et al[5] .They examined two prototype pipeline steels containing 0.05%C,1.65%Mn,058%Nb,0.008%B, with and without an 0.015%Zr addition. The steels were rolled to 12mm thick plate using thermo- mechanical control processing with a cooling rate of 12 ºC/s and a final cooling temperature of 300-350ºC, which resulted in a bainitic microstructure. Gleeble 2000 equipment was used to simulate weld HAZ's with heat inputs, H, of 3, 6 and 10kJ/mm. The microstructural evolution and the impact toughness were investigated, and some of the results

shown in Fig 29.When H was 3kJ/mm, the impact toughness was retained to a high level of ~50J at -20ºC for both specimens, but after increasing the heat input to 6kJ/mm, the impact toughness was reduced to ~30J for the zirconium free steels , but to only ~40J for the zirconium steel. A further increase in H to 10kJ/mm, resulted in the toughness decreasing sharply to ~10kJ/mm for the zirconium -free steel, whereas it remained at a higher level of ~30J in the zirconium-bearing steel.Coarsening curves for the austenite grain size in both steels are given in Fig 30.The grain diameter, D, increased slowly in both steels when the austenitizing temperature was below 1000ºC, but above this temperature, D in the zirconium-free steel increased sharply compared with the zirconium-bearing steel. At 1250ºC, D in the zirconium-free steel was an average of ~65μm compared with ~45 μm in the zirconium-bearing steel. The reason for the improvements in the zirconium –bearing steel was considered to be due to the larger volume fraction of smaller well distributed MnS inclusions. In the zirconium -bearing steel, there was selected area electron diffraction evidence that MnS was nucleated by ZrO_2 particles, so that the inclusions consisted of a core of ZrO_2 surrounded by a layer of MnS. More recent work by Zheng et al[169] studied the austenite grain size in the HAZ of a steel containing 0.08%C,0.02%V,0.01%Nb,0.02%Ti, 0.06%Zr,0.0047%N,0.0004%B.The grain size was recorded after different high heat input welding conditions, Fig 31, simulated by a Gleeble -1500 thermal-mechanical simulator. When the temperature was lower than 1200ºC, the grain size increased slowly, while above 1200ºC it increased rapidly. Models, developed as part of this work, demonstrated that the final grain size was not influenced by the initial grain size, but only by the heat input and the peak temperature. The successful choice of the zirconium-titanium steel for this work, confirmed by the results, was based on the expectation that zirconium and titanium would form precipitates of a size and shape that can pin austenite grain boundaries, and also that larger precipitates or inclusions containing zirconium and titanium are known to promote

acicular ferrite which can improve the toughness in the coarse grained HAZ. However, no particle characterisation was in fact undertaken.

Cast structures of 0.02%C cerium treated steels, either zirconium –free or containing 0.236%Zr,where compared by Arumalla. [94]However,the nitrogen content of his steels was not given. For the experimental zirconium –free steel ingot, the microhardness across the traverse sections, averaged over nine readings, was 340VHN, while that of the zirconium steel was 120VHN. No explaination was given for this data.

A number of papers authored by Dobuzhskaya, for example ref.170, dealing with rail steels containing 0.007-0.010%Zr and 0.009N, which precipitated zirconium oxides, are not considered in detail here, as they are out with the chemical composition range of microlloyed steels and suggest problems with the deoxidation practice employed.

9 Summary

While zirconium additions alone have little influence on strength of steels, enhancement in the ductility and toughness properties are indubitably linked to the high stability of zirconium compounds formed during the steelmaking process. This in turn is very dependent on steel composition and steel processing route. Even in the early work of Field [2], allowance was made for the loss of some zirconium to the slag as zirconium oxide, leaving the remainder to form sulphides or nitrides. Table 6 is a useful reminder of the extent of this problem. Modern steel-making methods normally avoid such high losses, which result in more zirconium combining to form useful precipitates. Zirconium additions to low carbon and microalloyed steels have been shown to be effective in improving toughness and ductility by forming (Mn,Zr)S inclusions, which are less plastic than MnS inclusions, and through grain refining of austenite, leading to a finer ferrite grain size. For high sulphur steels, ~0.02% S, Bucher[90] considered that the minimum zirconium addition to improve ductility was 0.015%.Others, such as Heisterkamp et al[130] and Meyer et al[131] showed that significant improvements in

impact toughness were found when the zirconium addition exceeded about 0.05%. Milhelich et al [22] have provided a composition range above or below which, no improvements in properties were recorded. With a good deoxidation practice combined with a low sulphur (~0.005wt%) content in the steel, zirconium has been shown to combine with carbon and with nitrogen, resulting in pinning of austenite grain boundaries by Zr(C,N) particles .[26] There is some evidence that under certain circumstances, zirconium additions when combined with vanadium and or niobium can result in an increase in strength. For example, increases in the yield strength were noted in Zr-Nb steels in the work of He and Baker[25]. Very few research publications on zirconium alloyed steels have attempted to understand mechanical properties through a study of microstructural parameters. Despite a detailed survey of the literature, rarely have papers been found in which the level of zirconium, the precipitate size or grain size have been related to yield stress or the impact transition temperature. The only paper dealing with this aspect in detail appears to be that of Li et al[30] who studied a DRTS Zr-V microalloyed steel, with zirconium additions added as a possible replacement for, or in combination with, the transition metals niobium, titanium and vanadium, and found increases in the yield strength through grain size control and /or dispersion strengthening by precipitation of fine nitrides. Here, a low carbon (0.05%), high nitrogen (0.01%) steel with an addition of zirconium of 0.008% and vanadium of 0.10%, produced a ferrite grain size of ~4.8μm combined with significant dispersion plus dislocation strengthening component of ~145MPa, after equalisation at 1050ºC. The data was used in the Hall- Petch and Petch relationships. Similar data was given by Michel and Buršak.[133]

Several of the studies which have examined the microstructure, recorded zirconium containing particles greater than 1μm in radius, which are not expected to have a major effect on grain boundary pinning. Also, to date, there have been no reports of ferrite grains being nucleated by zirconium particles, but many instances of grain refinement in

steels with zirconium additions. In general, the effect of zirconium has been presented in terms of the level of alloying additions and also as the Zr/N ratio. In some research, characterisation of carbide and nitride precipitates of zirconium was undertaken. In one such example, Shiraiwa et al [69] observed cubic inclusions of ZrC and ZrN , but also cases where ZrCN existed in the core surrounded by ZrC. He and Baker [26] found that Zr(C, N) contained either a high N or high C content, depending on the Zr/N ratio, and these particles resulted in austenite grain refining, as did MnS nucleated by ZrO_2 particles, noted by Guo et al [5],while Mihelich[22]obseved that the (Mn, Zr)S particles nucleated on a ZrN core. There is also information on the role of zirconium oxides and (Mn, Zr) sulphides. Suzuki et al[82] verified zirconium sulphides as Zr_3S_2, in a rod or plate- like morphology, when the molar ratio of Zr/Mn was in the range 0.4~ 3.5.The inclusions changed to globular $(Zr, Mn)_3S_2$ when the manganese content of the steels was ~1 wt.-%. Pacey et al[163] found that small amounts of zirconium initially slightly increased the percentage of acicular ferrite, but at levels of 0.011%Zr and above, increased the percentage of bainitic laths and replaced inter-ferritic carbides with M-A phase. These effects were interpreted as the addition of zirconium lowering the transformation temperature.

As this review shows, zirconium additions can significantly increase the toughness through both sulphide shape control and austenite grain refinement. There is evidence to show that in microalloyed steels, zirconium is more effective in combination with vanadium and /or, niobium, which in addition to increasing toughness and ductility, can also improve strength through dispersion strengthening. With a worldwide distribution of zirconium containing ores, it is timely for research to be undertaken to explore in more depth, the potential of zirconium additions to microalloyed steels.

Acknowledgements The author wishes to thank Dr.W.B.Morrison, formerly of British Steels and Corus, for introducing him to zirconium microalloyed steels and then supporting

several pieces of research in this area, Dr. David Crowther, formerly of Corus now Tata Steels for his support and Mr. Peter Mitchell, formerly of Vanitec who supported financially the DCTS research, and all three for many useful and enjoyable discussions. Also, Dr. Michael Arrowsmith is thanked for providing information from his selected area electron diffraction work on zirconium compounds which he identified in steels, and Aileen Petrie for her patience in re -editing the figures and tables.

References

1. C. A. Beiser: ASM preprint no138, 1959, Metals Park, OH, Am. Soc. Met.
2. A L Feild: Trans. Am . Inst. Mining Met. Engrs., 1923, 69, 848-894.
3. F. M. Becket: Trans. Amer. Electrochem. Soc., 1923, 43, 261-269.
4. T. H. Xi, X. Chen, P H Li: Acta Metall. Sin. (Engl. Lett.) 2006, 19, 319-327.
5. A. M. Guo, S. R. Li, J. . Guo, Q. F. Ding, K. M. Wu and X. L. He: Mater. Char., 2008, 59**,** 134-139.
6. H. R. Wang, W Wang and J. Q. Gao: Mater. Lett., 2010,64, 219-222.
7. F. G. Wilson and T. Gladman: Inter. Met. Revs., 1988, 33, 221-288.
8. A. J. DeArdo: Inter. Met. Revs ., 2003, 48, 371-402.
9. F. B. Pickering: in 'Titanium technology in microalloyed steels', (ed. T. N. Baker), 1997, 10-43, London, The Institute of Materials.
10. T. N. Baker: Mater. Sci. Technol., 2009, 25, 1083-1107.
11. G. T. Motock and C. M. Offenhauer: 'Boron, calcium, columbium and zirconium', 462, 1957, New York, Wiley.
12. C. E. Sims and F. B. Dahle: Trans. Amer. Foundrymens Association, 1938, 46, 65-132.
13. C. E. Sims, A. Saller and F,W. Boulger: Trans Amer. Furn. Soc.,1949,57,233-247.
14. C. E. Sims:Elect. Furn. Proc., AIME 1952, 10,152-168.
15. C. E. Sims and C. W. Briggs: Elect. Furn. Proc., AIME, 1959,17,104-124.
16. C. E. Sims: Trans. Met. Soc. AIME, 1959, 215, 367-393.
17. E. J. Lichy, GC Duderstadt and N L Samways: J. Met., 1965, 17, 769-775.
18. H. A. Vogels :Arch. Eisenh, 1962, 33, 649-659.
19. W. Dahl, H. Hengstenberg and C. Düren: Stahl Eisen, 1966, 86,796-817.
20. M. Wahlster, H. Heimbach and K. Forch: Stahl Eisen,1969,89,1037-104.

21. A. G. Franklin and W. J. M. Tegart: J Iron Steel Inst., 1964,202, 588-592.

22. J. L Mihelich, J. R. Bell and M. Korchynsky: J Iron Steel Inst., 1971,209, 469-475.

23. T. Sawai, M. Wakoh, Y. Ueshima and S. Mizoguchi: ISIJ International, 1992, 32, 169-173.

24. J. W. Halley: Trans. Am. Inst. Mining Met. Engrs. 1946,167, 224-236.

25. K He and T N Baker: Mater Sci Eng 1996, A215, 57-66.

26. K He and T N Baker: Mater Sci Eng 1998, A256, 111-119.

27. K. He and T. N. Baker: in 'Titanium technology in microalloyed steels', (ed. T. N. Baker), 115-132, 1997, London, The Institute of . Materials.

28. K He, D. N. Crowther and T. N. Baker, **Proc, THERMEC 97**, (ed. T. Chandra and T. Sakai), 925-930, 1998. TMS,

29. A. R. B. Maia, C. R. Guinâncio, R. L. Germano, P. R. Rios and I. de S. Bott: Advan. Mater. Res**.,** 2007, 15-17, 834-839.

30. Y. Li, J. A. Wilson, D. N. Crowther, P. S. Mitchell, A. J. Craven and T. N. Baker: ISIJ Internal., 2004,44,1093-1102.

31. G. L. Miller: 'Zirconium', 1954, Butterworth Scientific Publications, London.

32. G. L. Miller: 'Zirconium', 2nd edn, 1957, Butterworth Scientific Publications, London.

33. W. J. Kroll, A. W. Schlechten and L. A. Yerkes: Trans. Electrochem. Soc., 1946, 89, 263-276.

34. W. B. Blumenthal: 'The chemical behaviour of zirconium', 1958, Van Nostrand Company, Princeton, NJ.

35. D. R. Lade editor: 'Zirconium', CRC Handbook of Chemistry and Physics, 4, (2007-2008),42, New York, CRC Press.

36. The Columbia Encyclopedia, 6th edn. Copyright© 2004, Columbia University Press.

37. W. Hume-Rothery,R. E. Smallman and C. W. Howarth: 'The structure of metals and Alloys' 5th edn, 262,1969, The Institute of Metals, London

38. A D Schwope: Symp. Amer. Soc. Metals: 'Zirconium and zirconium alloys' 111, 1953, Cleveland, Ohio.

39. W. Hume-Rothery and G. V. Raynor: 'The structure of metals and alloys' ninth printing (revised), 100-104,218-222,1956,The Institute of Metals, London.

40. G Hägg: Z. Physikal Chem., 1931, [serB], 12, 33-6.

41. H. K. D. H. Bhadeshia: ISIJ International, 2001, 41, 626–640.

42. A H Cottrell: ‘Chemical Bonding in Transition Metal Carbides’, 1, 1995, The Institute of Materials, London.

43. K W Andrews and H Hughes: JIron Steel Inst.,1959,193,304-311.

44. P. L. Brown: ‘Chemical Thermodynamics of Zirconium’, vol. 8. of Chemical Thermodynamics, 2005,, Elsevier, Amsterdam.

45. H. J. Goldschmidt ‘Interstitial alloys ’, 1957, Butterworths, London.

46. L. E Toth, ‘Transition metal carbides and nitrides’, 1971, Academic Press, New York and London.

47. H. O. Pierson, ‘Handbook of Refractory carbides and nitrides’, 1996, Noyes publications, New Jersey.

48. R. Kiessling, S. Bergh and N Lange: J Iron Steel Inst., 1963,201**,** 965-967.

49. H. Hahn, B. Harder,U. Mutshke and P. Hess: Z. Anorg. Allg. Chem.,1957, 292, 82-96.

50. H. Harldsen Acta Chemica Scandinavia: 1963, **17**, 1283-1292.

51. B. R. Conrad and H. F. Franzen : High Temp. Sci.,1971,**3**,49-55

52. H. Kudielka and K Rohde: Z. Krist., 1960, 114, 447-456

53. R. Kiessling and J. T. Norton: J. Metals, 1950,2, 1060-1061

54. J. T. Norton, H. Blumenthal and S. J. Sindeband, J. Metals , 1949,1, 749-751

55. L. Brewer, D. L. Sawyer, D. H. Templeton and C. H. Dauben: J. Amer. Cerm. Soc., 1951, 34, 173-177.

56. R. Kieffer, F. Benesovsky and E. R. Honak: Z. Anorg. Chem.,1952,268, 191-200.

57. B. Post and F. W. Glaser:J. Metals, 1952, 4, 631-632

58. R. Kiessling and J. T. Norton: J. Metals,1950,2,1060-1061

59. ‘ASM Handbook, Alloy Phase Diagrams’, . 2. 87, 3, 1992, ASM International, Ohio.

60. V. Raghavan : ‘Phase diagrams of ternary iron alloys’, 455- 458, Part 6A ,1992, Indian Institute of Metals, Calcutta.

61. J-W Park, K-K Jee and W-S Jung: Scripta mater.,2001, 44, 587-592.

62. R. V. Sara: J. The system zirconium –carbon, Am. Cerm. Soc., 1965**, 48**, 243-245.

63. H. Okamoto J. Phase Equil.,1990, 17, 162. ,

64. A. F Guillermet: J. Alloys Cpds, 1995. , 217,69-89.

65. J. W. Mallet: Amer. J. Sci, 1859, 28, 346-349.

66. E. Wedekind: Berichte der deutschen chemischen ghemellschaft: 1912, 45, 1298-1315.

67. R. F. Domagala, D. R. McPherson and M. Hansen: J. Met., 1956, 98-105.

68. ASM Handbook, Alloy Phase Diagrams, 2-300, 3, 1992, ASM International, Ohio,

69. T Shiraiwa, N. Fujino and J. Murayama: Trans ISIJ. 1970, 10**,** 406-412.

70. C. B. Alcock, K. T. Jacob and S Zador: 'Zirconium: Physicochemical properties of its compounds and alloys. 1. Thermochemical properties', 7-65,1976, Spec. Issue, Atomic energy Rev.
71. J. P. Abriata, R Versaci and J Garcés: ASM Handbook, Alloy Phase Diagrams, 2-326, 3, 1992, ASM International, Ohio.
72. R. Srinivasan, M. B. Harris, S. F. Simpson, R. J. De Angelis and B. H. Davis: Mater. Res. Soc., 1988, 3,787-797.
73. A. L. Feild: Trans. Am. Inst. Mining Met. Engrs.,1924, 70, 201-223.
74. E. Fremy: Ann. Chem. Phys., 1853, 38, 312-344.
75. R. Kiessling and N. Lange: 'Non-metallic Inclusions in Steel' 2nd edn, 138-139,1978, Metals Society, London.
76. S. R. Shatynski: Oxidation of Metals, 1977, 11, 307-320
77. F. Jellinek: Ark. Kemi, 1963, 20, 447-480.
78. W. Koch and E. Artner: Archiv. für das Eisenhüttenwesen, 1958, 29, 737-744.
79. W. J. M. Tegart and A. D. Wadsley: Australian J Chem, 1958, **11,** 445-457.
80. D. Charquet: J Nucl. Mater., 2002, **304,**246-248.
81. K. Nartita, Y. Yamaguchi, N. Yagi and T. Tetsu- to- Hagane, 1976, **62,** 885-894.
82. K-I Suzuki, A. Ejima and K. Nakanishi: ISIJ International, 1985,25,433-442.
83. R. Vogel and H. Hartung: Archiv. für das Eisenhüttenwesen, 1942, **15**, 413-418.
84. C. Frick and H. Rohde: Archiv. für das Eisenhüttenwesen 1960, **31**, 419-422.
85. J. M Arrowsmith: Identification of embrittling phase in zirconium steels, BISRA Report SNW(C)/E7/21, Aug 1968. [cited by Little and Henderson 84]
86. J. H. Little and W. J. M. Henderson: Proc. Conf. on ' Effect of second phase particles on mechanical properties of steel, 182-189,1971, The Iron Steel Institute, London.
87. J. H. Schneibel, C. L. White and M. H. Yoo: Metall. Trans A, 1985, 16A, 651-660.
88. S. F. Urban and J. Chipman:Trans ASM,1935,**23**, 93-112.
89. A. M. Portevin and R. Castro: J Iron Steel Inst., 1937, 135, 223P-254P.
90. J. H. Bucher, G. C. Duderstadt and K. Piene: J Iron Steel Inst.,1969, 207, 225-229.
91. D. J. McCullough, L. Brewer and L. A. Bromley: Acta Cryst. 1948, 1, 287-289.
92. F. Jellinek: Acta Chem. Scand. Ser. A, 1962, 16, 791- 792.
93. K Narita: Trans. ISIJ, 1975, 15,145-152.
94. S. R. Arumalla: Trans. Indian Inst. Met.,1990, 43, 202-206.
95. J Wadsworth,J. H. Woodhead and S. R. Keown: Met. Sci.,1976,10,342-348.
96. T. Gladman: 'Physical metallurgy of microalloyed steels',1997, London, Inst. Materials.

97. M. T. Nagata, J. G. Speer and D. K. Matlock:Metall. Mater. Trans., 2002,33A, 3099-4110.

98. D. B. Evans and R. D. Pehlke: Trans Met. Soc. AIME, 1965, 233, 1620-1624.

99. Z. Morita, T. Tanaka and T. Yanai: Metall. Trans. B, 1987, 18B, 195-202.

100. H. Ono, K. Morita and N. Sano: Metall. Mater. Trans, 1995, 26B, 991-995.

101 S. Matsuda and N. Okumura: Trans Iron Steel Inst. Japan, 1978, 18, 198-205.

102. D. C. Houghton: Acta metall. mater, 1993, 41, 2993-3006.

103. H. L. Zhou and J. S. Kirkaldy: Metall. Trans. 1991, 22A**,** 1511-1524.

104. Z-K Liu: Scripta Mater. 2004, 50, 601-606.

105 K.Xu, B.G.Thomas and R.O'Malley: Metall. Mater. Trans, 2011, 42A, 524-539.

106. V. Raghaven: J Phase Equilibria, 2002, 23, 523-524.

107. M. Jiang, K. Oikawa,T. Ikeoshoji,L. Wulff and K. Ishida: J. Phase Equilibria,2001, 22, 406-417.

108. H. Holleck and F. Thummler: 'Structure, fabrication and properties of high melting point compounds and systems', KfK report 2826B, 73-76,1979, Kernforschungzentrum, Karlsruhe, Germany.

109. V. Raghaven; 'Phase Diagrams of Ternary Iron Alloys', 133-140, 1987, ASM

110. K. C. Mills: 'Thermodynamic data for inorganic sulphides, selenides and tellurides', 845, 1974, Butterworth, London.

111. I. Barin: ' Thermodynamic data of pure substances', 1738, 2004,Wiley VHC.

112. N. J. Petch: in 'Fracture' (ed. G. T. Hahn et al),91, 1959,Cambridge M. A. MIT Press.

113. N. J. Petch:Acta Metall.,1986,34,1387-1393.

114. J. W. Martin: 'Micromechanisms in particle-hardened alloys', 150,1. 980, Cambridge University Press, UK

115. R. D. Doherty and J. W. Martin: J. Inst. Metals,1962-3,91,332-338.

116. C. S. Smith:Trans. Metall. Soc. AIME, 1948, 175, 15-51.

117. T. Gladman and F. B. Pickering: J. Iron Steel Inst., 1967, 205, 653-664.

118. F. J. Humphreys and M. Hatherly: 'Recrystallization and related annealing Phenomena', 1st edn, 1995, Oxford, Pergamon Press.

119. P. A. Manohar, M. Ferry and T. Chandra:, ISIJ International, 1998, 38**,** 913-. 924.

120. T. Gladman, I. D. McIvor and F. B. Pickering: J Iron Steel Inst., 1971,209, 380-390.

121. D. T. Gawne and G. T. Higgins: J Mat. Sci., 1971, 6**,** 403-412.

122. D. T. Gawne and G. T. Higgins: J Iron Steel Inst., 1971, 209,562-566.

123. C. Kamma and E. Hornbogen: J Mat. Sci., 1976, 11, 2340-2344.

124. H. Masayoshi: Tetsu-tu-Hagane, 1951, no37, 73-283.

125. H. Masayoshi: Tetsu-tu-Hagane, 1951, no37, 579-588.

126. W. Crafts and J. L Lamont: Trans. Am. Soc. Metal, 1939, 27, 268-288.

127. J. Falce, J. M. Henry, E. A. Hanne and C. Parrini, Joint ASM-AIM Symposium Welding of HSLA Steels, November 1976, 440-466, Rome.

128. H. A. Akbarzadeh,M. Tamizifar, Sh. Mirdamadi and A. Abdolhossein: ISIJ International. 2005, 45, 1201-1204.

129. H. Aliakbarzadeh, Sh. Mirdamadi and M. Tamizifar: Mater. Sci. Technol.,2010, 26, 1373-1376

130. F. Heisterkamp, D. Lauderbod. L. Meyer C. Straussbu: Effect of zirconium on toughness of weldable high strength structural steels containing niobium or vanadium, Stahl Eisen, 1970,**90**,1255-1262.

131. L. Meyer, F. Heisterkamp and C. Straussburger: Proc. Symp., Low Alloy High Strength Steels' , May 21-23, 1970. 9-15,Nuremberg.

132. W. B. Morrison: Scan J. Metall. 1980,9, 83-90.

133. U. Michel and M. Buršak: Phys. Met. Metall.,1987, 64,173-178.

134 B. Mintz, A. Williamson, H. Su, and W.B. Morrison: Mater. Sci. Technol., 2007, 23, 63-71.

135. J. J. Egan, W. Crafts and A. B. Kinzel: Trans A. S. Steel Treat., 1933, 21, 1136-1152.

136. R. Tull: Heat Treat. Forging, 1932, 18, 471-473.

137. K. Kato: Tetsu-to-Hagané, 1962, 48, 753-759.

138. B Pollard: Metal Technol., 1974, 1,343-347.

139. D. Battacharya: Metall Trans A, 1981,12A, 973-985.

140. D. T. Llewellyn and R. C. Hudd: 'Steels: Metallurgy and Applications', 163-167, 1998, Butterworth: Heinemann, Oxford.

141. K.B. Gove and J.A. Charles: Metals Technol.,1974, 1,145-

142 T. J. Baker, K. B. Grove and J. A. Charles: Metals Technol., 1976, 3, 183-193

143J. A. Charles and I. Uchiyama : J Iron Steel Inst., 1969,207, 979-983.

144. T. J. Baker and J. A. Charles: J. Iron Steel Inst., 1972,210, 702-706**.**

145. R. B. G. Yeo: J. Metals, 1967, 19, part 1, June, 29-32, part11, July 23-27.

146. V. Karmazin: Stal', 1940, 5-6, 24-30.

147. B. I. Edelson and W. M. Baldwin: Trans. ASM, 1962, 55**,** 230-250.

148. T. Gladman, B Holmes and F. B. Pickering: J Iron Steel Inst., 1970,208, 172-183.

149. R. Kiessling: J Metals, 1968, 20, 20-21.

150. W. Crafts and D. C. Hilty: Proc. Elect. Furn. Conf.,1953, 121-150.
151. T. J. Baker and J. A. Charles: J Iron Steel Inst., 1972,210, 680-690.
152. E. Scheil and R. Schell: Stahl und Eisen 1952, 72, 683- 687.
153. P. J. H Maunder and J. A. Charles: J Iron Steel Inst., 1968,206, 705-715.
154 A. J. Mardinly, L. H. VanVlack and W. F. Hosford: Tex. Micros.,1993, 22,127-138.
155. E. J. Paliwoda: Trans. ASM, 1955, 47, 680-691
156. A. Ejima: 24-26th Nishiyama Memorial Seminar, ISIJ, 1975,100.
157. L. Luyckx, J. R. Bell, A. McLean and M. Korchynsky: Met. Trans., 1970**,** 1, 3341-3350.
158. J. E. Croll: J. Australastian Inst. Metals, 1975, 20, 171-179.
159. Y. Yamaguchi, T. Shimohata, T. Kaneda and S. Furusawa: Proc. Int. Sym. 'Influence of metallurgy on machinability of steel', Japan, 289, 1977, Metals Park, OH, ASM.
160. T. Arakawa,T. Yamamoto and T. Aizawa: Tetsu to Hagane, 1971, 57, 2067-2075.
161. A H. Koukabi, T H North and H B Bell: Met Constr. 1979, 7, 639-642.
162. U Schriever: J. Met., 1965, 17, 115.
163. A. J Pacey, S. Kayali and H W Kerr: Can. Metall. Quart., 1982, 21,309-318.
164. E. S. Kayali, A. J. Pacey and H. W. Kerr: Can. Metall. Quart., 1984, 23, 227-236.
165. Y. Tomita, N. Saito, and T Tsuzuki,Y. Tokunaga and K. Okamoto: ISIJ International, 1994, 34, 829-835.
166. G. M. Evans: Weld J., 1995, 74, S249-S261.
167. F. Chai, C. F. Yang,H. Su, Y. Q. Zhang, Z. Xu and Y. H. Yang: Acta Metall Sin. (Eng. Lett.), 2008, 21, 220-226.
168. A. B. Fox, M. E. Valdez, J. Gisby, R. C. Atwood, P. D. Lee and S. Sridhar: ISIJ International, 2004, 44, 836-845.
169. L. Zheng, Z-x. Yaun, S-h. Song, S-h. Xi and Q Wang: J. Iron Steel Research International, 2012, 19, 73-78.
170. A. B. Dobuzhskaya, E. L. Kolosova and V. I. Syreyshchikova: Phys. Met. Metall., 1990,70, 121-128.

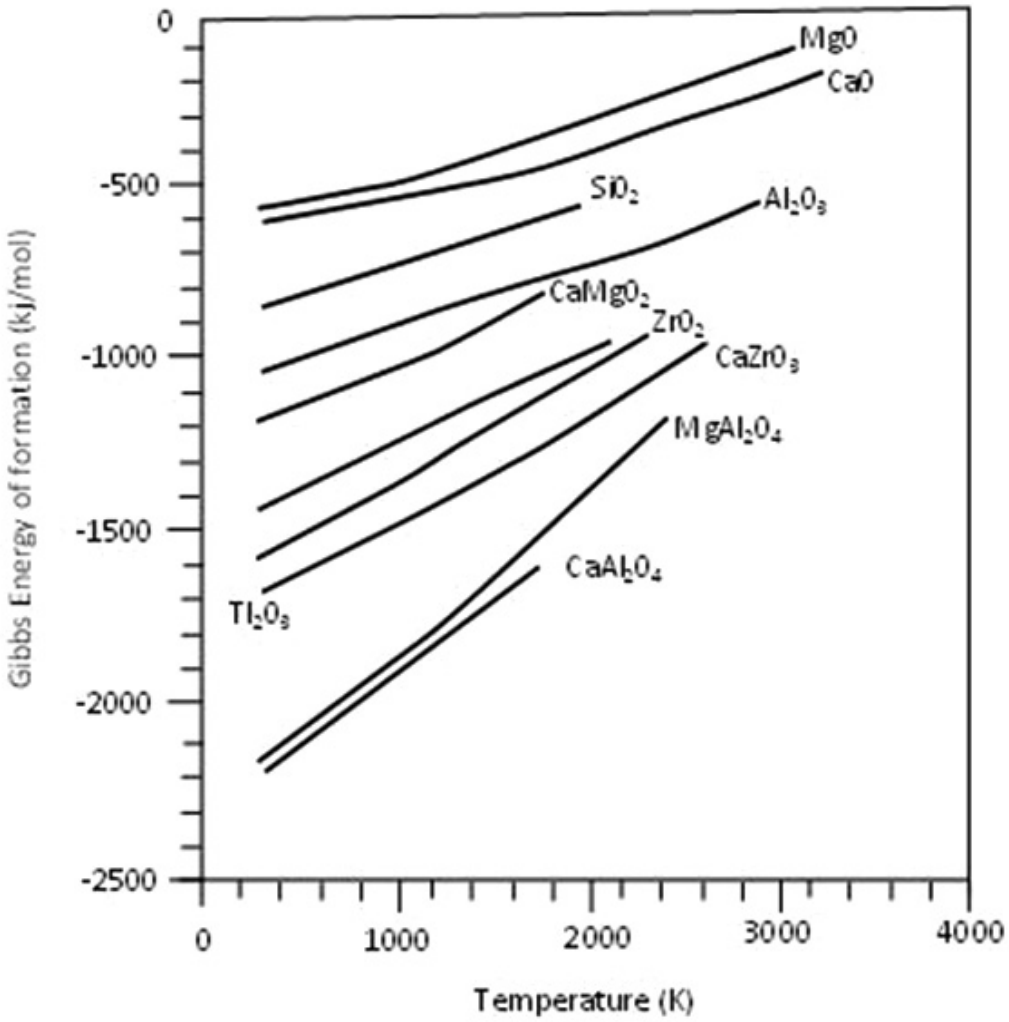

Figure 1 Thermodynamic data of oxides associated with steels, after Barin. [111]

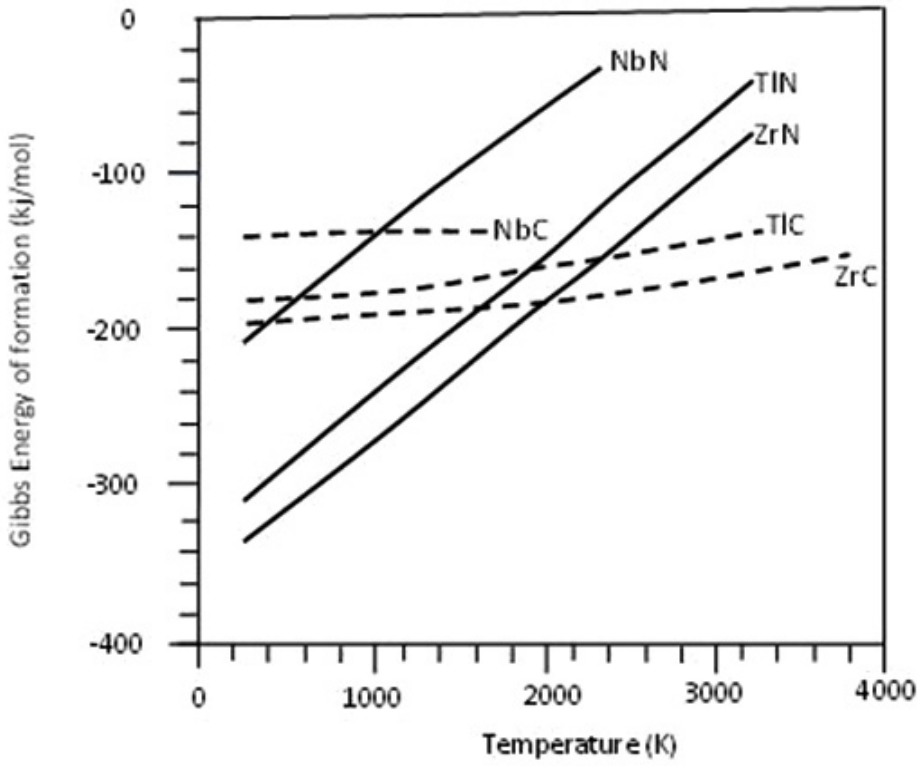

Figure 2 Thermodynamic data of carbides and nitrides oxides associated with steels, after Barin. [111]

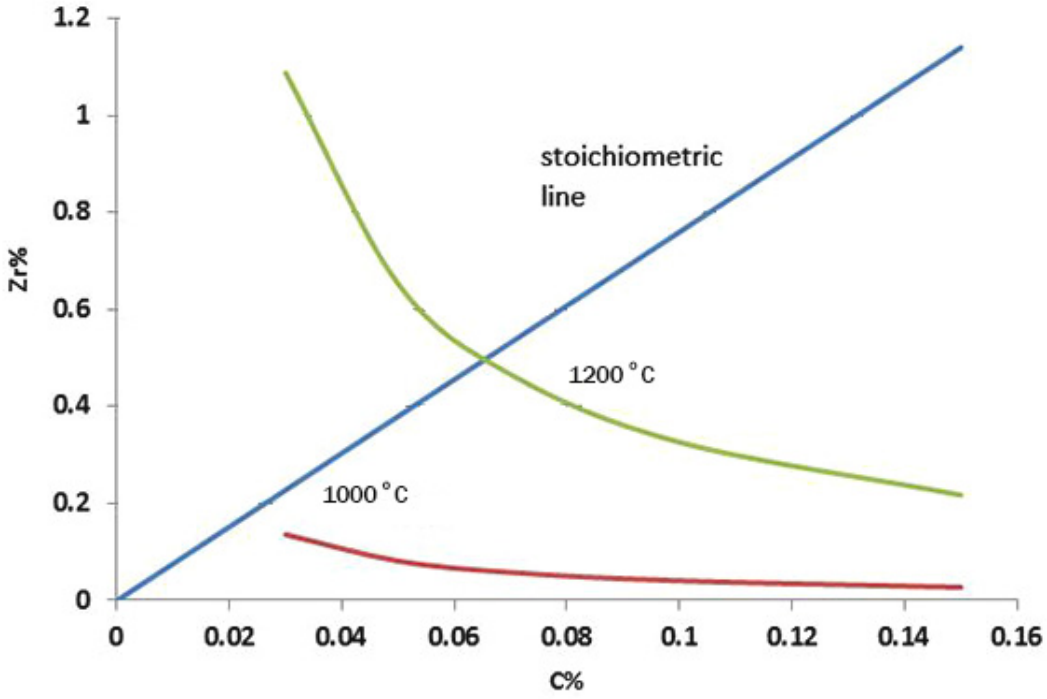

Figure 3 Solubility curves for ZrC in austenite at 1000°C and 1200°C, and showing the stoichiometric line, after Narita.[93]

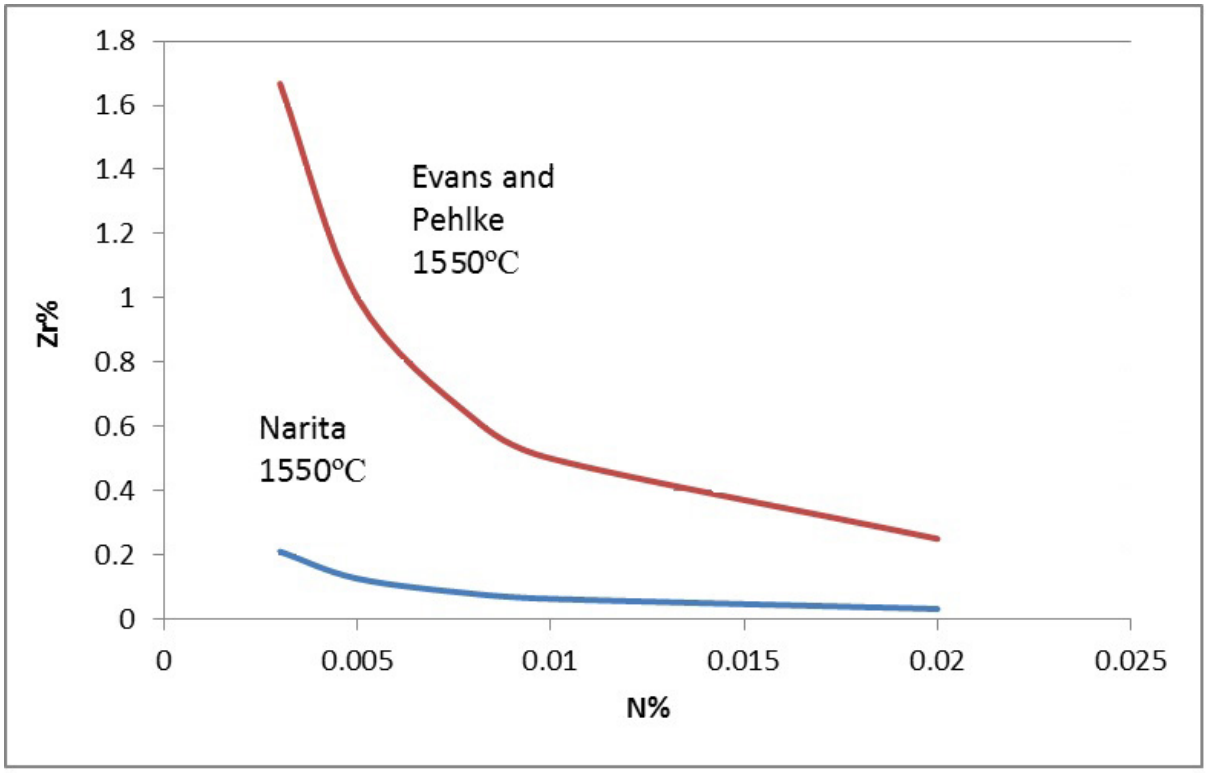

Figure 4 Solubility curves for ZrN in austenite and liquid iron at 1550ºC, after Narita.[93]

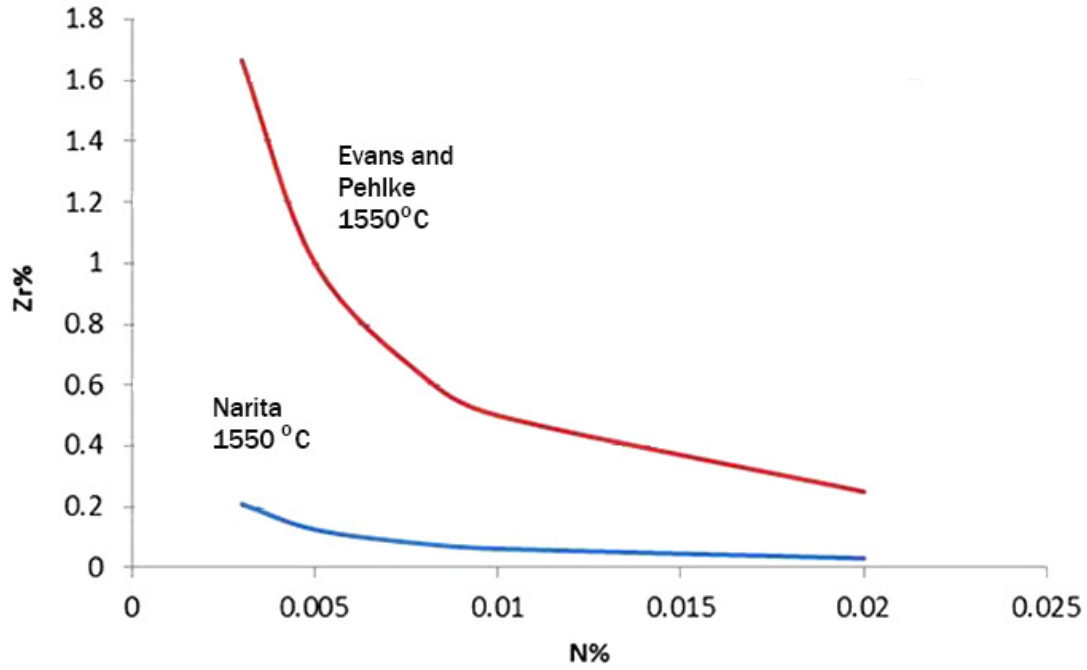

Figure 5 Comparison of solubility curves by Narita[93] and Evans and Pehlke[98] for ZrN in liquid iron at 1550°C.

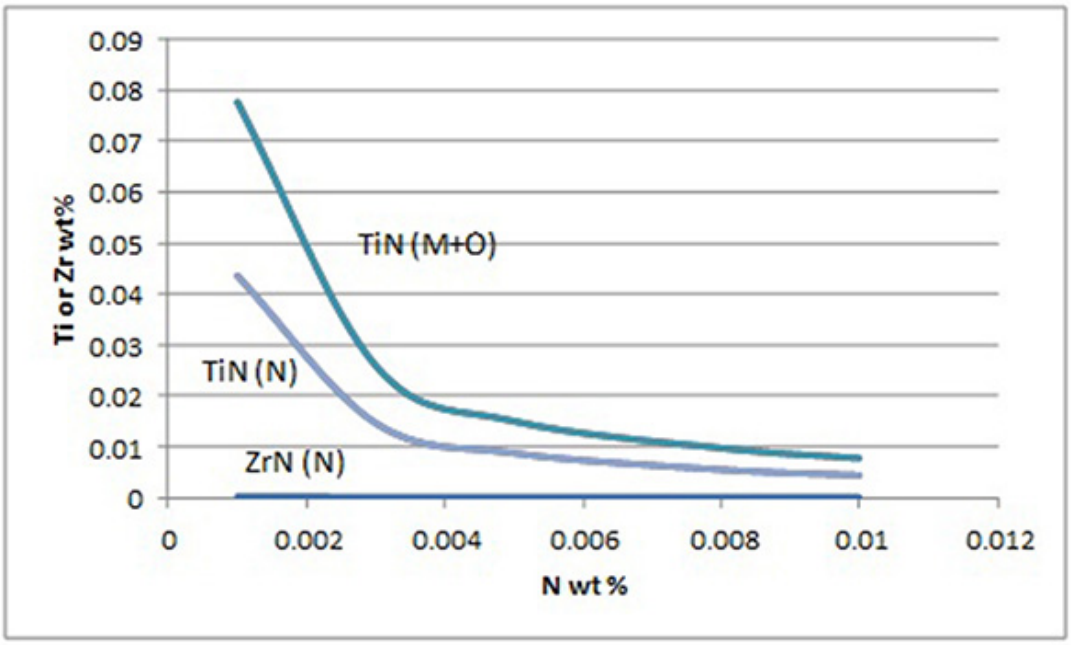

Figure 6 Comparison of solubility curves at 1200ºC for ZrN in austenite by Narita[93], TiN in austenite by Narita[93] and Matsuda and Okumua. [101]

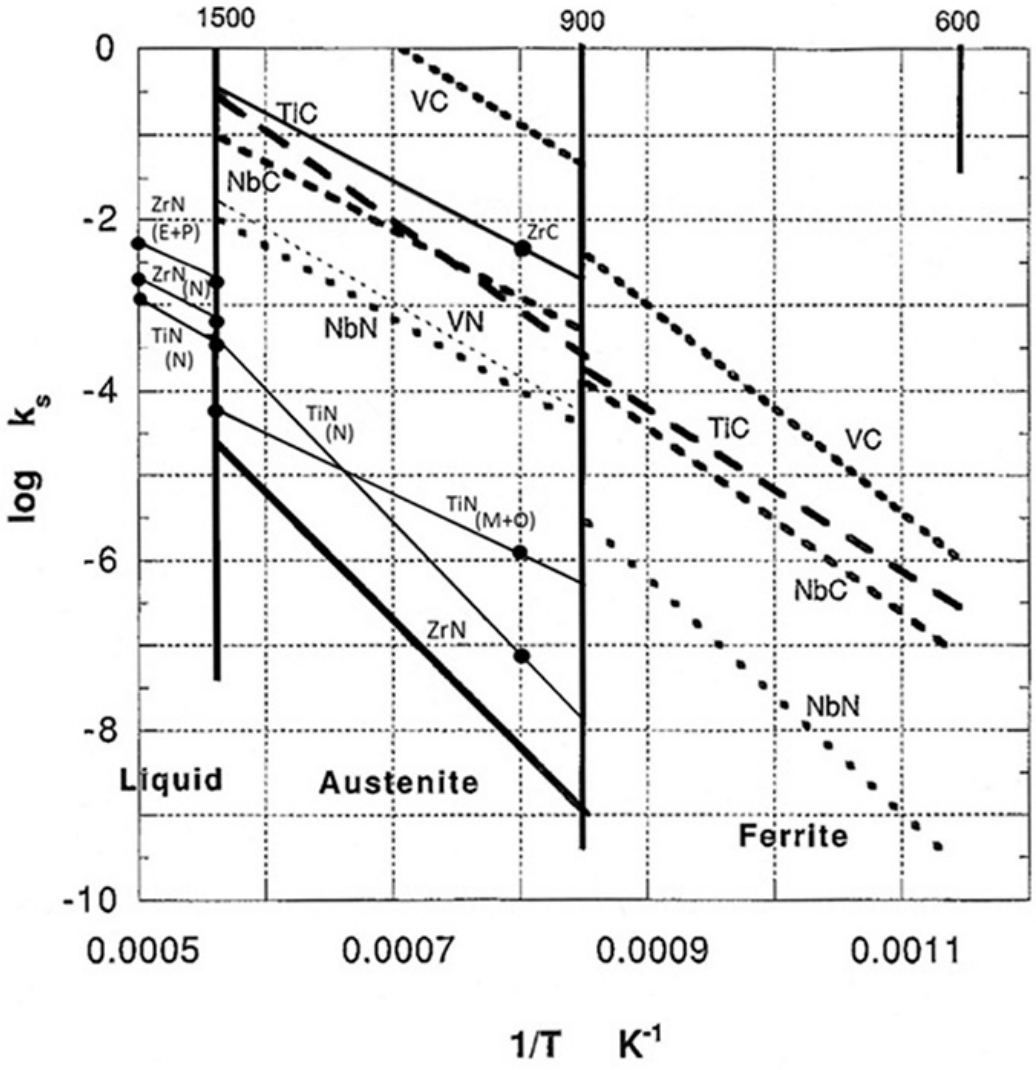

Figure 7 A comparison of solubility products of carbides and nitrides in microalloy steels. The top horizontal axis is ºC, after Gladman.[96]

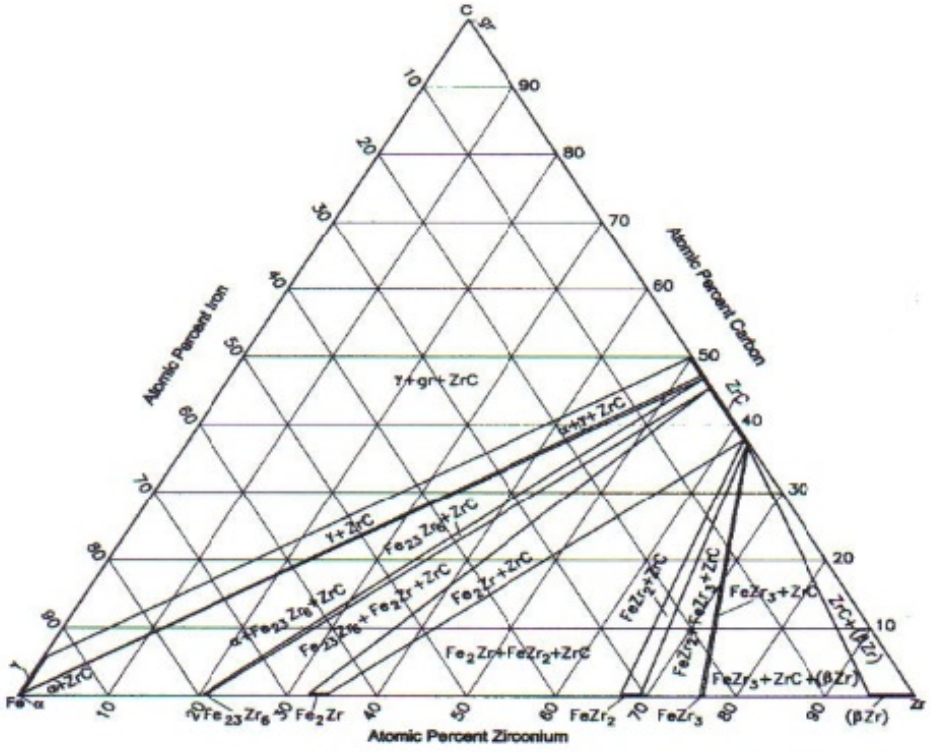

Figure 8 C-Fe-Zr computed isothermal section at 900ºC, Jiang et al. [107]

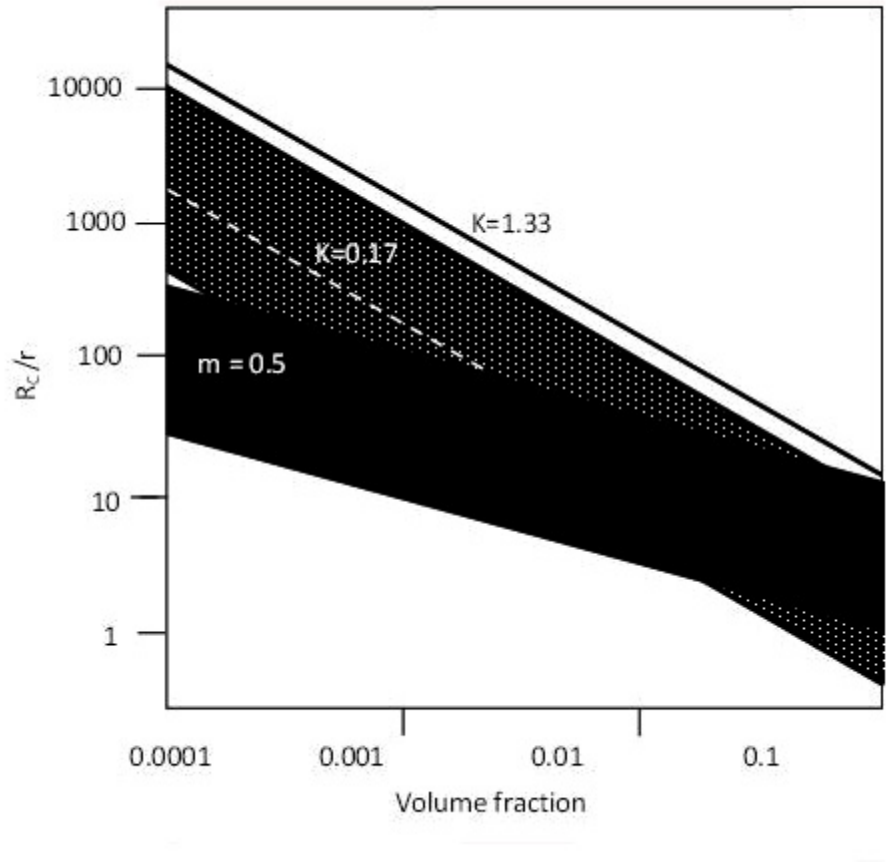

Figure 9 Ratio of limiting grain radius to particle radius (R_c/r) as a function of the volume fraction of particles(f).after Manohar et al. [119]

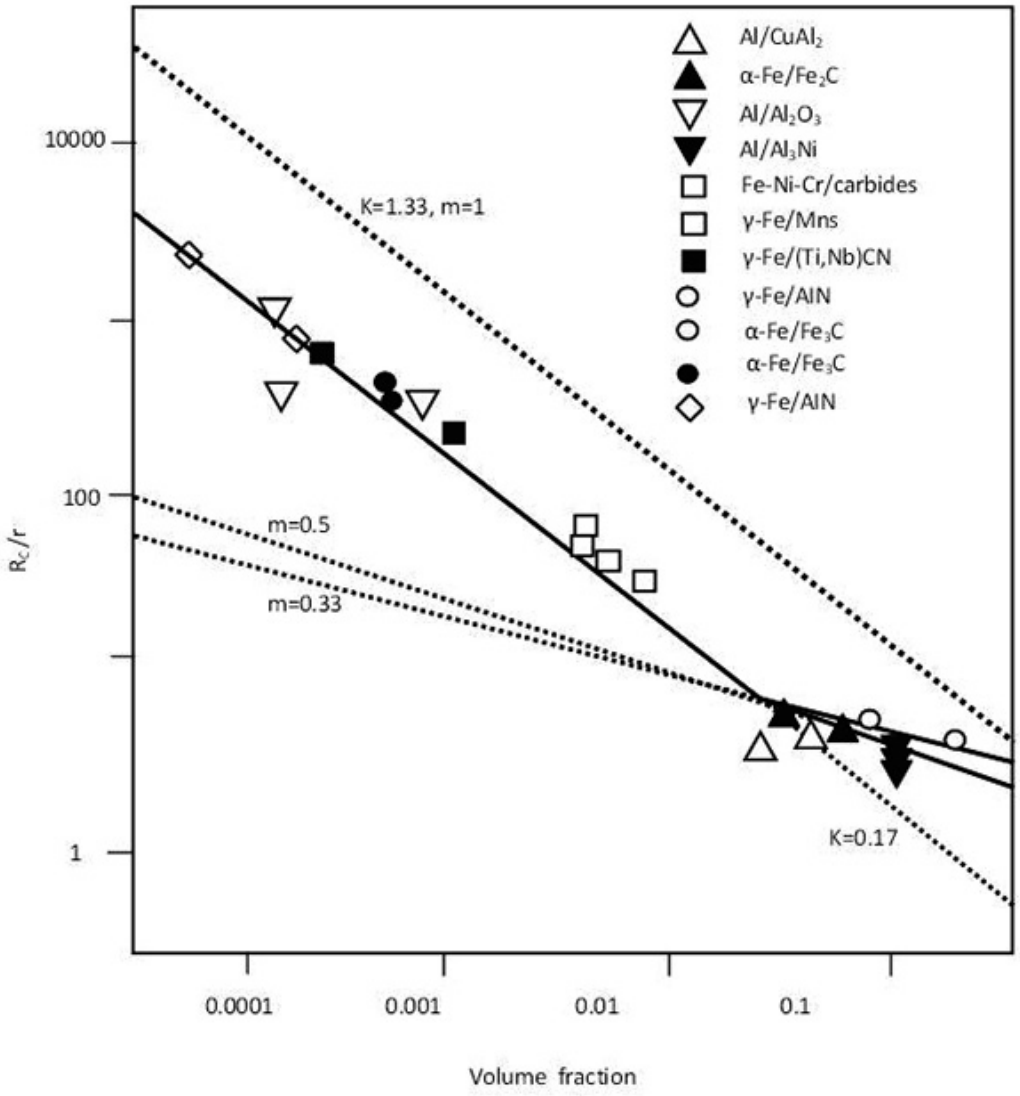

Figure 10 Experimental data of ratio of limiting grain radius to particle radius (R_c/r) as a function of the volume fraction of particles(f) for the alloy systems collated by Manohar et al. [119]

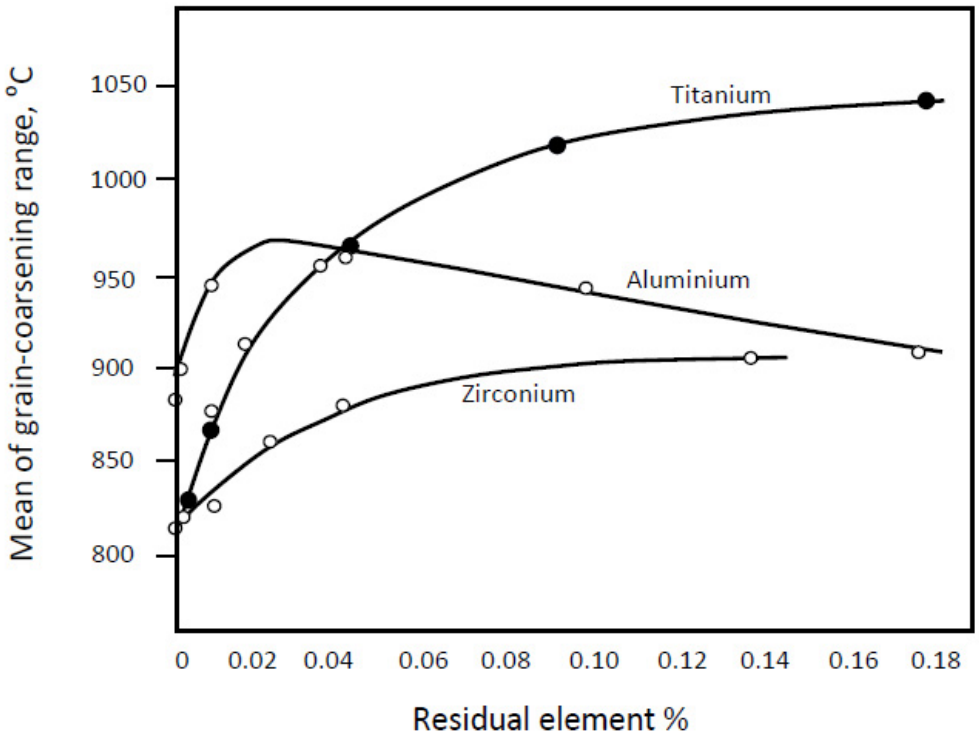

Figure 11 Effect of aluminum, titanium and zirconium on the grain coarsening temperature, after Halley. [24]

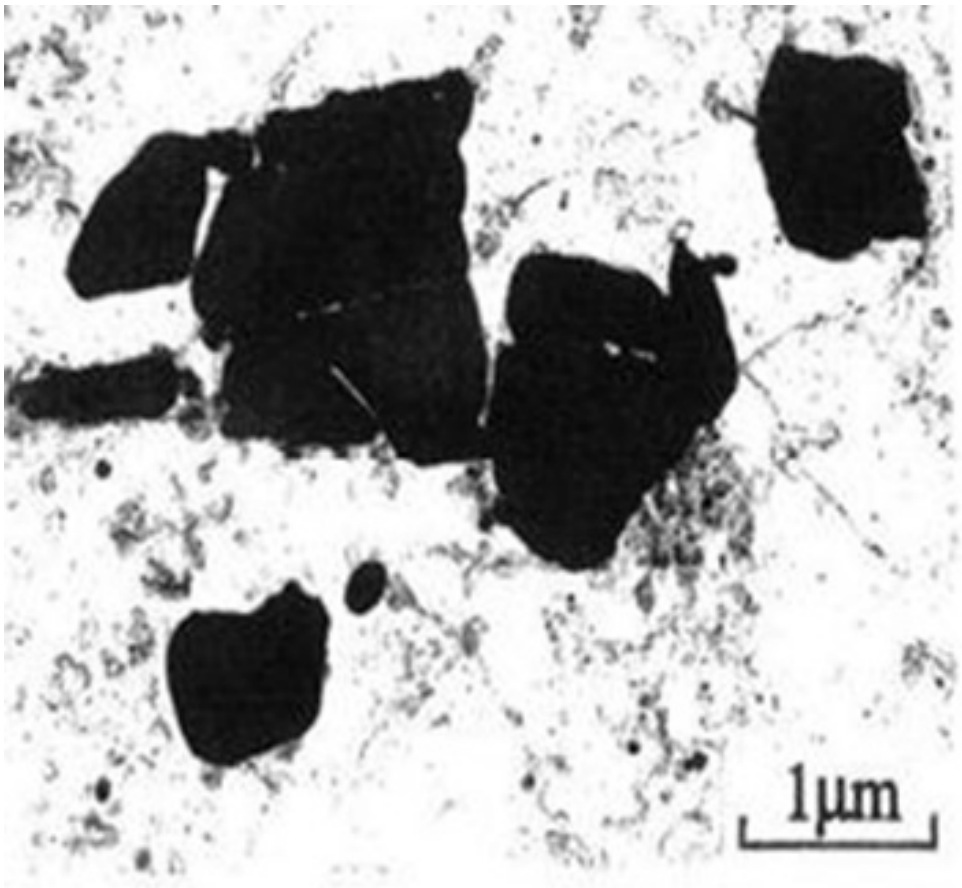

Figure 12 Large zirconium carbonitrides in a 0.12% Zr steel, He and Baker. [26]

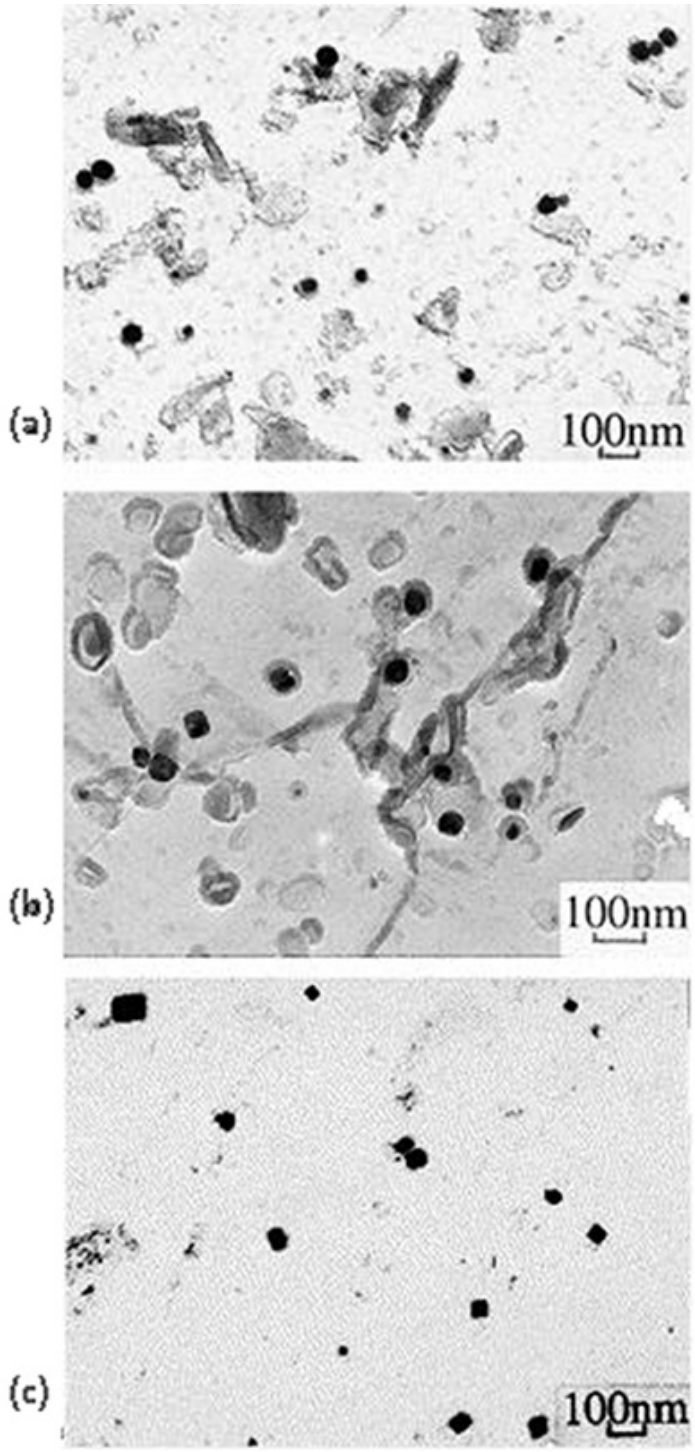

Figure 13 Shape change of zirconium carbonitrides with increasing temperature. 0.12%Zr steel (a) spherical zirconium carbonitrides after solution treatment (ST) and quenching (Q) from 1100ºC (b) angular and spherical zirconium carbonitrides particles after ST and Q from 1150ºC(c) angular carbonitrides after ST and Q from 1200ºC, He and Baker. [26]

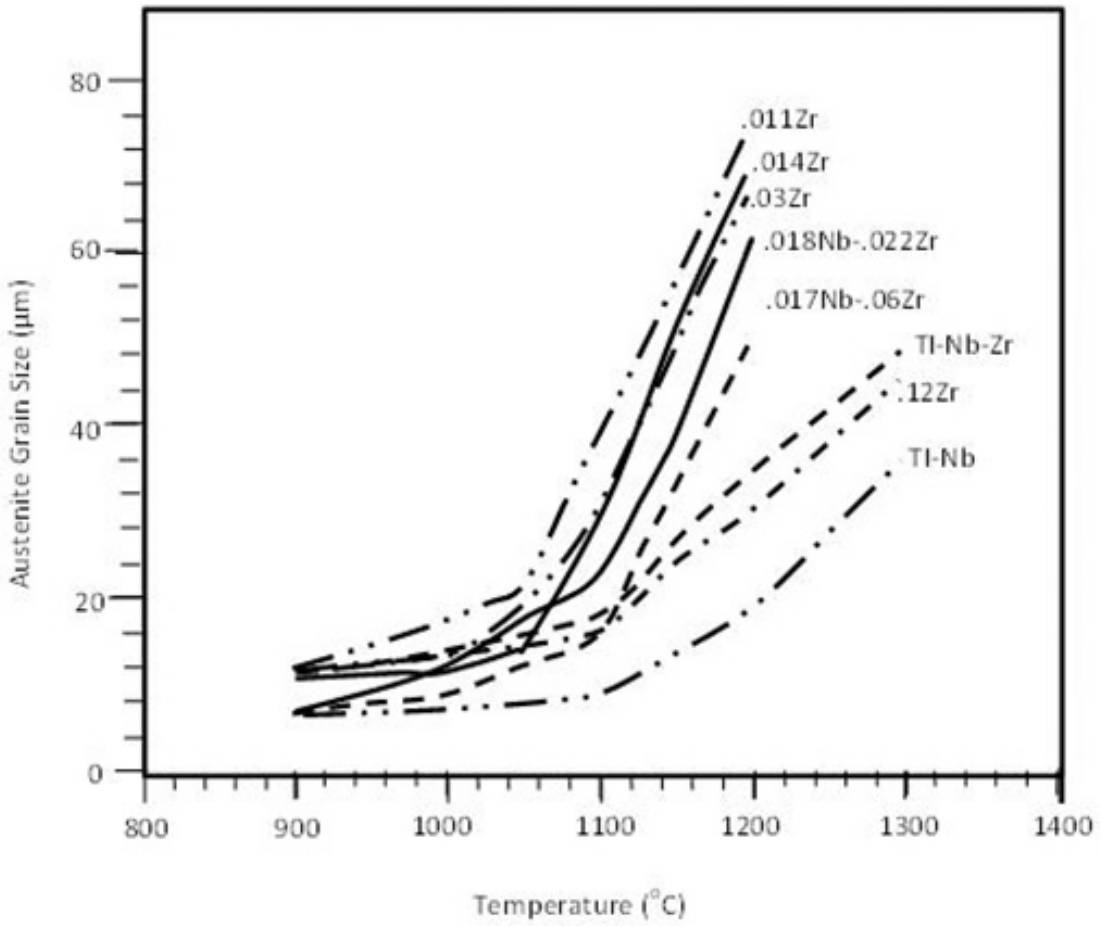

Figure 14 Austenite grain coarsening behaviour in zirconium treated and titanium treated steels , He and Baker.[26]

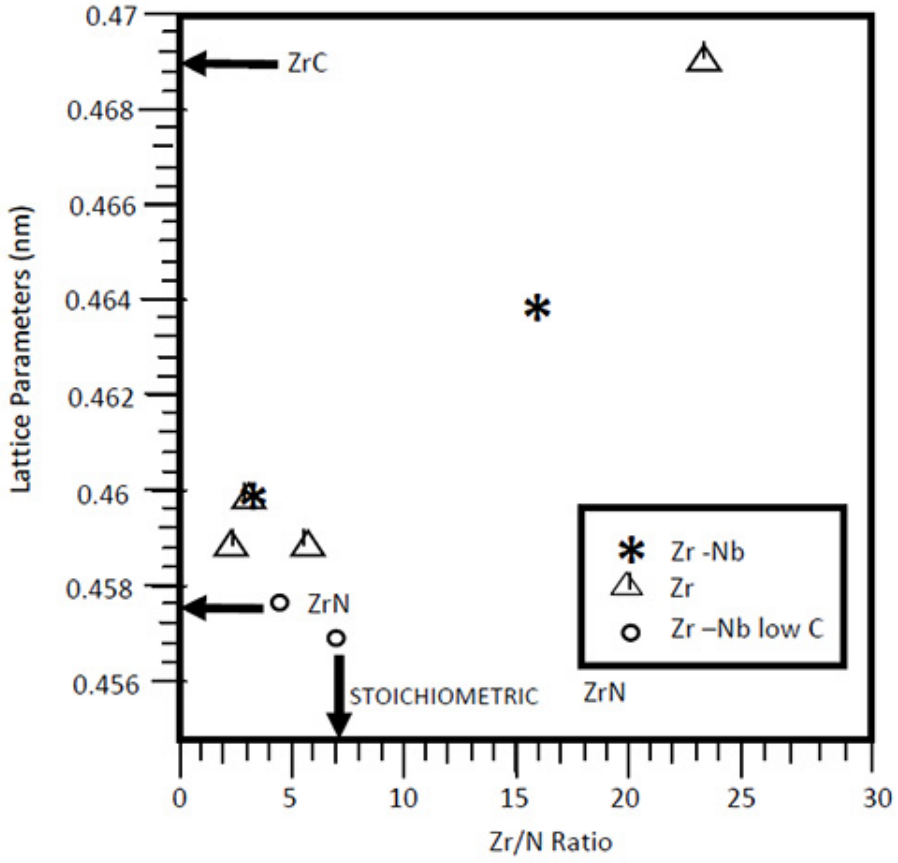

Figure 15 Effect of zirconium additions on lattice parameters of zirconium carbonitrides in the as –rolled condition ,He and Baker. [26]

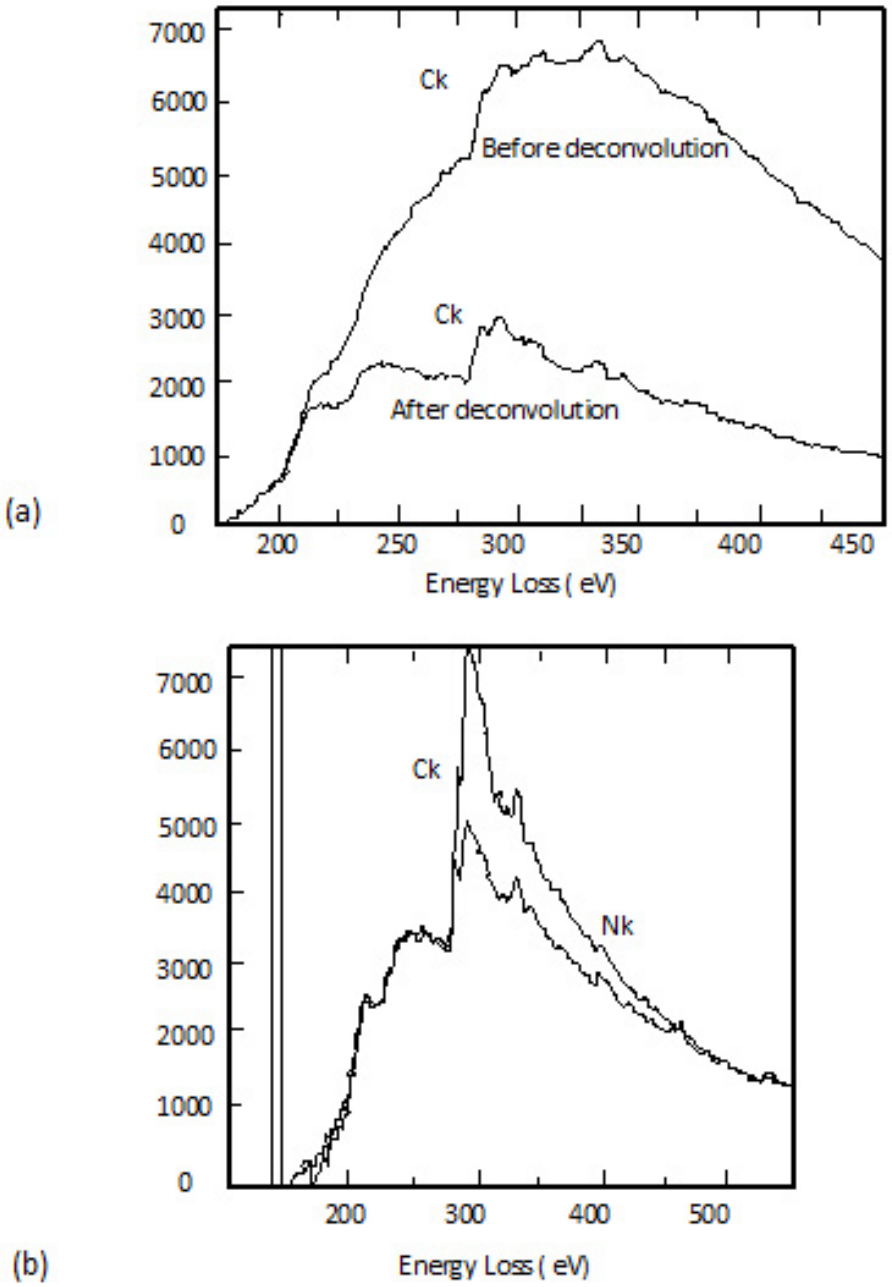

Figure 16 PEELS analysis of zirconium carbonitrides in Steel 4, Table 10.

(a)PEELS spectra from a particle overhanging a hole in a carbon replica , showing only the carbon edge, before and after deconvolution (b) PEELS spectra from two particles quenched from 1200ºC, showing N edges with different heights together with C edges, He and Baker. [26]

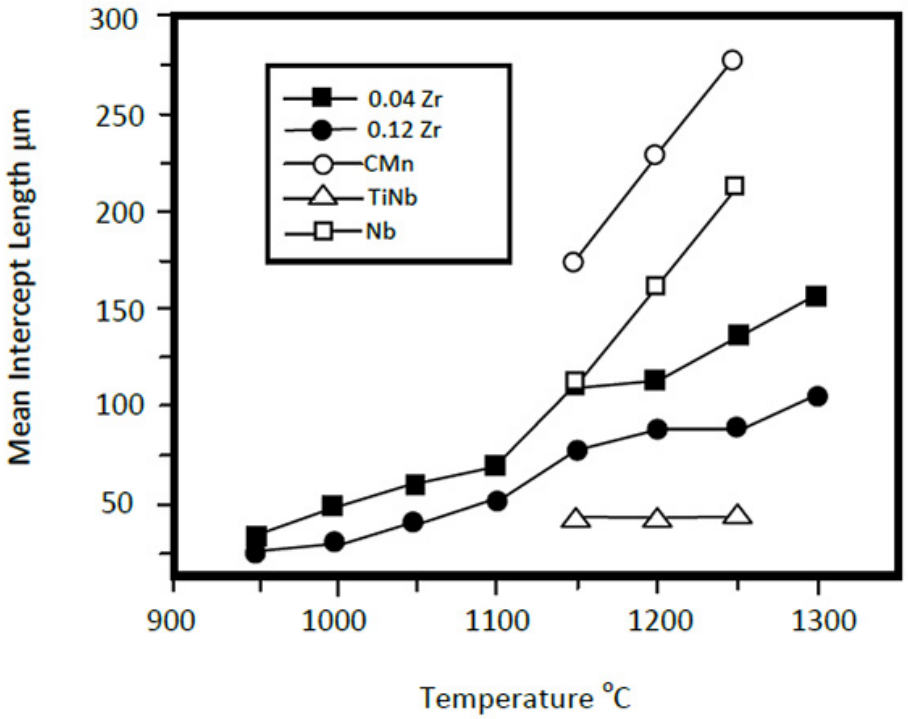

Figure 17 Austenite grain size (mean intercept length) versus holding temperature, Maia et al. [29]

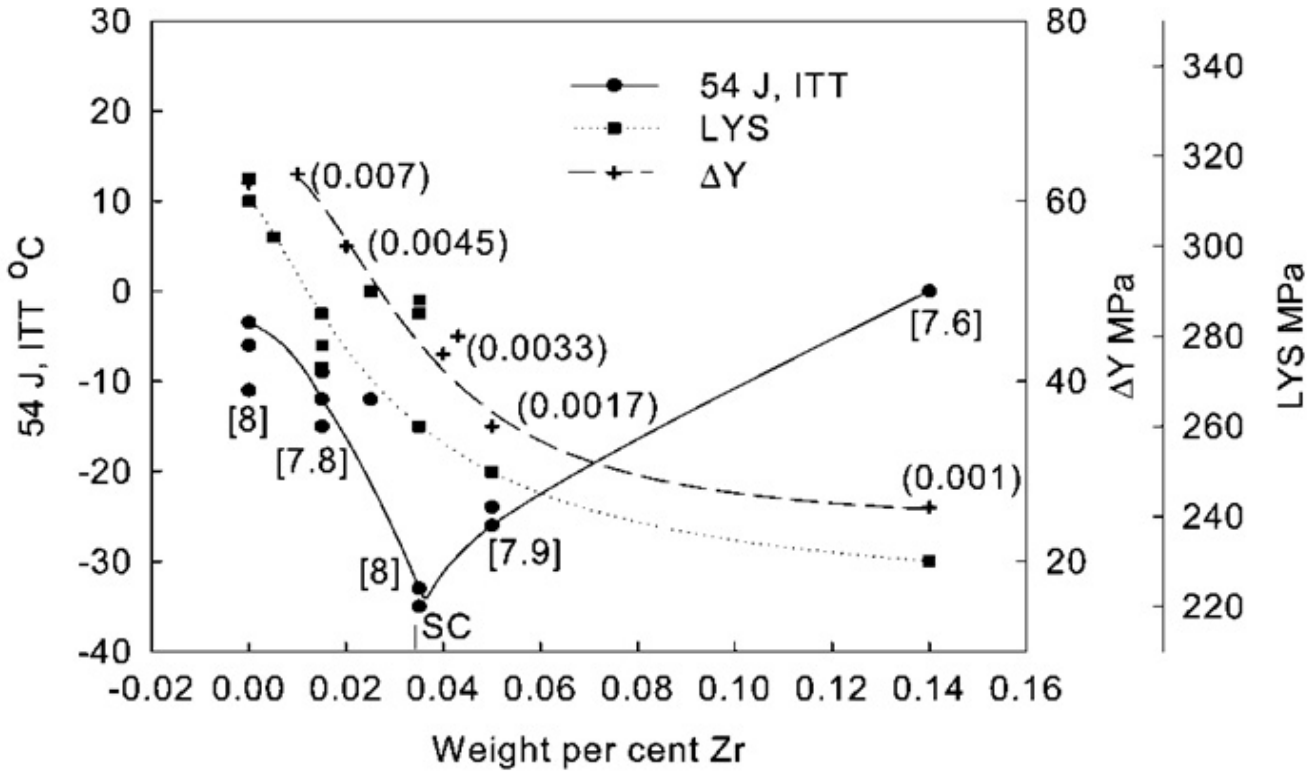

Figure 18, Influence of Zr on impact and lower yield point of hot rolled 0.18%C, 0.6%Mn, 0.3%Si and 0.005%N steels: grain size range was 7.5–8.5 mm21/2; figures in ( ) and [ ] brackets are free N values and average grain size values for composition; SC is stoichiometric composition Zr–N for steel with 0.005%N, Mintz et al.[134]

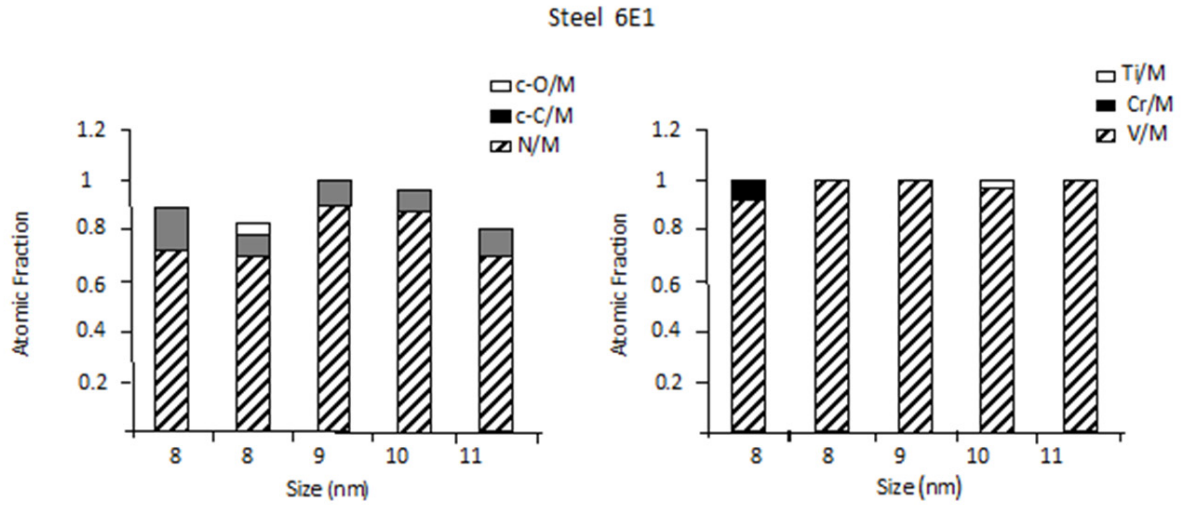

Figure 19 PEELS analysis data from five 8 to 11 nm sized particles, extracted on to a carbon replica from a Zr-V-N steel[steel6E1]. They contained mainly vanadium and nitrogen.

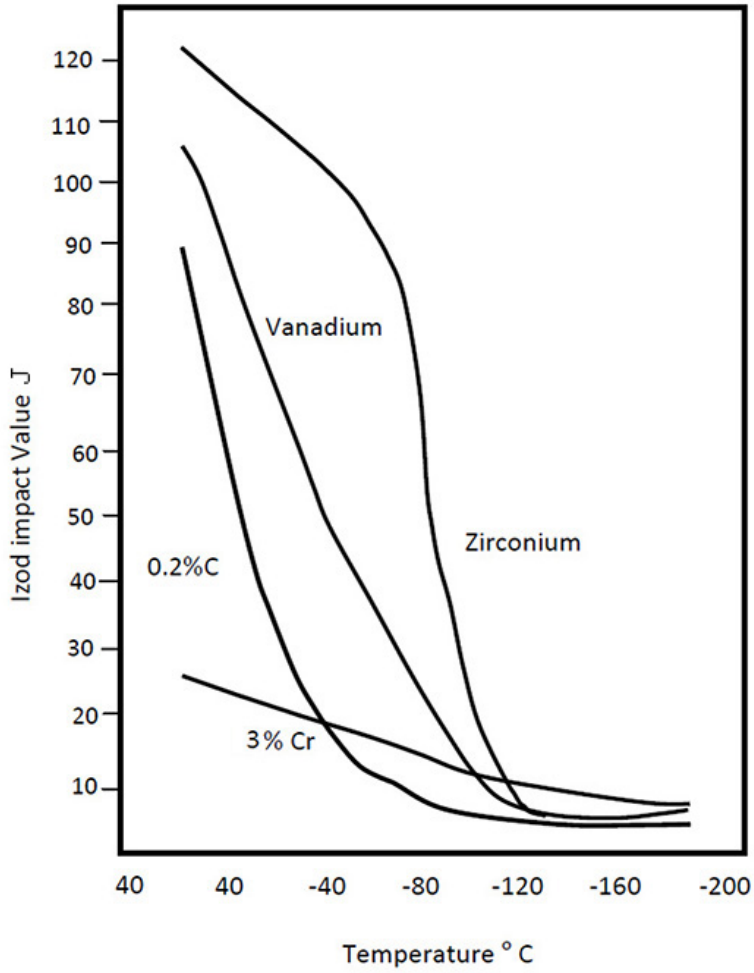

Figure 20 Impact values of three alloy steels compared with a mild steel,

Egan et al.[135]

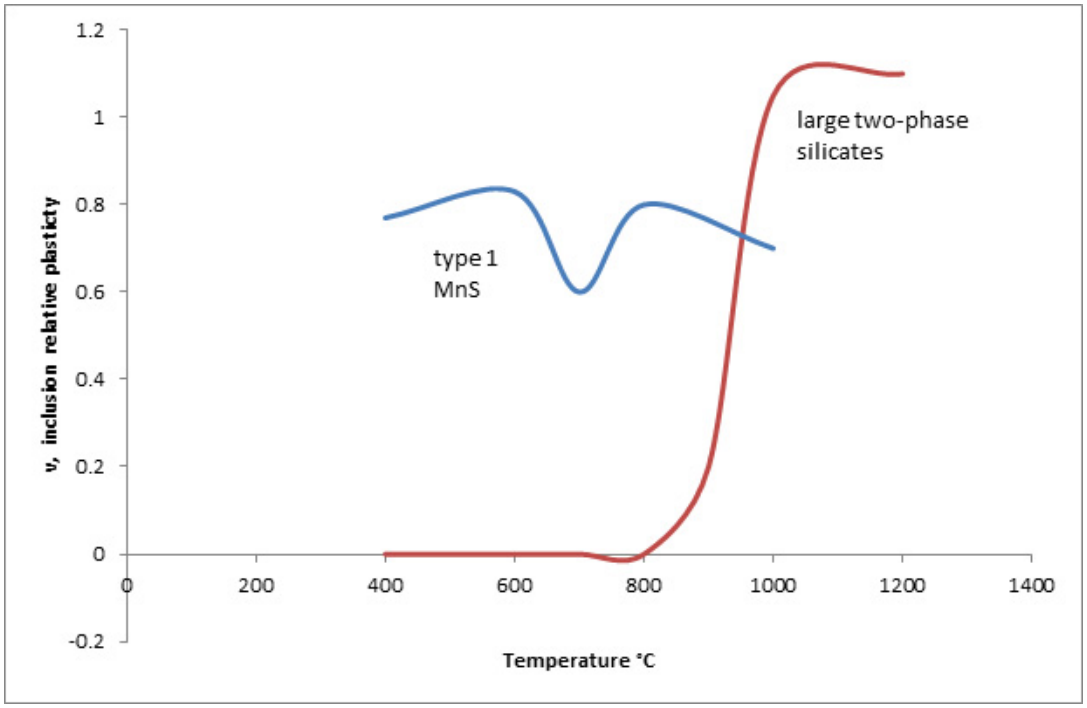

Figure 21 A comparison of the relative plasticity ν, as a function of temperature for large two- phase silicates and type1MnS inclusions. Compiled from the data in Baker et al.[142]

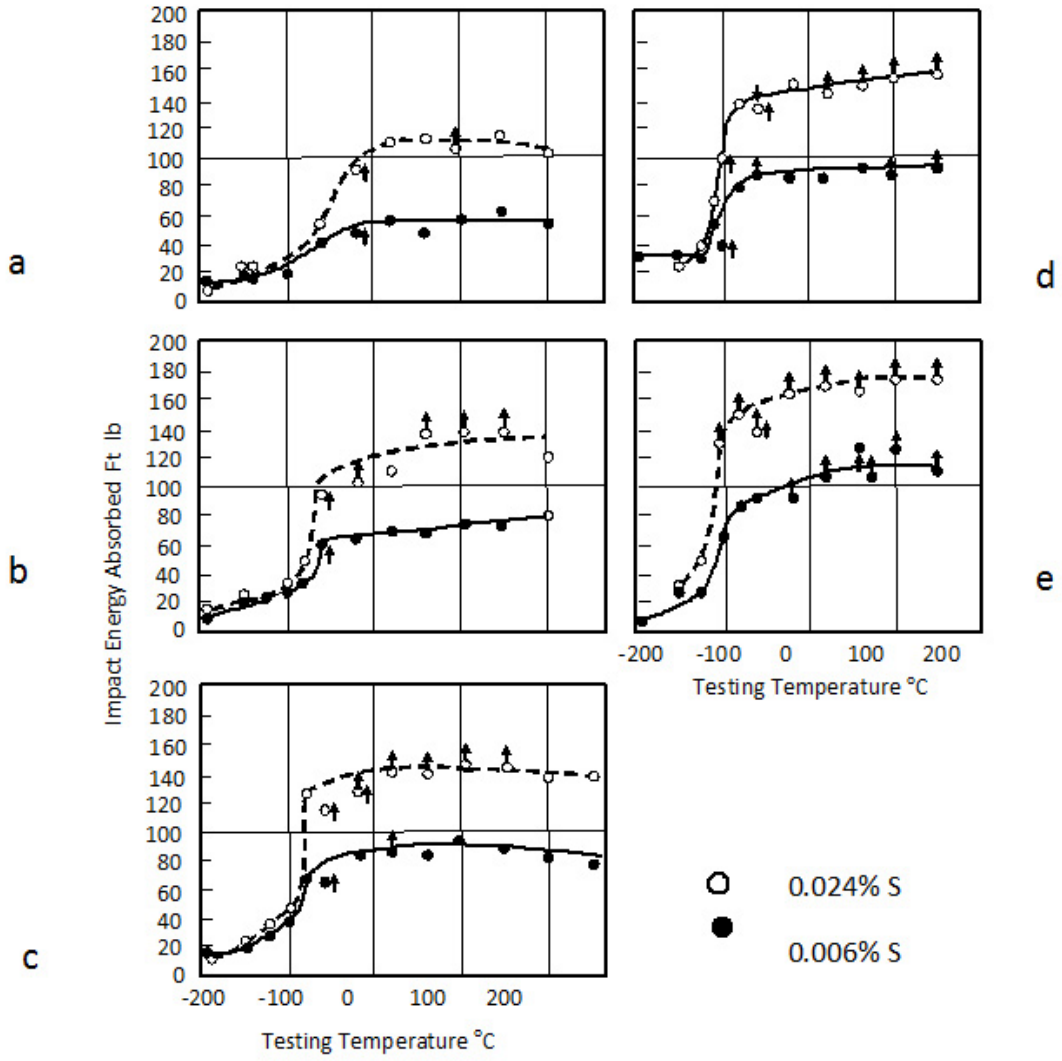

Figure 22 Effect of sulphur on the impact strength of 1%Cr-Mo steel at different tensile strengths in MPa (a)1034(b)965(c)896(d)827(e)758, after Franklin and Tegart.[21]

[40ft.lbs ≡ 55J]

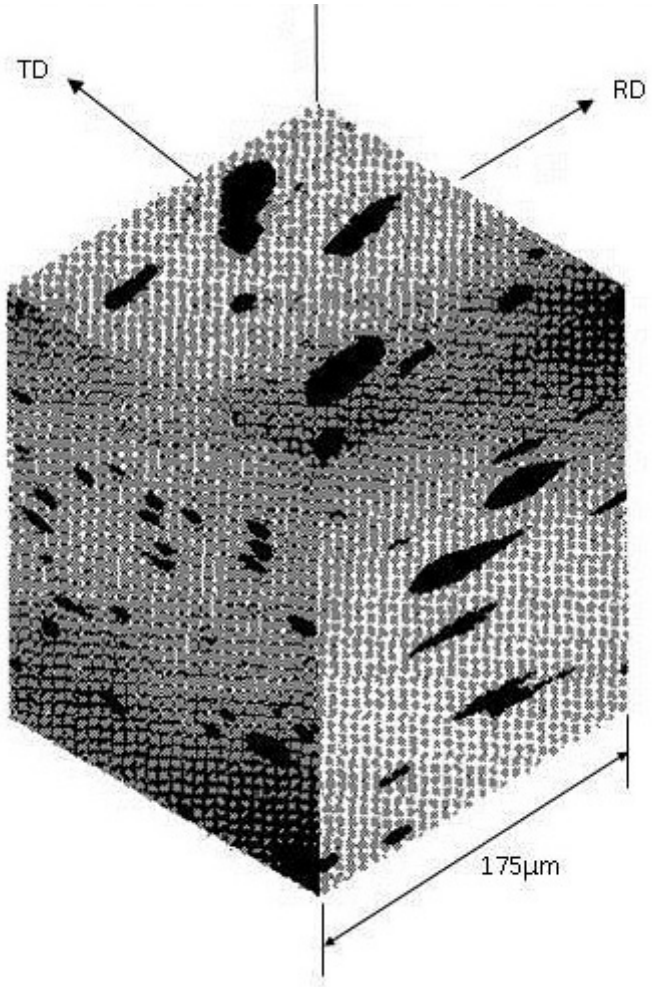

Figure 23 MnS inclusions in a hot rolled steel after a rolling strain of 1.0, Mardinly et al.[154]

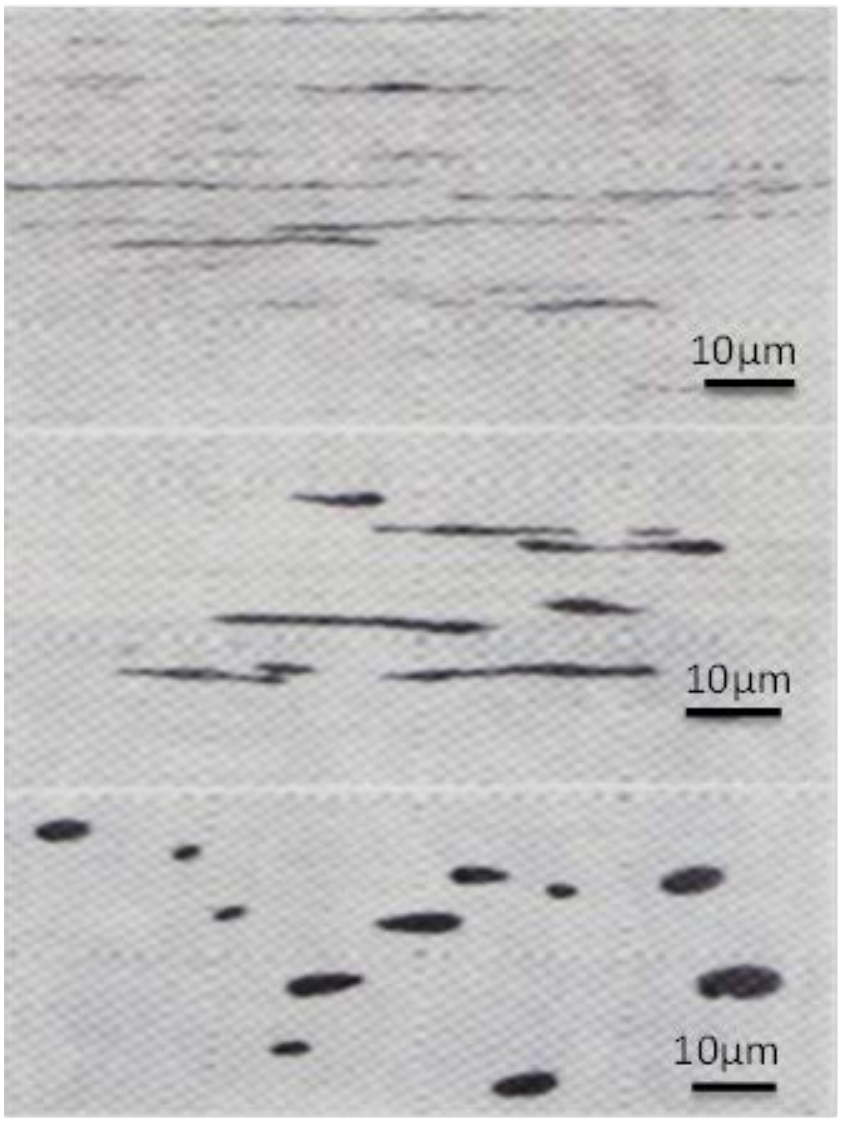

Figure 24 Micrographs showing the effect of zirconium on sulphide inclusions,

Top, 0%Zr, middle, 0.03%Zr, bottom, 0.08%Zr.

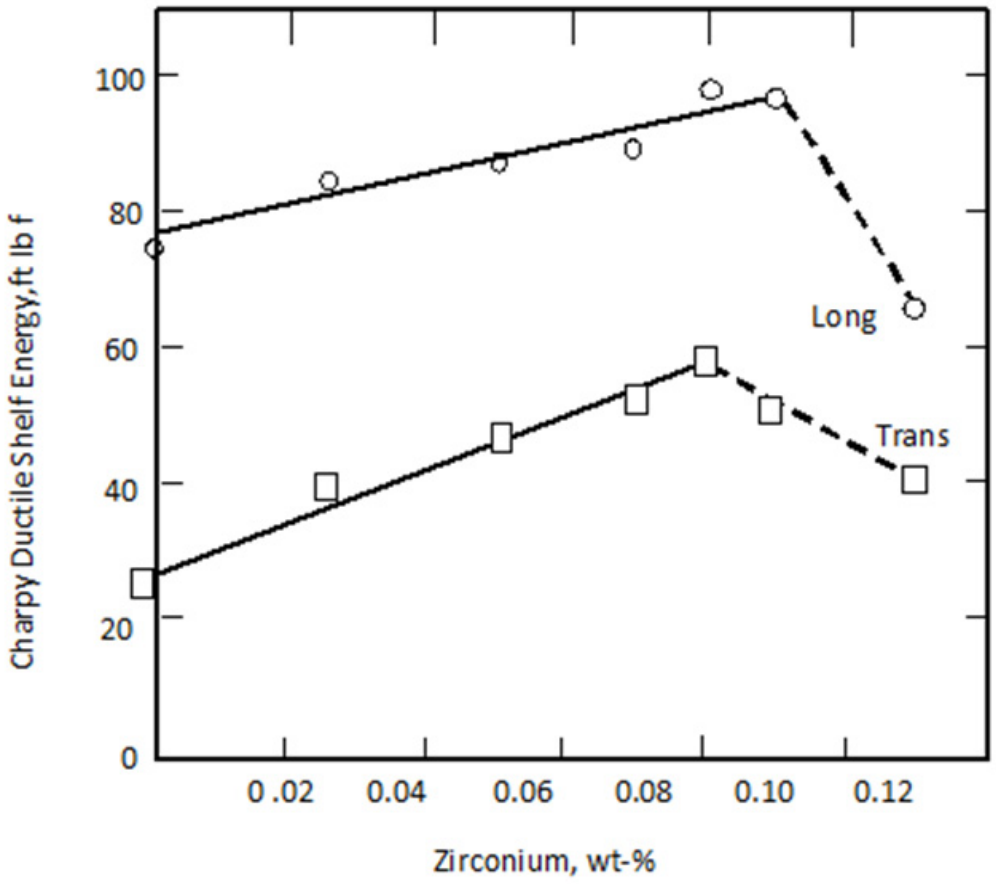

Figure 25 Effect of zirconium on the corrected Charpy ductile shelf energy, series 2 zirconium melt , Little and Henderson. [86]

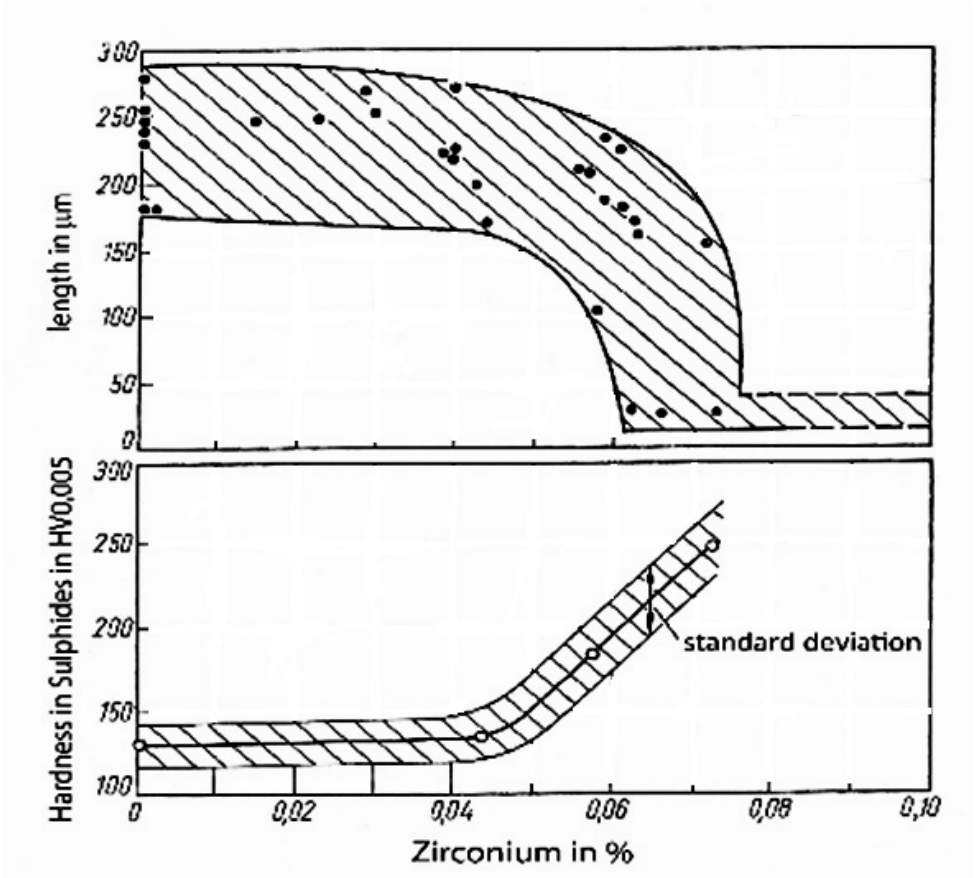

Figure 26 Influence of zirconium addition on the inclusion length and hardness for all 19 steels investigated ,after Heisterkamp et al.[130]

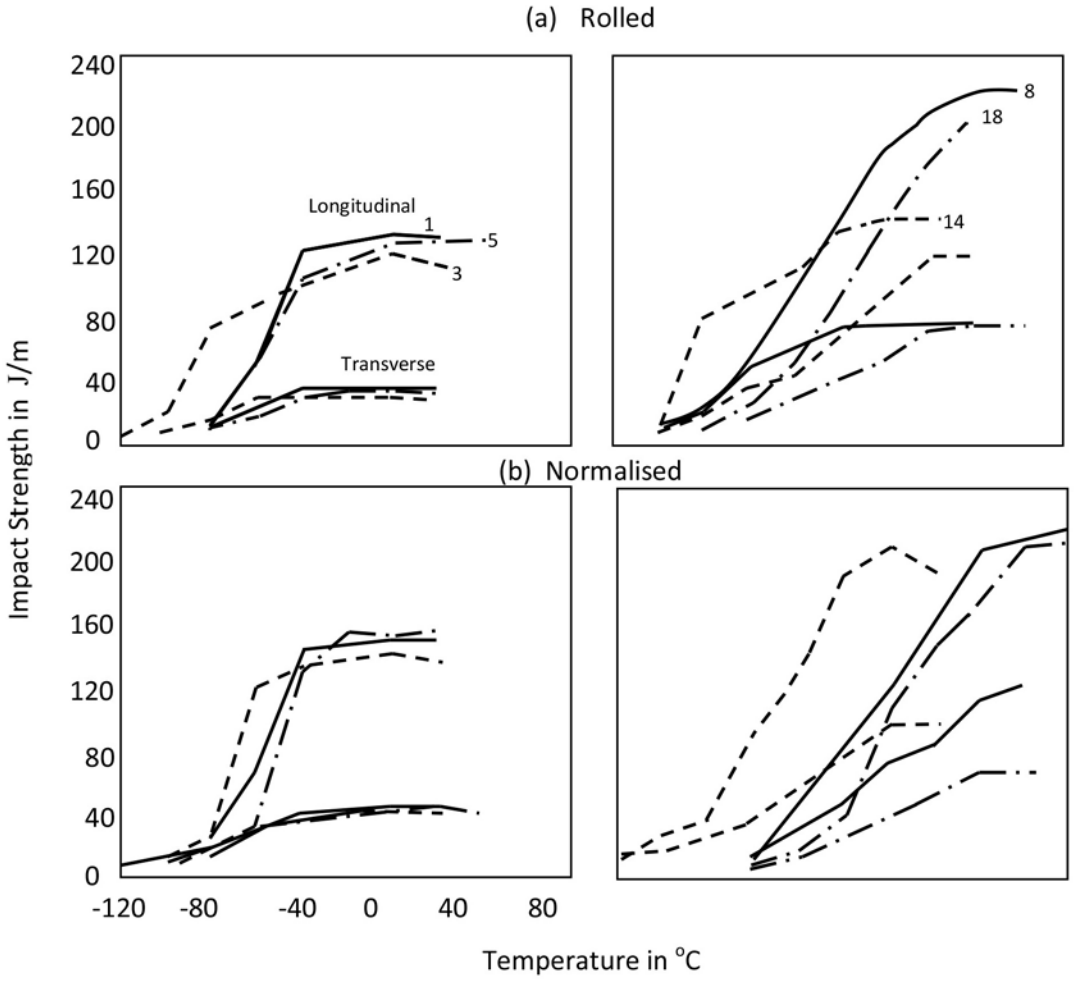

Figure 27 Comparison of the impact strength of three steels, (1)-plain carbon, (3) 0.035%Nb, (5) 0.057%V with three zirconium steels (8) 0.072%Zr, (14) 0.053%Zr+0.049%V, (18) 0.070%Zr+0.031%Nb, all in the as-rolled and normalized states, Heisterkamp et al.[130]

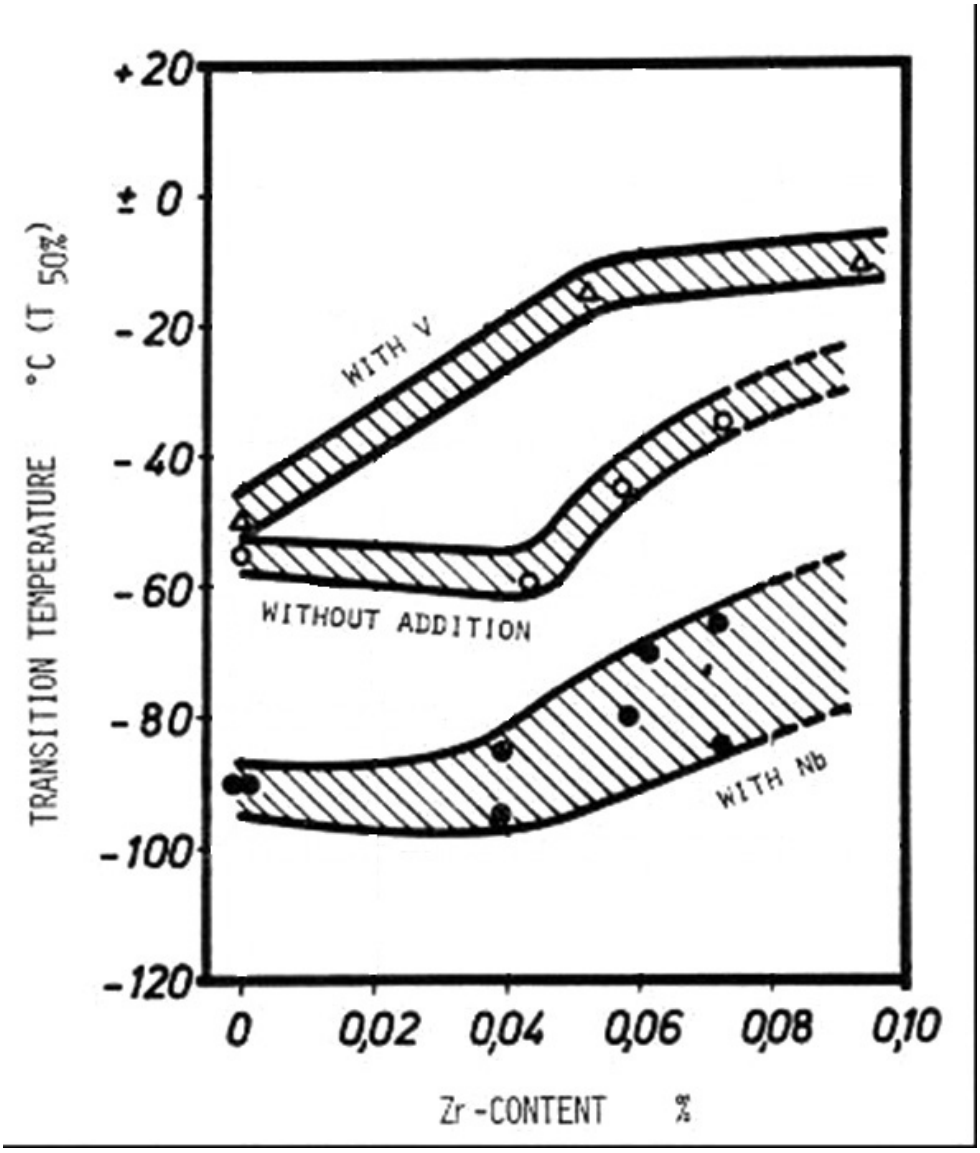

Figure 28 Effect of zirconium on the transition temperature of strip in the as-rolled condition and containing niobium or vanadium (0.18%C, ISO-V longitudinal tests), Meyer et al. [131]

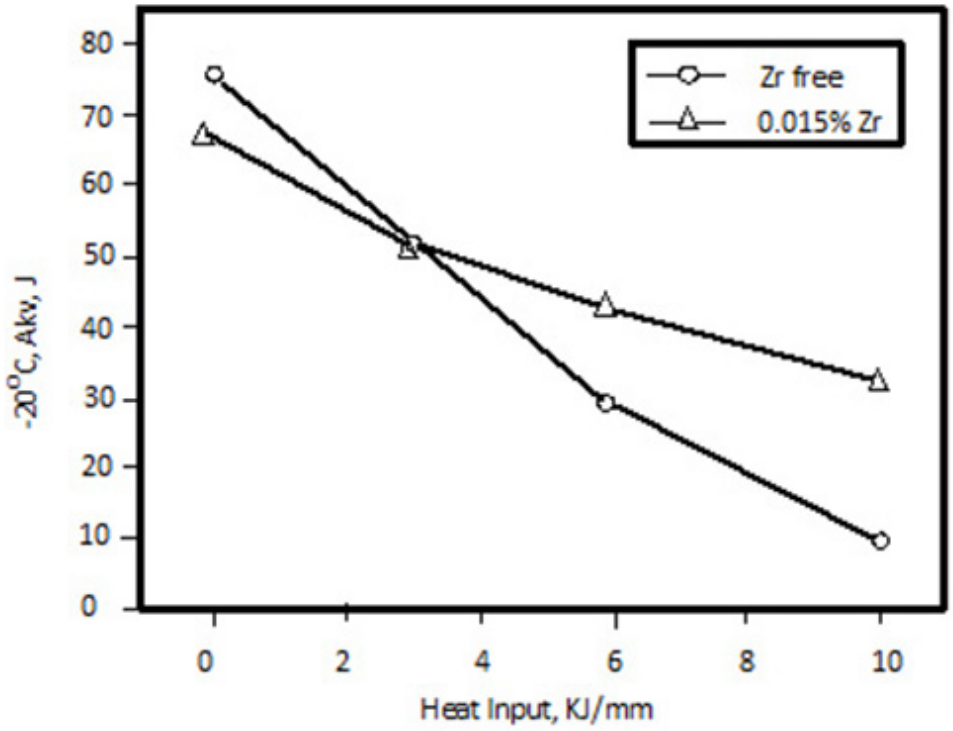

Figure 29 Variation of impact toughness in coarse grained HAZ with different weld heat inputs[H] in zirconium–bearing and zirconium -free specimens, Guo et al.[5]

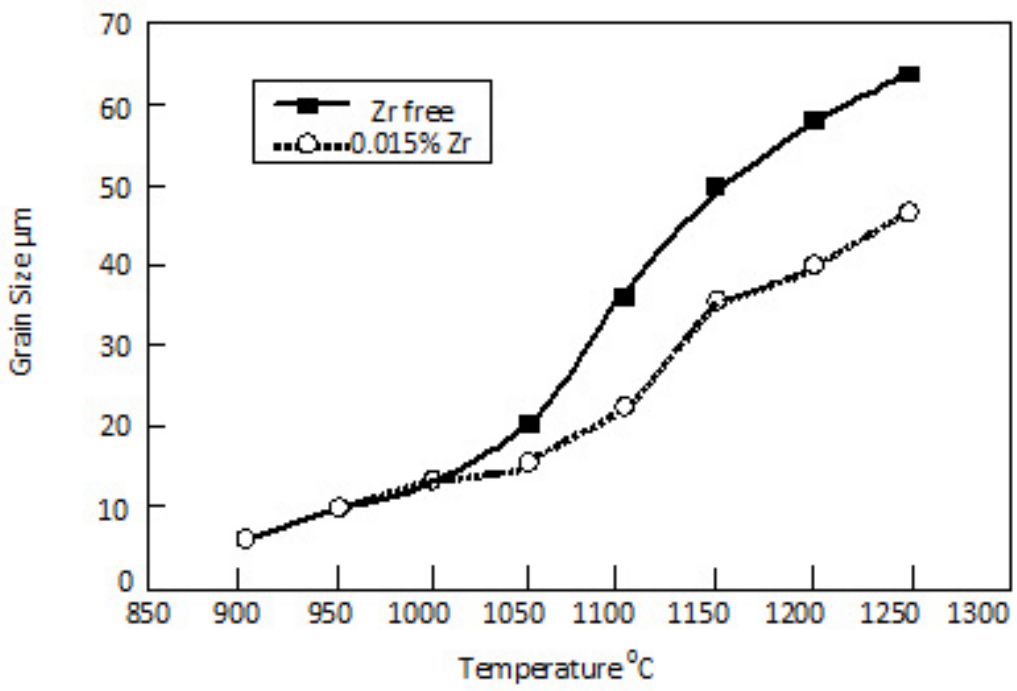

Figure 30 Relationship between austenite grain size (D) and reheat temperature for zirconium–bearing and zirconium-free specimens, Guo et al. [5]

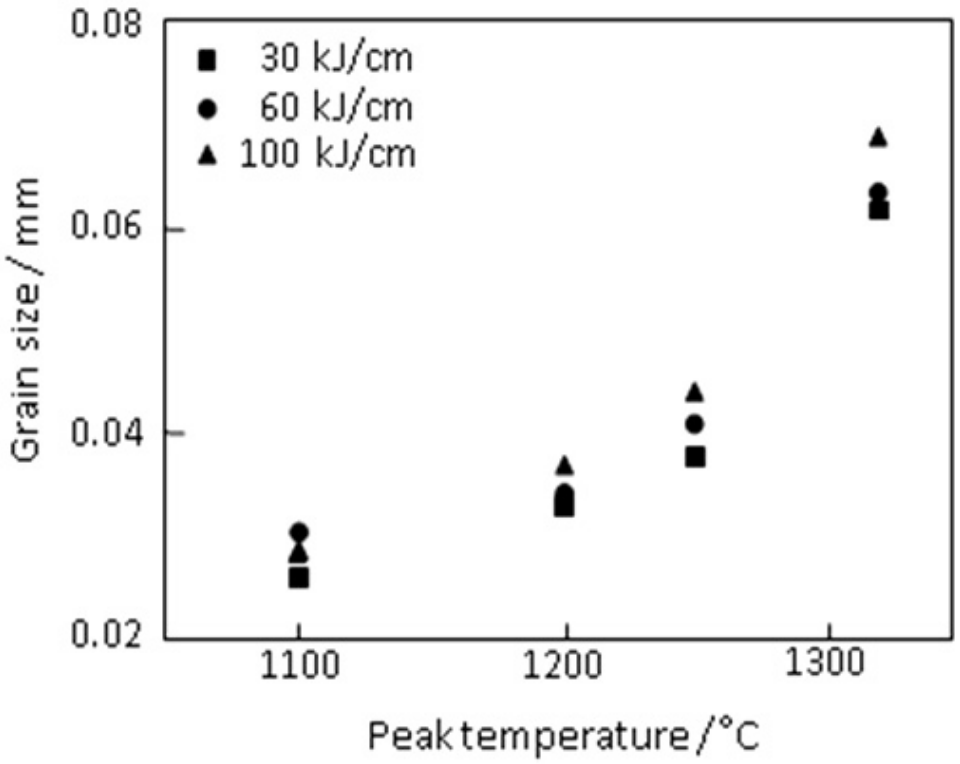

Figure 31 Measured prior austenite grain size in HAZ as a function of different heat inputs, Zheng et al. [169]